

SECURITY CLASSIFICATION OF THIS PAGE (When Data Entered)

| REPORT DOCUMENTATION PAGE   |                       | READ INSTRUCTIONS<br>BEFORE COMPLETING FORM  |
|---|-----------------------|--|
| 1. REPORT NUMBER<br>AVRADCOM TR 82-F-4  | 2. GOVT ACCESSION NO. | 3. RECIPIENT'S CATALOG NUMBER  |
| 4. TITLE (and Subtitle)<br>QUALITY CONTROL AND NONDESTRUCTIVE EVALUATION<br>TECHNIQUES FOR COMPOSITES - PART IV:<br>RADIOGRAPHY - A STATE-OF-THE-ART REVIEW   |                       | 5. TYPE OF REPORT & PERIOD COVERED<br>Final Report -<br>12/1/80 to 5/15/81                 |
|   |                       | 6. PERFORMING ORG. REPORT NUMBER   |
| 7. AUTHOR(s)<br><br>F. Alberti  |                       | 8. CONTRACT OR GRANT NUMBER(s)<br><br>IPA05-3363   |
| 9. PERFORMING ORGANIZATION NAME AND ADDRESS<br><br>University of Lowell<br>Lowell, Massachusetts 01854  |                       | 10. PROGRAM ELEMENT, PROJECT, TASK<br>AREA & WORK UNIT NUMBERS<br><br>D/A Project: 1807119 |
| 11. CONTROLLING OFFICE NAME AND ADDRESS<br>US Army Aviation Research and Development Command<br>ATTN: DRDAV-EGX<br>4300 Goodfellow Blvd., St. Louis, Missouri 63120   |                       | 12. REPORT DATE<br>June 1982   |
|   |                       | 13. NUMBER OF PAGES<br>75  |
| 14. MONITORING AGENCY NAME & ADDRESS (if different from Controlling Office)<br><br>Army Materials and Mechanics Research Center<br>ATTN: DRXMR-K<br>Watertown, Massachusetts 02172  |                       | 15. SECURITY CLASS. (of this report)<br><br>Unclassified                                   |
|   |                       | 15a. DECLASSIFICATION/DOWNGRADING<br>SCHEDULE  |
| 16. DISTRIBUTION STATEMENT (of this Report)<br><br>Approved for public release; distribution unlimited.   |                       |  |
| 17. DISTRIBUTION STATEMENT (of the abstract entered in Block 20, if different from Report)  |                       |  |
| 18. SUPPLEMENTARY NOTES<br><br>AMMRC TR 82-40   |                       |  |
| 19. KEY WORDS (Continue on reverse side if necessary and identify by block number)<br><br>Composite materials      Quality control      Voids<br>Quality assurance      Gamma radiography      Neutron radiography<br>Nondestructive evaluation      X-radiography      Image enhancement |                       |  |
| 20. ABSTRACT (Continue on reverse side if necessary and identify by block number)   |                       |  |

(SEE REVERSE SIDE)

Block No. 20

## ABSTRACT

Radiography is perhaps the most commonly known method of nondestructive examination, its origins dating back to the early 1920's. Using the penetration and absorptive properties of gamma or X-radiation to impart an image of the item under examination onto radiographic film, radiographic inspection has become a standard technique for inspecting modern industrial and advanced composite materials.

Earlier uses of radiography were limited to the examination of metallic items, such as welds, castings, forgings, and various other metal parts to reveal imperfections (voids, inclusions, density variations, and other fabrication irregularities). Today's applications include a wider range of materials comprising metallic, nonmetallic, and composite materials to insure the integrity of components for industrial needs, military needs, aircraft elements, aerospace components, and numerous other applications. In composite materials, the radiographer has had to deal with a wide spectrum of reinforcement and matrix material systems, together with a number of associated types of defects. In particular, some of the defect considerations investigated with radiography include: bond evaluations, curing effects, damage considerations, flaw content and growth, voids, failure mechanisms, fatigue behavior, fiber characteristics and fiber breaks, fracture characteristics, moisture effects, physical properties, resin content, and thermal effects. The need for detection of these types of defects and the general nature of composite systems has brought about a number of advancements in the traditional straightforward radiographic technique and has spurred the development of some new and promising techniques.

This report reviews and relates the procedures, variables and techniques for producing a quality radiograph to past and ongoing research aimed at improving the radiographic technique as a nondestructive evaluation method, with emphasis on composite material investigations. In particular, the report includes discussions of state-of-the-art techniques such as micro radiography, stereoradiography, and neutron radiography. Fluoroscopy is discussed along with recent developments in filmless techniques of radiographic imaging, electronic image enhancement, and use of opaque additives and penetrants.

AVRADCOM

Report No. TR 82-F-4

ADA 137156

MANUFACTURING METHODS AND TECHNOLOGY  
(MANTECH) PROGRAM

QUALITY CONTROL AND NONDESTRUCTIVE EVALUATION  
TECHNIQUES FOR COMPOSITES, PART IV: RADIOGRAPHY -  
A STATE-OF-THE-ART REVIEW

FRANK P. ALBERTI  
University of Lowell  
Lowell, Massachusetts 01854

June 1982

FINAL REPORT

Contract No. IPA05-3363



Approved for public release;  
distribution unlimited

U. S. ARMY AVIATION RESEARCH AND DEVELOPMENT COMMAND

The findings in this report are not to be construed as an official Department of the Army position, unless so designated by other authorized documents.

Mention of any trade names or manufacturers in this report shall not be construed as advertising nor as an official indorsement or approval of such products or companies by the United States Government.

#### DISPOSITION INSTRUCTIONS

Destroy this report when it is no longer needed.  
Do not return it to the originator.

## PREFACE

This project was accomplished as part of the U.S. Army Aviation Research and Development Command Manufacturing Technology Program. The primary objective of this program is to develop, on a timely basis, manufacturing processes, techniques, and equipment for use in production of Army material. Comments are solicited on the potential utilization of the information contained herein as applied to present and/or future production programs. Such comments should be sent to: U.S. Army Aviation Research and Development Command, ATTN: DRDAV-EGX, 4300 Goodfellow Blvd., St. Louis, MO 63120.

The work described in this report was accomplished under a contract monitored by the Army Materials and Mechanics Research Center. Technical monitor for this contract was Dr. R. J. Shuford.

## CONTENTS

|  | Page |
|--|------|
| SECTION 1. INTRODUCTION. . . . .                                 | 1    |
| SECTION 2. RADIATION SOURCES                                     |      |
| X-Rays . . . . .   | 4    |
| Gamma Rays . . . . .   | 7    |
| SECTION 3. MAKING A RADIOGRAPH . . . . .                         | 11   |
| Geometric Factors. . . . .                                       | 11   |
| Object Effects . . . . .   | 16   |
| Scattered Radiation. . . . .                                     | 17   |
| Film Effects . . . . .   | 20   |
| SECTION 4. EXPOSURE FORMULATION. . . . .                         | 24   |
| X-Ray Exposure Charts. . . . .                                   | 28   |
| Gamma Ray Exposure Charts. . . . .                               | 29   |
| Control of Scattered Radiation . . . . .                         | 30   |
| Penetrameters and Radiographic Sensitivity . . . . .             | 34   |
| Viewing and Interpreting Radiographs . . . . .                   | 37   |
| SECTION 5. COMPOSITE MATERIAL INVESTIGATIONS                     |      |
| Typical Applications . . . . .                                   | 39   |
| Microradiography . . . . .                                       | 42   |
| Automatic Computer-Based Radiographic Image Enhancement. . . . . | 46   |
| Stereoradiography. . . . .                                       | 51   |
| Opaque Additives and Image Enhancement . . . . .                 | 53   |
| Neutron Radiography. . . . .                                     | 59   |
| APPENDIX   |      |
| Exposure Calculations. . . . .                                   | 64   |
| LITERATURE CITED. . . . .  | 66   |
| BIBLIOGRAPHY. . . . .  | 67   |

## SECTION 1. INTRODUCTION

Perhaps the most commonly known method of nondestructive examination is radiography, which uses the penetration and absorptive properties of gamma or X-radiation to impart an image of the item under examination onto radiographic film. Today, these types of radiographic inspection are widely used for inspecting modern industrial and advanced composite materials. Another type of radiation imaging, neutron radiography, has recently been developed and improved for use in numerous specialized applications. Due to its inherent differences in processing, techniques, and applications, neutron radiography will be treated separately (see Section 5). Sections 1 through 5 are primarily a study of gamma and X-radiography.

Earlier uses of radiography were limited to the examination of metallic items, such as welds, castings, forgings, and various other metal parts to reveal imperfections (voids, inclusions, density variations, and other fabrication irregularities). Radiography is now applied to a wider range of materials comprising metallics, non-metallics, and composites, to insure the integrity of components for industrial and military needs, aircraft elements, aerospace components, and numerous other applications. In composite materials, radiography is used to detect and identify such defects as void content (porosity), unpolymerized resins, irregular matrix content, fiber-matrix unbonds, interlaminar unbonds, foreign inclusions, fiber and laminate misalignments, fiber breaks, moisture content, and others.

X-rays and gamma rays comprise part of the electromagnetic spectrum, which can be described, on the basis of wavelength, as follows:

|   |                           |
|---|---------------------------|
| X-rays                                    | 0.0004 - 0.5 Å            |
| Gamma Rays                                | 0.005 - 0.1 Å             |
| Ultraviolet                               | 10 - 4,000 Å              |
| Visible                                   | 4,000 - 7,500 Å           |
| Infrared                                  | 7,500 - $4 \times 10^6$ Å |
| Radio Waves                               | $10^6$ - $10^{13}$ Å      |
| (Here, Å = Angstrom unit = $10^{-8}$ cm.) |                           |

The following is a list of some of the properties and characteristics of gamma and X-rays, and is included, together with Figure 1, as an introductory aid toward the understanding of their processes and effects.

1. Invisible electromagnetic radiation
2. Can penetrate matter
3. Absorption dependent on material density and thickness



4. Travel in straight lines at 186,000 miles/second
5. Produce photochemical effects in photographic emulsions
6. Ionize gases through which they pass
7. Unaffected by electrical or magnetic fields
8. Liberate photoelectrons
9. Cause some substances to fluoresce
10. Damage or destroy living tissue

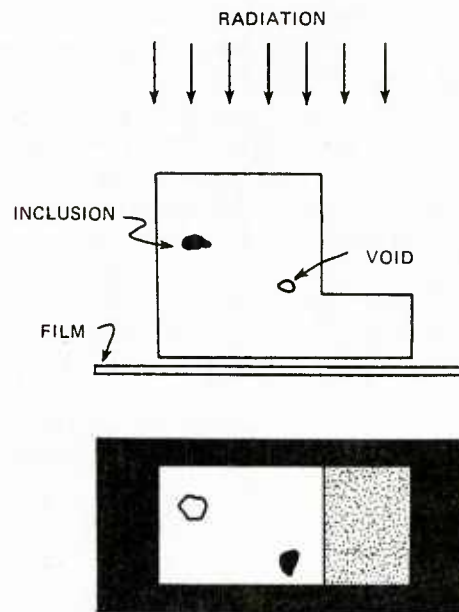


Figure 1. Basic radiographic set-up.

X-rays and gamma rays are each a type of electromagnetic radiation with identical form and properties. However, they arise from different sources and have different spectral (frequency content) characteristics. X-rays are produced in a cathode ray tube when high energy electrons strike a metallic anode target at high speed. As these electrons collide with the anode atoms and decelerate, they emit packets of energy, or photons, called X-rays.

Gamma radiation, on the other hand, is produced when atomic nuclei are put into a state of high excitation. Gamma ray sources can be either man-made isotopes, such as Cobalt 60 or Iridium 192, or natural isotopes, such as radium. While gamma and X-radiation are similar in form and properties, the quality of radiation, penetration ability, and absorption depend on the energy of the source used. X-rays can be made more penetrating by increasing the kilo-voltage across the X-ray tube. The thickness of a specific material which can be investigated



is therefore limited to the maximum voltage capacity of the X-ray tube; thicker, denser items under investigation would obviously require the use of higher kilovoltage tubes. The quality of gamma radiation depends on the activity of the isotope selected or the amount of radioactive material. Isotope activity is initially dependent on the nature of neutron bombardment used in creating a man-made isotope, and decays in energy level with time. The time required for the radiation activity of an isotope to decay to one-half of its initial value is termed its "half-life," and is a basic characteristic of each specific isotope. Isotope activity and gamma-ray quality are also affected, naturally enough, by the size of the isotope source. The size effect, however, is not linearly proportional, as might be assumed, since active nuclei internal to an isotope emit gamma rays which are absorbed by surrounding material. Further discussion on the nature and properties of radiation sources will follow in the next section.

The production of a quality radiograph requires not only the selection of an appropriate radiation source, but also thorough understanding and control of the geometric, spacial, equipment, material, and film variables involved. In addition, proper film development techniques are necessary to produce a readable radiograph prior to the final steps of film interpretation and item evaluation. The treatment of some of these variables is discussed later in Section 3, "Making a Radiograph."

Before deciding on the radiographic technique for a particular nondestructive evaluation, it is important to understand its limitations and advantages. The major advantages of radiographic inspection are as follows:

1. It provides a permanent visual representation of the interior of an item.
2. It is applicable for most materials.
3. It can be used as a quality control procedure to reveal the internal nature of an item and eliminate those which fail to meet a previously established acceptance-rejection criterion.
4. It can disclose errors in manufacturing procedures and fabrication processes, as well as indicate possible corrective action.
5. It can be utilized for easily accessible items which can be examined periodically in a preventive maintenance program.

The limitations of radiographic inspection include safety, economic, and geometric considerations as follows:

1. Due to the danger of exposing personnel to radiation sources, strict compliance to safety regulations is required, entailing specialized and costly protective equipment.
2. The cost of radiographic supplies, X-ray films and their processing is high relative to other NDE techniques. Large items of complex geometry which require multiple exposures and multiple films for complete examination are therefore quite expensive to radiograph. Conversely, smaller items of simple geometry are

easier to handle and are much more economical to investigate with radiography due to their higher rate of inspection.

3. The problem of complex item geometry is, in itself, an inherent limitation, since it is necessary to maintain a proper object-film orientation in order to minimize image distortion. In some instances of highly complex geometry, therefore, it can become impossible to produce a readable radiograph.
4. Since radiography is a penetration technique, it requires that the item under investigation be accessible from two sides, a source side and a film side.
5. Since radiographic images are brought about by density and thickness differences in the item under investigation, small laminar-type defects (particularly interlaminar unbonds or those along a fiber-matrix interface) are particularly difficult to detect, since they do not constitute a measurable density difference when radiographed perpendicular to their orientation. It is necessary in these instances, therefore, to align the radiation parallel to the expected discontinuity direction. Fortunately, this can often be easily accomplished with items of known fiber direction and laminate orientations.

Recently a number of experiments have been conducted using opaque additives, such as tetrabromoethane (TBE) and diiodobutane, to enhance the radiographic image of laminar-type defects. Radio-opaque penetrants have also been developed to detect surface defects such as crazing and surface-connected delaminations and voids. Further discussions of the use of opaque additives for the determination of crack growth and failure mechanisms will be included in some of the following sections. In addition, the procedures, variables, and techniques for producing a quality radiograph will be reviewed and related to discussions of past and ongoing research aimed at improving the radiographic technique as a nondestructive evaluation method, with emphasis on composite material investigations. In particular, this will include discussions of state-of-the-art techniques such as microradiography, stereoradiography, the use of opaque additives, and neutron radiography. Fluoroscopy will also be discussed along with recent developments in filmless techniques of radiographic imaging and automatic computer-based image enhancement.

## SECTION 2. RADIATION SOURCES

### X-Rays

In a typical high vacuum X-ray tube, an incandescent filament at the negative cathode electrode releases or "boils off" electrons as it is heated. These electrons are made to accelerate across the tube by a voltage difference applied across the electrodes (see Figure 2). X-rays are produced by these bombarding electrons as they undergo deceleration while moving into the positive anode target material. The X-rays or photons (energy packets) emitted comprise a range or spectrum of intensities similar to that shown in Figure 3, the characteristic peaks shown being dependent upon the type of anode target material. This characteristic radiation is of specific wavelength and small energy content, and can be neglected in considering the effects of X-radiation. What is important to recognize is that X-rays reaching

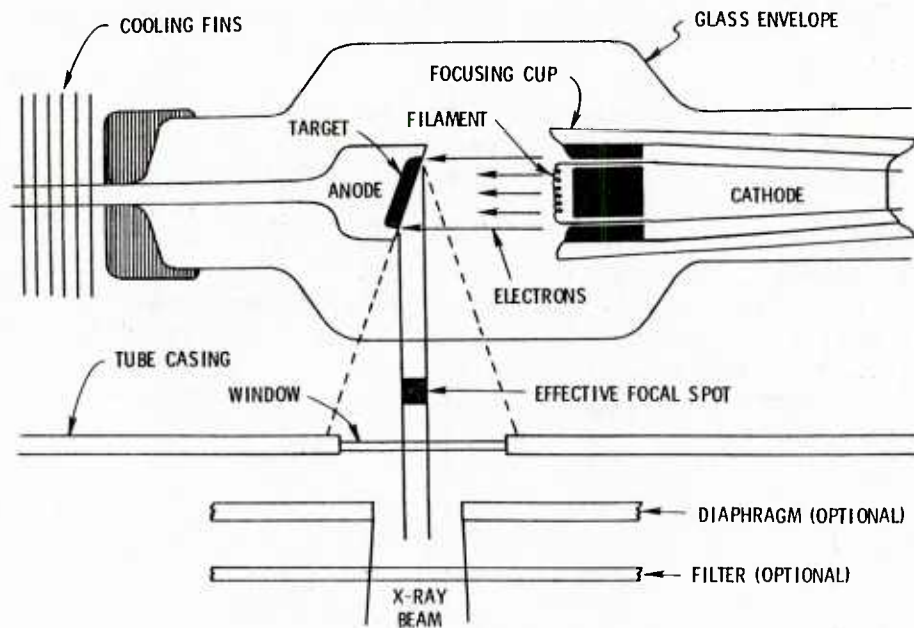


Figure 2. Typical X-ray tube.

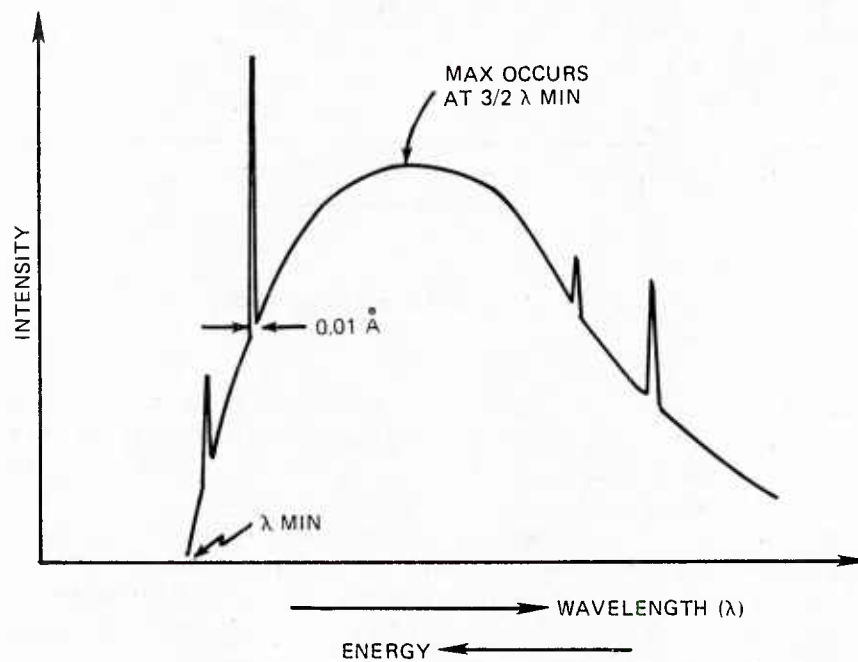


Figure 3. X-ray spectrum.

an item under investigation comprise a spectrum of intensities with a range of wavelengths. The high-energy (short wavelength) rays have greater penetrating ability and are termed hard X-rays. The lower energy (long wavelength) rays have little penetrating power and are more easily scattered within the item material. These are called soft X-rays.

Since X-ray intensity is dependent upon the energy (or velocity) of the electrons bombarding the anode target, an increase in voltage across the X-ray tube will produce more short wavelength X-rays (see Figure 4). This is important to the radiographer, since it indicates that X-ray penetrating ability is increased as tube voltage is increased. That is, higher voltages produce more shorter-wavelength penetrating rays. However, the relationship is not linear, and no general analytical expression exists which can describe the relationship between voltage increase and X-ray penetrating ability. Such a relationship, if desired, would have to be experimentally derived for each particular X-ray tube. It is not necessary, however, to do this in order to produce a quality radiograph, as we shall see later in Section 4, Exposure Formulation.

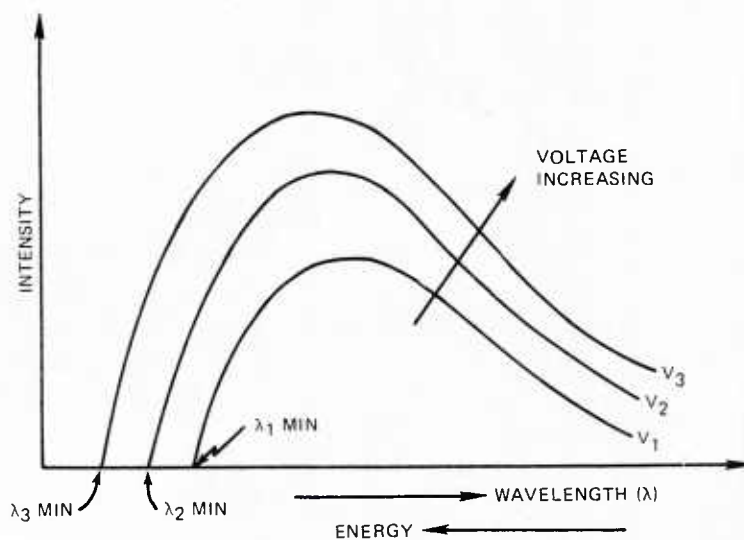


Figure 4. Effect of voltage change on X-ray quality.

Since the exposure ( $E$ ) needed to produce a radiograph is equal to the product of X-ray intensity ( $M$ ) and time ( $t$ ), a second relationship of importance is that between the number of target bombarding electrons and X-ray intensity. The number of bombarding electrons is commonly referred to as tube current. The tube current depends upon the temperature of the cathode incandescent filament, usually made of tungsten, where more electrons are "boiled off" at higher temperatures. Figure 5 illustrates the effect of change in tube current on the X-ray beam spectrum. Note that the X-ray output or intensity of each wavelength increases in proportion to tube current. The spectrum of wavelengths produced, however, remains the same. Therefore, penetrating ability is not improved by increasing tube current, but, since  $E = M \times t$ , increased X-ray intensity reduces the required exposure time.



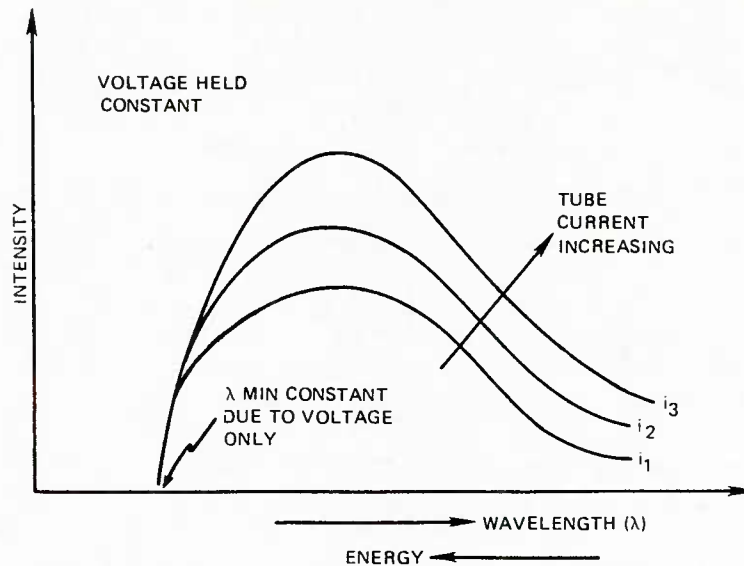


Figure 5. Effect of change in tube current on X-ray intensity.

In the design of X-ray tubes, it is important to realize that most of the energy imparted to the anode target is transformed into heat, and only a small portion is used to generate X-rays. For this reason, the anode target material must be of high atomic number and have a high melting point. Tungsten is one such material and is generally selected for the target material. In addition, tube designs generally incorporate some type of cooling system, usually radiating fins and circulating liquid, to carry off the heat generated at the anode target (see Figure 2). Note that the bombarding electrons are focused to travel in a straight line to the target, and that the target is oriented at a small angle. This creates a small "effective focal spot" at the anode. The size of the effective focal spot is very important in defining the sharpness of the object image on the X-ray film. The smaller the effective focal spot, the sharper and more well defined the resulting radiograph will be.

The tube window is made of a low absorptive material, usually glass or beryllium, and allows X-rays to escape the tube casing. The term "inherent filtration" is used to describe the radiation filtering that takes place through the tube window. Beryllium windows provide less inherent filtration than glass windows. That is, they allow more low energy, long wavelength (soft) radiation to pass through, along with high energy radiation, to the object. Low filtration is advantageous for low voltage X-ray work, including radiography of thin metal sections not exceeding 0.25 inch of aluminum or equivalent, and low density composite materials. For these applications, the use of glass windows, moreover, does not afford the required sensitivity for viewing low density fibers. If desired, tubes can also be equipped with high absorptive diaphragms to limit the extent of the X-ray beam. In applications requiring maximum X-ray penetration, special filters, usually made of copper, can be added at the tube window to eliminate the low energy, soft X-rays. Further discussion on the use of diaphragms and filters will be included in a later section.

## Gamma Rays

Gamma rays are produced when the nuclei of radioactive isotopes disintegrate. An isotope is dissimilar to its parent element in that it has a different atomic

weight due to a different number of neutrons. The number of protons, or atomic number, is the same. Isotopes with excessive neutron differences are inherently unstable and release energy in the form of gamma rays, alpha particles and beta particles as they disintegrate. Of these, the penetrating powers of alpha and beta particles are negligible, and only the gamma rays are useful in radiography.

While some natural elements such as radium are inherently unstable and radioactive, man-made radioactive isotopes can be created. Cobalt 60, thulium 170, and iridium 192 are isotopes used in radiography and are created by bombarding their parent elements with neutrons. A second method of creating an artificial radioactive isotope is through a by-product of nuclear fission. Cesium 137 is an example of this process. The number assigned to each of these isotopes denotes its mass number and distinguishes it from its parent element and other isotopes of the same element.

An important distinction between gamma and X-rays is the spectrum of wavelengths generated. While X-rays are produced over a broad band of wavelengths as shown in Figure 3, gamma ray sources emit rays of only certain discrete wavelengths characteristic of the isotope, as shown in Figure 6. Gamma rays are usually specified in terms of their energy of radiation rather than by wavelength. For example, cobalt 60 emits radiation at only two discrete energy levels, 1.17 MeV and 1.33 MeV, with corresponding wavelengths of approximately 0.01 angstroms. It has a penetrating power (hardness) roughly equivalent to that of a 2 MeV X-ray machine, and is used to radiograph steel, copper and other medium-weight metals up to 9 inches thick.

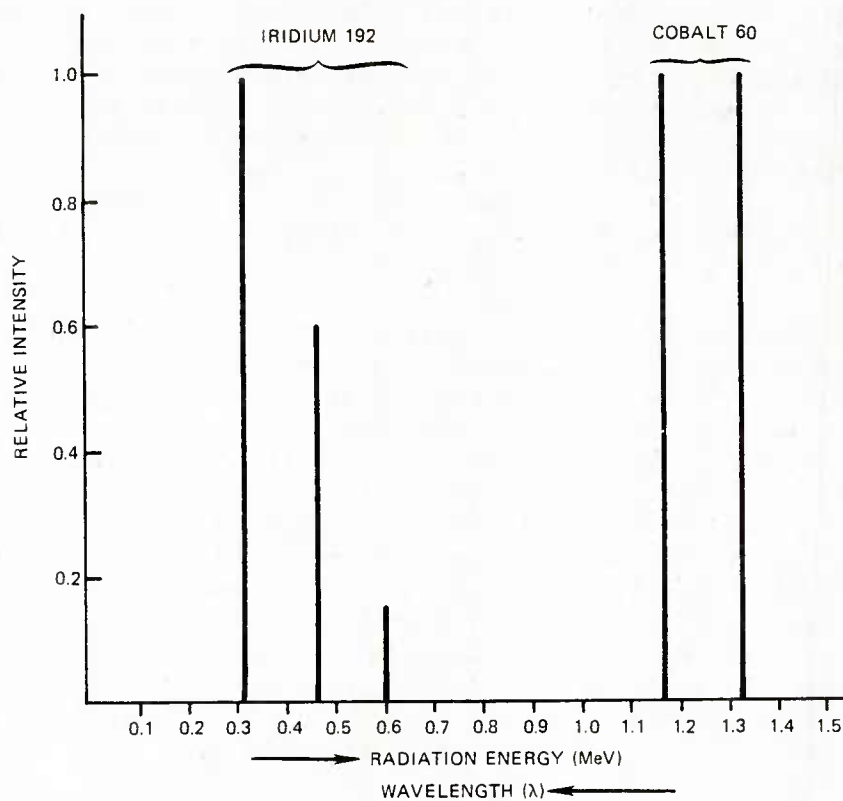


Figure 6. Gamma ray spectrums of Cobalt 60 and Iridium 192.

Since gamma rays are available only at discrete energy levels, the radiation quality (hardness) cannot be varied as was the case with X-rays. If softer, less penetrating gamma rays are required, another isotope such as iridium 192 would have to be selected. Iridium 192 emits radiation principally at 0.31, 0.47, and 0.60 MeV, which corresponds to wavelengths from 0.04 to 0.02 angstroms (higher energies producing shorter wavelength rays). It is roughly comparable in penetrating power to a 600 kV X-ray machine and is used to radiograph medium weight metals from 0.25 to 3.0 inches thick.

The intensity of gamma radiation reaching an item under investigation is dependent upon the source activity, the distance between source and object, and time. The source activity (amount of radioactive material) is dependent upon the effectiveness of the fission process or neutron bombardment that creates the isotope. Source activity is measured in curies ( $3.7 \times 10^{10}$  disintegrations per second).

The effect of source-to-object distance upon radiation intensity conforms to the law of light, where intensity varies inversely with the square of the distance. Gamma ray intensity at the object, therefore, is given as the radiation emission activity over a given period of time at a fixed distance, and is measured in roentgens per hour at one foot (rhf).

Another factor to be considered is source size, since gamma radiation emitted in the center of the source can be absorbed (self-absorption) by the surrounding material. This is particularly true of those isotopes emitting low energy radiation. For this reason, small or moderate-sized sources of high radioactive concentration are preferable for most applications. The term "specific activity" is used to define radioactive concentration, and is usually expressed in units of curies per gram or curies per cubic centimeter. For the radiographer, specific activity and source size are important, since a smaller source will produce a sharper, more well-defined image.

In addition, it is also important to note that the source activity decreases with time. The length of time required for the activity of a radioactive isotope to decay to one-half of its initial strength is termed "half life" and is characteristic of a specific isotope. The decay rate is non-linear, and a dated decay curve, supplied by the isotope manufacturer, must be used to adjust exposure time calculations over the life of the isotope.

Most isotopes used in radiography are right cylinders whose diameter and length are approximately equal. For this reason any surface can be used as the focal spot since all surfaces emit rays over an equal area.

The following is a brief description of the most common sources used in gamma radiography together with some of their characteristics and applications.

#### a. Radium

Radium is a natural radioactive element with a half-life of 1600 years. Radium itself does not produce useful gamma rays but through decomposition produces radon, a radioactive gas, and other radioactive daughter products. It is the disintegration of these that produces useful gamma rays. By the encapsulation of the radon gas, a constant rate of gamma ray emission can be produced. However, because of its low specific activity, radium is little used in industrial radiography.



b. Cobalt 60

Cobalt 60 is an artificial isotope, created by neutron bombardment of cobalt, with a half-life of 5.3 years. It can be used for the investigation of steel, copper, brass, and other medium-weight metals ranging in thickness up to 9 inches. Because of its intensity and penetrating ability, it requires heavy shielding with corresponding handling difficulties.

c. Iridium 192

Iridium 192 is another artificial isotope created by neutron bombardment with a half-life of approximately 75 days. It is used to radiograph steel and other similar metals from 0.25 to 3.0 inches thick. Because of this lower radiation energy level, lower penetrating ability and higher specific activity, it is relatively easy to shield, more portable, and more easily handled. It is obtainable in the form of a small-capsuled pellet providing a small focal spot producing sharp, well-defined images.

d. Thulium 170

Thulium 170 is created by neutron bombardment of thulium and has a half-life of approximately 130 days. It emits radiation only at the 84 keV and 52 keV energy levels, which are soft rays similar to X-rays generated in the 50-100 kV range. It is most widely used in the radiography of thin medium-weight metals up to 0.5 inch thick, or for light-weight metals and other materials of low density such as composites. Because of its soft radiation, it requires only light shielding and is therefore extremely portable and easy to handle.

e. Cesium 137

Cesium 137 is a by-product of the fission process and has a half-life of 30 years. It emits gamma radiation at the 0.66 MeV level, which consists of hard, penetrating rays similar to the radiation of a one MeV X-ray machine. It is used to radiograph steel and other medium-weight metals from 1.0 to 2.5 inches thick. Due to its high strength and penetrating ability, cesium 137 requires heavy shielding and is therefore very difficult to handle.

Radiation from radioactive materials producing gamma rays cannot be shut off, nor can it be regulated. For this reason, gamma ray equipment is designed primarily to provide safe storage and remote handling capabilities of the radiation source. The United States Nuclear Regulatory Commission (USNRC) and various state agencies prescribe safety standards for the storage and handling of radioisotopes under their control. For example, the USNRC recommends double encapsulation of cesium 137 in containers constructed of silver-brazed stainless steel. The positioning of the source during an exposure is accomplished with remote handling equipment called isotope cameras, which position the source through the use of various types of cable-and-reel assemblies.

The selection of an appropriate gamma ray source, with its characteristic strength and penetrating ability, and of the appropriate handling equipment, is often difficult to make. The choice will depend on a number of variables, among which are the size, thickness, density, and accessibility of the item under investigation, and

the allowable exposure time and shielding measures required. Each item investigation calls for a thorough understanding of the variables involved and a reliance on accumulated past experiences.

### SECTION 3. MAKING A RADIOGRAPH

A radiograph image is imparted onto film in much the same manner as a shadow is cast from a light source past an object onto a flat surface; that is, a radiograph is essentially a shadow graph. The important difference between a shadow and a radiograph is that in radiography, the radiation penetrates and passes through the object, thereby creating not only a peripheral outline, but also an image of the internal structure of the object. In so doing, radiation is differentially absorbed and scattered, causing variations in film density (blackness) and image clarity. The radiographer seeks to optimize the readability of a radiograph by controlling the distribution of film density and creating a clearly defined image. In order to do this, he must have a thorough understanding of some basic concepts of image formulation, and a basic knowledge of some of the factors relating object and film radiation effects to image quality. This includes a study of geometric spacial relationships, the effect of object shape and density, and the effect of film properties on radiation as it travels from its source into and through the object and into the film emulsion. It is therefore advisable to discuss the factors involved in making a quality radiograph by separating them into geometric, object, and film variables. Later in Section 4, the effects of these variables will be interrelated and shown to be the primary factors in formulating a correct radiographic exposure. Before proceeding, however, it is necessary to briefly define the term "exposure" or "radiographic exposure." In general, the term "exposure" means the subjection of a recording medium to radiation for the purpose of producing a latent image. More specifically, exposure is defined as the product of the intensity of radiation reaching the film and the time over which it acts. Mathematically,  $E = Mt$ , where  $E$  is the exposure,  $M$  the radiation intensity, and  $t$  the exposure time. As discussed earlier, the radiation intensity,  $M$ , for X-rays is proportional to the tube current, and for gamma rays it is dependent on the source strength. For X-rays, therefore, the units for exposure are milliamper-minute or milliamper-seconds, and for gamma rays, millicurie-minutes or millicurie-hours. Notice that, with all other variables held constant, the amount of exposure necessary for a required image density can be obtained from numerous combinations of radiation intensity,  $M$ , and exposure time,  $t$ , provided their product is unchanged.

#### Geometric Factors

In establishing the optimum radiographic set-up, it is important to understand the effects of the spacial arrangement of the object, source, and film, as well as the effects of source size. Figures 7, 8, and 9 indicate the effects of these variables on the image imparted by a simple disc-shaped object.<sup>1</sup> Figure 7 indicates the effects of varying the source-to-object and object-to-film distances. Minimizing the object-to-film distance (Figures 7A and 7B) improves image sharpness by reducing penumbral shadows, and minimizes object enlargement. Image sharpness (see Figure 7C) is also improved by maximizing the source-to-object distance. In general, therefore, the object should be in intimate contact with the film, unless prohibited by the shape of the object, and the source should be as far as possible from the film. Keep

1. Army Materiel Command Pamphlet, *Quality Assurance Guidance to Nondestructive Testing Techniques*, AMCP-702-10, April 1970, p. 30-31.

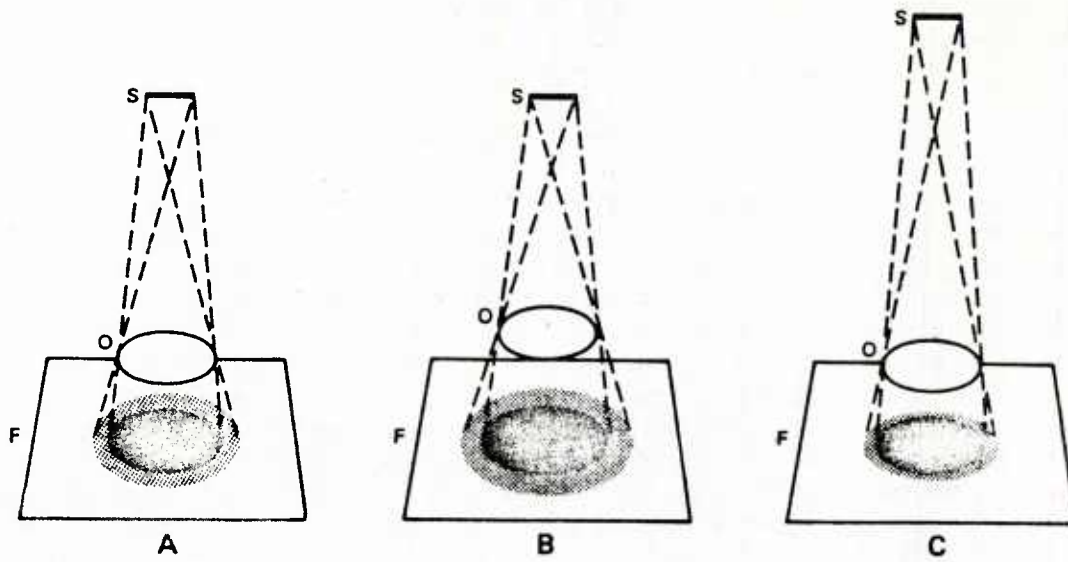


Figure 7. Image sharpness, penumbral shadow.<sup>2</sup>

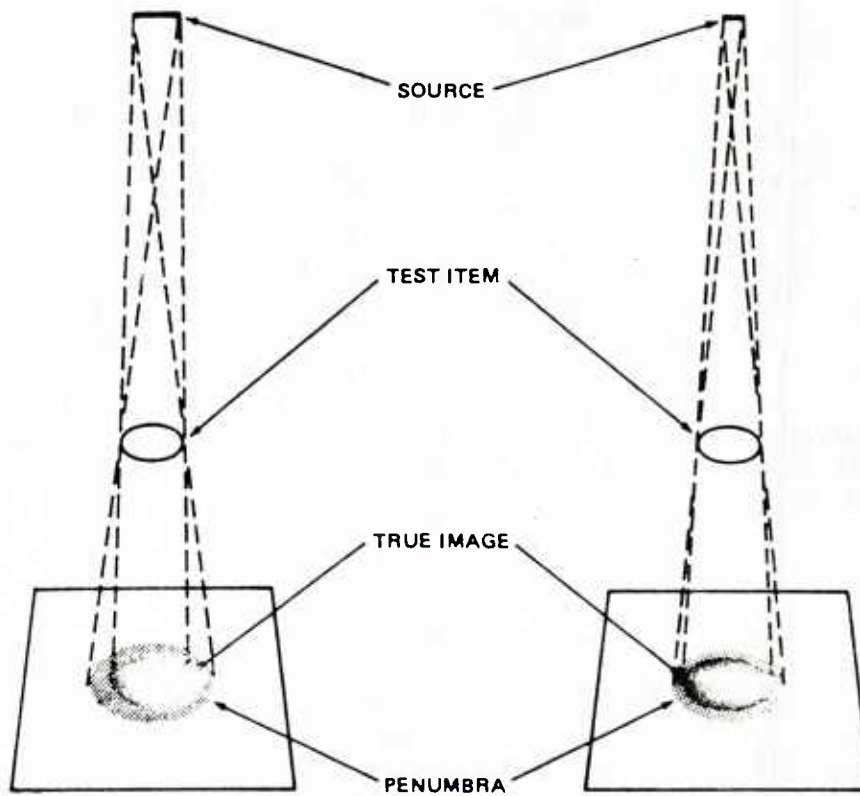


Figure 8. Effect of source size on image sharpness.<sup>2</sup>

2. Army Materials and Mechanics Research Center, DARCOM Training Handbook 5330.19, Radiographic Inspection, p. 2-17.

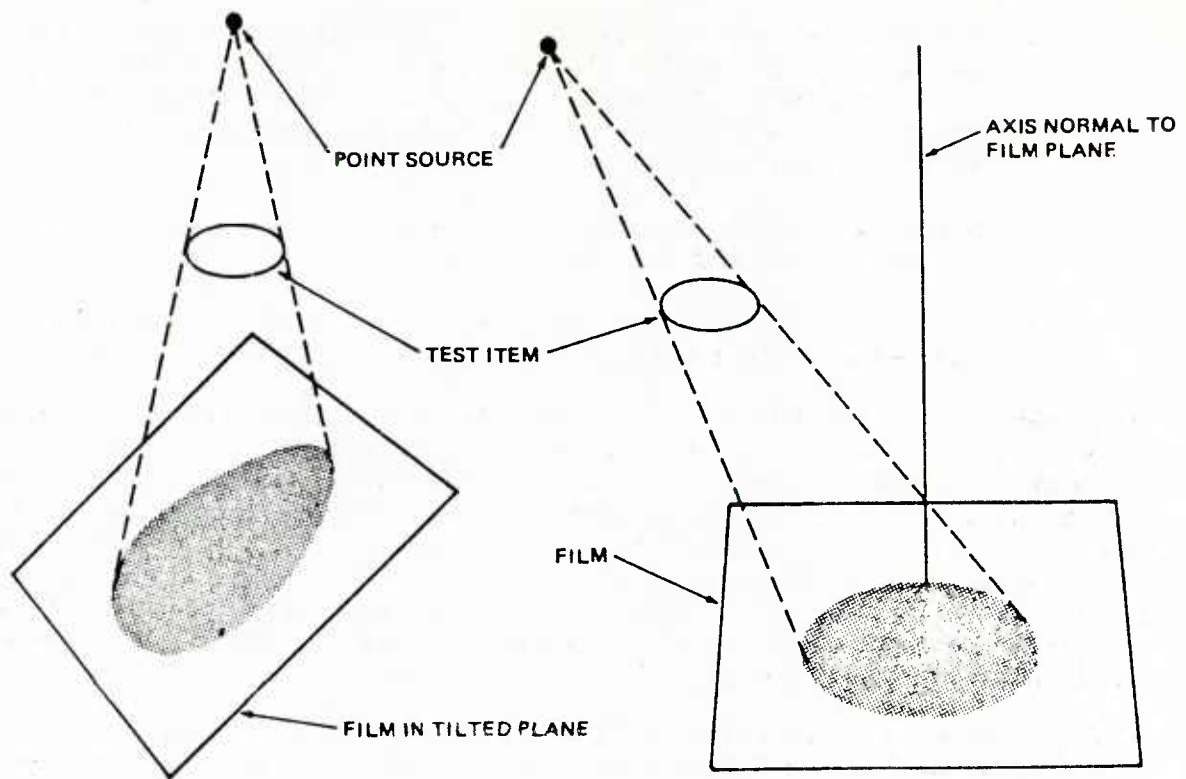


Figure 9. Angular image distortion.<sup>2</sup>

in mind, however, that increasing source-to-film distance decreases the intensity of radiation striking the object and its image-forming ability. The source-to-film distance, therefore, can only be maximized to an amount limited by the source strength.

Figure 8 indicates the effect of source size on image sharpness. The smaller the source, the sharper the image produced. As the source size increases, each point of the source emits its own radiation, producing overlapping images, resulting in a larger penumbral shadow. While a smaller source (gamma ray isotope) or smaller effective focal spot (X-ray anode) improves image sharpness, it also limits radiation intensity. A minimum source size is therefore governed by the source strength required for image formation and the characteristics of the gamma isotope or anode target material.

Figure 9 shows the effect of deviating from the prescribed perpendicular source-object-film spacial relationship. If the film is tilted, or if the source is displaced from the normal to the film plane, the object image will be distorted. Note that image distortion is an angular effect, independent of the factors contributing to image sharpness, and that both can be optimized by adherence to the following:

1. The source size, or focal spot size, should be as small as possible while producing the required radiation intensity.
2. The object-to-film distance should be as small as possible, maintaining intimate contact whenever practical.



3. The source-to-object distance or source-to-film distance should be as large as possible. Large source-to-film distances are particularly helpful when radiographing thick objects in order to minimize geometric unsharpness produced by parts of the object furthest from the film.
4. The source should be oriented as nearly perpendicular to the film as possible to reduce spacial distortion.
5. For objects of uneven shape, the area of major interest should be maintained as parallel as possible to the film plane.

In radiography, the term "definition" refers to the clarity and sharpness of image details. It is generally used qualitatively in reference to the outline of an object and to its internal structure as recorded on film. The preceding five geometric guidelines, while particularly important in improving definition, are not sufficient alone; they must be combined with the proper selection of source and film variables. In addition, the decision of whether to use radiographic filters or screens will also affect image definition. These decisions are primarily dependent on the size and density of the object being radiographed, and will be discussed in detail later in Section 4, Exposure Formulation.

Another term used in radiography to define the width of peripheral, fuzzy shadow is "geometric unsharpness" (see Figure 10). A simple analysis of similar triangles leads to the following relationship:

$$U_g = f (d/D),$$

where  $U_g$  is geometric unsharpness,  $f$  the source size,  $d$  the object-to-film distance, and  $D$  the source-to-object distance. Distances are taken from the source side of the specimen. Note that the units of  $U_g$  will be the same as those for source size,  $f$ , usually stated in millimeters, and that the units used for the measurement of  $d$  and  $D$  must be the same, either inches or millimeters.

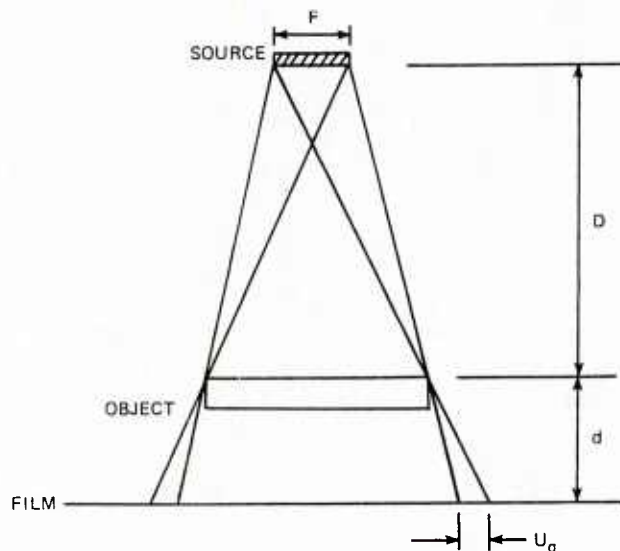


Figure 10. Geometric unsharpness.<sup>2</sup>

In the preceding discussion, it has been stated that, with a constant source strength, radiation intensity striking an object decreases as the source-to-object distance increases. However, this relationship is not linear, but varies as the distance squared. In radiography, the Inverse Square Law is given as follows:

$$\frac{M_1}{M_0} = \frac{D_0^2}{D_1^2}$$

The inverse square relationship (see Figure 11) is due to the fact that the divergent radiation beam intercepts an increasingly larger area as distance increases, with a corresponding lessening in intensity.<sup>2</sup>

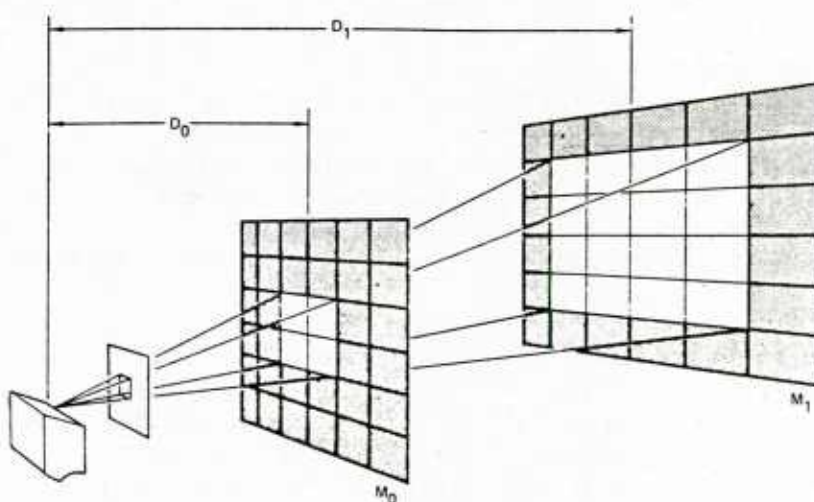


Figure 11. Diagram of the Inverse Square Law.<sup>2</sup>

Table 1. RADIOGRAPHIC EQUIVALENCE FACTORS

| MATERIAL  | X-RAYS KV |      |      |      |      |      |      | GAMMA RAYS |        |       |
|-----------|-----------|------|------|------|------|------|------|------------|--------|-------|
|           | 50        | 100  | 150  | 220  | 400  | 1000 | 2000 | Ir 192     | CE-137 | CO-60 |
| MAGNESIUM | 0.6       | 0.6  | 0.05 | 0.08 |      |      |      | 0.22       | 0.22   | 0.22  |
| ALUMINUM  | 1.0       | 1.0  | 0.12 | 0.18 |      |      |      | 0.34       | 0.34   | 0.34  |
| TITANIUM  |           | 8.0  | 0.63 | 0.71 | 0.71 | 0.9  | 0.9  | 0.9        | 0.9    | 0.9   |
| STEEL     |           | 12.0 | 1.0  | 1.0  | 1.0  | 1.0  | 1.0  | 1.0        | 1.0    | 1.0   |
| COPPER    |           | 18.0 | 1.6  | 1.4  | 1.4  | 1.1  | 1.1  | 1.1        | 1.1    | 1.1   |
| ZINC      |           |      | 1.4  | 1.3  | 1.3  | 1.1  | 1.0  | 1.1        | 1.0    | 1.0   |
| BRASS     |           |      | 1.4  | 1.3  | 1.3  | 1.2  | 1.2  | 1.1        | 1.1    | 1.0   |
| LEAD      |           |      | 14.0 | 12.0 |      | 5.0  | 2.5  | 4.0        | 3.2    | 2.3   |

## Object Effects

As radiation penetrates an object, part of it is absorbed, some is scattered, and the remainder passes through unobstructed. The undeviated, primary radiation reaching the film forms the object image, and it is this differential absorption-transmission effect which causes variations in film blackening and makes radiography possible. Scattered secondary radiation also reaches the film, but it is not image-forming, and serves only to fog a radiograph. This is a problem which radiographers must acknowledge and control as much as possible.

The amount of primary radiation reaching the film depends in part upon the level of radiation energy, and can be controlled either by varying the voltage at the X-ray tube, or by selecting a proper gamma ray source. As was discussed earlier, both higher voltage X-rays and gamma ray sources of high discrete energy levels produce more penetrating radiation. The amount of radiation absorbed depends, as expected, upon the thickness and density of the object (Figure 1). Moreover, for industrial metallic materials, absorption also depends on the internal atomic structure of the object material. The influence of atomic number and material composition on radiation absorption is known to be more important than either thickness or density for these particular materials. This effect, while complex, has received thorough investigation resulting in empirically determined radiograph equivalence factors as shown in Table 1.<sup>2</sup>

A careful review of the factors in Table 1 points out that the differences in material absorption properties decrease as kilovoltage increases, indicating less dependence upon atomic structure. This fact, while important for radiography of high density materials at high voltages, has little bearing on the radiography of composites, which are of low to medium density, and therefore are radiographed at low voltage. Radiographic equivalence factor tables do not exist for composite materials. However, the equivalence factor for a particular material at a chosen energy is easily calculated from mass absorption value for the constituent materials.

Another term generally used in radiography, "half-value layer" (HVL), refers to the thickness of a specified substance which, when introduced into the path of a given beam of radiation, reduces its intensity to one half its original amount. The half-value layer, therefore, is not simply half the thickness of the object, but depends upon the intensity of the radiation used, as well as the density, composition and internal atomic or molecular structure of the material. Figure 12 shows an example where the same object is radiographed using low and high energy radiation. In Figure 12a, assuming that, with low energy, the half-value layer is  $d$ , the transmitted radiation intensities would be  $I_0/16$  and  $I_0/4$  through the thick and thin portions respectively (a contrast of 4-to-1), where  $I_0$  is the incident radiation intensity. In Figure 12b, assuming that the incident radiation energy is increased (producing more hard radiation) so that the half-value layer becomes  $2d$ , the transmitted radiation would then be  $I_0/4$  and  $I_0/2$  respectively, reducing contrast to 2-to-1. In radiography, the ratio (or logarithm of the ratio) of the highest-to-lowest radiation intensities transmitted by selected portions of the specimen is termed "subject contrast." In general, therefore, radiographs should be made with the lowest energy level possible which will both produce sufficient penetration and result in improved subject contrast, while exposure (milliampere-minutes) should be sufficient to produce adequate film blackness, or density. Areas which are too light for adequate flaw detection, such as the thicker portion shown in Figure 12a, should receive greater exposure while maintaining low radiation intensity. This will not alter the high overall subject contrast,



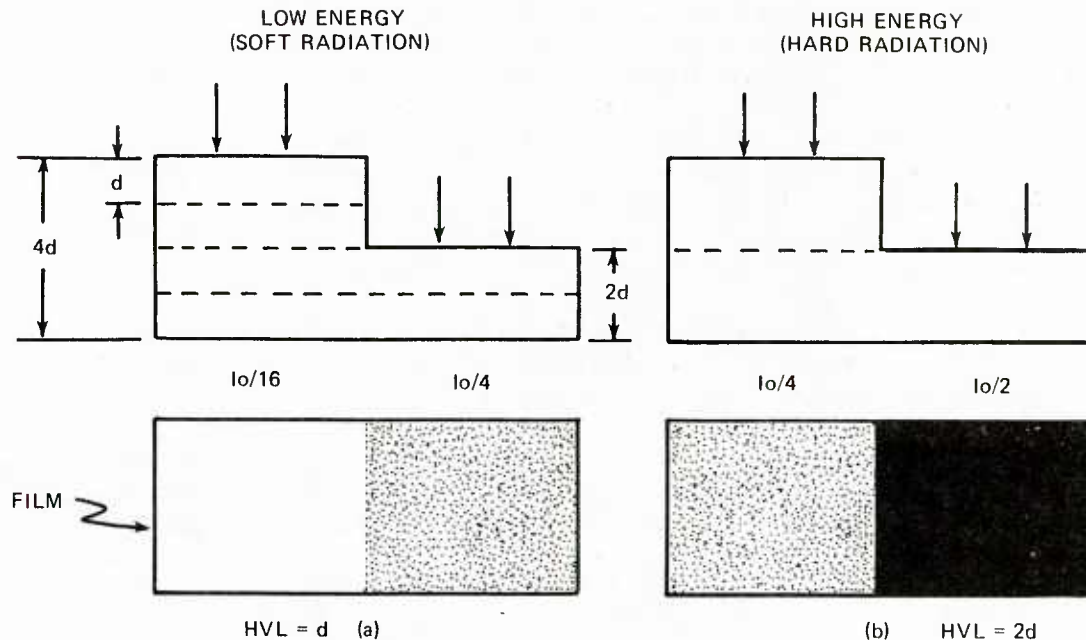


Figure 12. Half value layer (HVL).

but rather increase overall density and detection ability. Consideration should also be given to taking more than one radiograph when shooting objects of large thickness or density variations. This would allow the radiographer to use optimum settings for different portions of the object to obtain the definition needed for flaw detection. Later, the discussion will be directed to "film contrast" and the combined effects of both subject and film contrast on radiographic contrast, image quality and detecting ability.

### Scattered Radiation

As discussed earlier, when electromagnetic radiation penetrates an object, much of it passes through, but a large part of it is either absorbed or scattered as it comes in contact with the atoms of the material. The problem of scattering is a phenomenon of both X-rays and gamma rays. In the following discussion, differential absorption and scattering will be presented in terms of X-rays, but the same general phenomena occur also with gamma rays.

X-rays have no mass or weight, but rather can be considered packets of energy (photons) which travel at the speed of light. As they come in contact with object material atoms, energy is either partially or totally lost by various processes. During these processes, energy is transferred to the material atoms. As a result, orbiting electrons are set free to move about randomly with different velocities and directions. These free electrons then collide with the surrounding matter and generate secondary X-rays. These secondary X-rays are a minor component of what is termed scatter radiation or "scatter." The major component of scatter is low energy radiation, which is produced as higher energy radiation and is weakened during the scatter process. Scatter radiation, therefore, is of uniformly low-level energy content and random direction. It is non-image-forming and serves only to fog the radiograph.

In the radiography of composites, which are comprised of low and medium density materials, scattered radiation forms a high percentage of the total radiation reaching the film. This is due to the nature of the soft, low voltage radiation used to radiograph these materials, which is inherently less penetrating and more subject to scatter. However, if higher, more penetrating voltages were used, excessive overall film density could occur, resulting in reduced contrast and a radiograph unreadable in terms of flaw detection. Scatter is, therefore, a major problem when radiographing composites. In general, this presents a paradox for the radiographer since, as we have seen, low voltages are desirable for improving subject contrast, but lead to fogging of the image due to scatter, which, in turn, reduces subject contrast. Later we shall discuss some of the commonly used methods of reducing the effects of scattered radiation in radiographs of industrial metallic materials and the application of these methods to the radiography of composites.

As might be expected, internal scatter arising within the object itself is the major source of scattered radiation affecting image quality. For specimens of one thickness and density, scatter is generally uniform across the image, but with more complex shapes the effect of scatter is more pronounced. Figure 13 shows that internal scatter causes a blurring of the specimen outline and alters the image shape of the hole in the center.<sup>2</sup> Internal flaws such as voids, cracks, porosity and inclusions are also obscured, primarily by internal scatter.

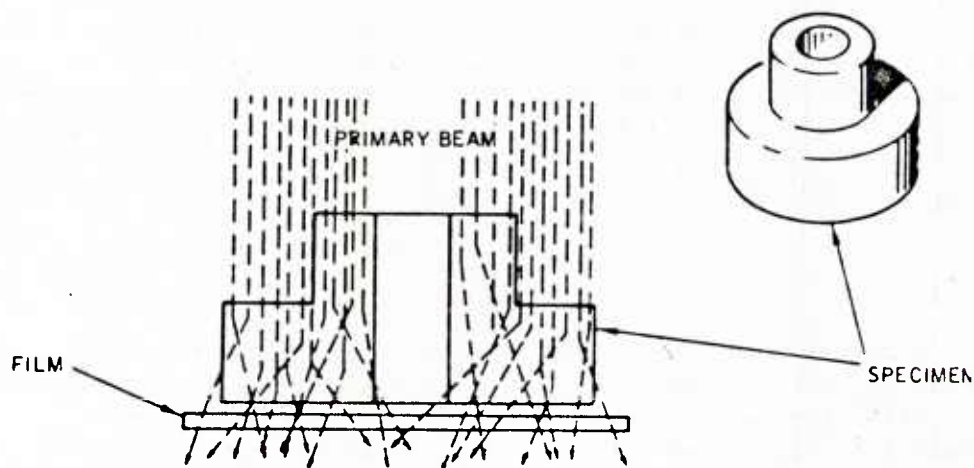


Figure 13. Internal scatter.<sup>2</sup>

Another source of scattered radiation, side scatter (as shown in Figure 14), is scatter from walls or objects adjacent to the specimen, or from portions of the specimen itself.<sup>2</sup> Again, specimen outline is blurred by this type of scatter. One measure of the harmful image effects of scatter can be obtained by comparing the dimensions of the object itself with the dimensions of the radiographed image.

An additional source of scatter arises from objects such as floors, benches or tables beneath the specimen (see Figure 15).<sup>2</sup> This type of scatter usually occurs only when the film and specimen are not in contact with a supporting surface. It can easily be detected by attaching a lead letter "B" to the bottom of the film cassette; if a light B is produced on the radiograph, back scatter is present.

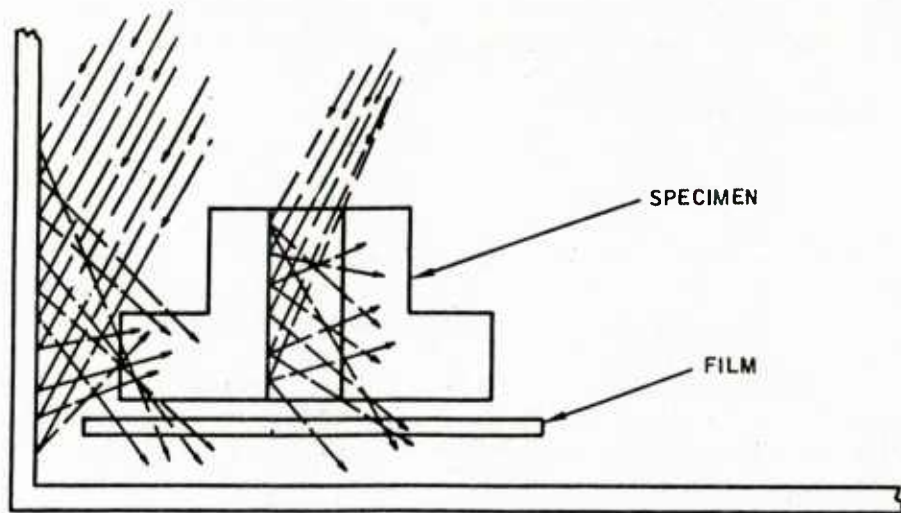


Figure 14. Side scatter.<sup>2</sup>

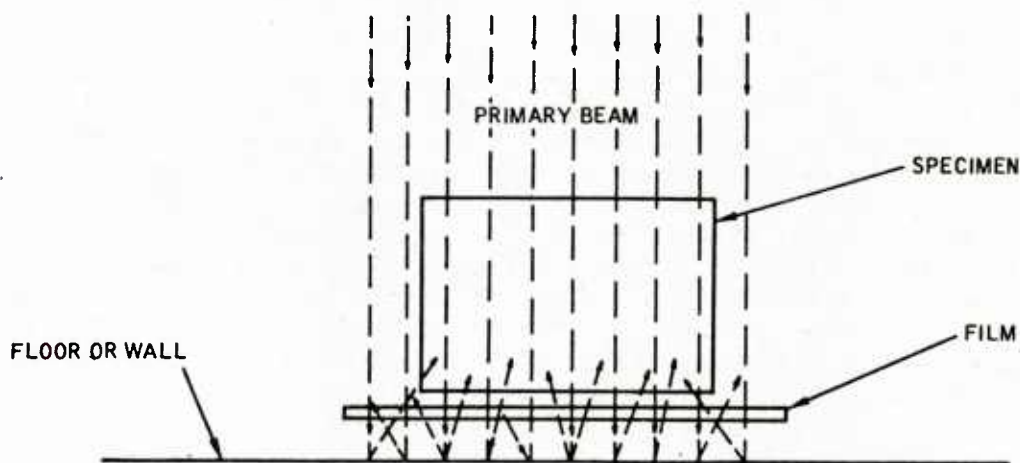


Figure 15. Back scatter.<sup>2</sup>

Another more indirect form of scatter occurs when the film holder or cassette extends beyond the edges of the specimen. As the cassette receives primary radiation, it becomes a source of scatter which can encroach upon the outline of the object image. This effect on image quality is termed "undercut" and can best be eliminated by using heavy density masking material. A discussion of masking techniques and other methods for controlling or eliminating scatter effects will be taken up later in Section 4. With specimens of complex shape, primary radiation can pass through a thin portion of a specimen adjacent to the edge and strike the film cassette, causing undercut scatter in the image outline. Yet another source of undercut is side scatter produced when two specimens are radiographed side-by-side on the same film. Scatter originating from the side of one specimen can intercept part of the edge of the other specimen and thereby cause an undercut effect.

The next section will present the effects of film variables on radiographic image quality, so that we might better understand the manner in which geometric, object, and film variables interact in the radiographic process, and how they can be properly selected and controlled

## Film Effects

Radiographic film is constructed of a base sheet of transparent cellulose material which is coated on one or both sides with a special gelatin emulsion containing microscopic silver halide salt crystals (primarily silver bromide). The emulsion is approximately 0.001-inch thick on either side of the base sheet. As X-, gamma, or visible light rays reach the emulsion, the silver halide grains become sensitized, and metallic silver is formed within the crystal. This is referred to as the latent image, since a subsequent development process is necessary to bring forth the final visible image.

The developing process can be carried out either by hand or automatic processing techniques, and should be accomplished following the recommendations of the film manufacturer. In general, the hand developing process consists of first immersing the exposed film in a chemical developer solution which reduces the radiation-affected silver halide salt crystals to black metallic silver, producing the radiographic image.<sup>3</sup> The unexposed halide crystals are left unaffected. Excessively long immersion will begin to reduce unexposed grains, causing uniform film darkening or fogging. The next step is the immersion of the film in a stop bath, and then in a fixer solution. The latter solution serves to harden the emulsion, making the image more permanent. The film is then rinsed in water and thoroughly dried.

The film is now ready for viewing in front of a high-powered illuminator capable of lighting either the entire film, or selected spot areas, at various light intensities. At this point, successful flaw detection inspection depends upon many factors -- the quality of the radiographic image, the quality of the illuminator, the skill and experience of the inspector, and the ability of the human eye to perceive differences in densities and flaw details as depicted on the radiograph. We will now turn our attention to the film variables affecting the quality of the radiographic image, but in a later section will return to some thoughts on how the human eye perceives and interprets a radiographic image, and the limitations on flaw detection ability.

We have been using the term density or film density as a quantitative measure of film blackening. More specifically, the amount of density is defined as the common logarithm of the ratio of the light intensity incident on the film to that transmitted through it, that is:

$$D = \log_{10} \frac{I_o}{I_t}$$

where D is the density,  $I_o$  is the incident light intensity and  $I_t$  is the transmitted light intensity. Notice that a density of 2.0 means that only 1/100 of the incident light has been allowed to pass through the emulsion. Density of a radiograph is measured with an instrument called a densitometer, which is capable of point-by-point readings of film blackening.

3. *Radiography in Modern Industry*. Eastman Kodak Co., 1979, p. 44-130.



Although film density increases continuously with exposure, the rate of increase in film density depends upon both the level of exposure and the type of film. Characteristic curves similar to those shown in Figure 16 are available from manufacturers for a wide variety of industrial and medical films, and are primarily used as a guide in film selection.<sup>4</sup> These curves are plots of film density versus the log of relative exposure, both being laid out on a linear scale. Relative exposure is used because there are no convenient units either to relate X-radiation quantities (milliamperere-minutes) to gamma ray quantities (millicurie-hours), or to take into account exposure variations due to kilovoltage, scattering effects, use of screens, etc. Therefore, the amount of film exposure is given in terms of a particular standard radiation quantity, established and agreed upon by film manufacturers, producing a relative scale. For radiographs which are to be taken under a different set of conditions, characteristic curves are used as a quantitative tool to adjust the preliminary exposure for changes in film type and desired density.

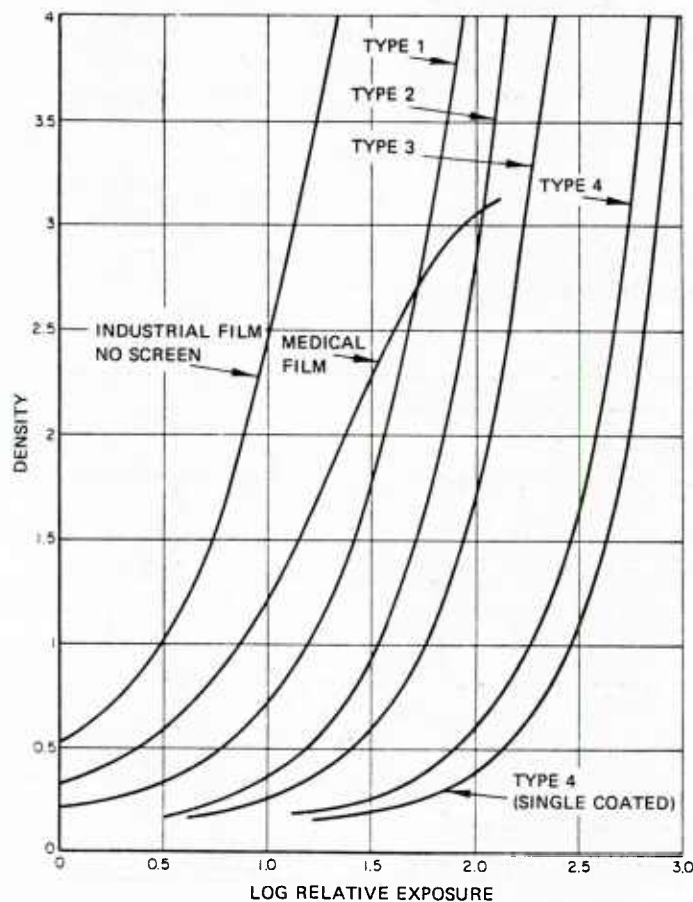


Figure 16. Characteristic curves of films used in industrial radiography.<sup>4</sup>

4. MIL-HDBK-333 (USAF), April 1974, p. 4-34.

Of particular importance to the radiographer is the capability of a particular type of film for detecting and recording film density differences in adjacent areas of a specimen (due to flaws, voids, inclusions, thickness, and matrix material density variations). It is this film density difference, or film contrast, which aids the human eye in distinguishing small imperfections. The ASTM defines film contrast as "a qualitative expression of the slope or steepness of the characteristic curve of a film; that property of a photographic material which is related to the magnitude of the density difference resulting from a given exposure difference."<sup>5</sup>

The importance of film contrast for detection ability is demonstrated by Figure 17, which indicates the film density differences recorded at two portions of a specimen.<sup>6</sup> A specimen similar to that shown in Figure 12 was radiographed at both low and high exposure levels. The amount of exposure reaching the film through the thick and thin portions of the specimen are  $E_A$  and  $E_B$  respectively, with the average film exposure level given as  $E_1$  or  $E_2$ . We see that the film density difference, or film contrast, is far greater at a high exposure ( $E_2 > E_1$ ) and that the presence of a flaw can thus be detected much more clearly. Moreover, at a low exposure, the film contrast may be so small as to approach the lower limit of the eye's ability to detect tonal differences. The radiographer can thus make most use of inherent film contrast capabilities by exposing the film to the highest densities readable with available illumination. In addition, if we recall that overall radiographic contrast is a combination of both film and subject contrast, we can think of film as a contrast amplifier. In general, a quality readable radiograph can best be produced by using the lowest voltage necessary for specimen penetration, together with an exposure sufficient to produce high readable densities. This will yield good subject and film contrasts and provide optimum detection ability.

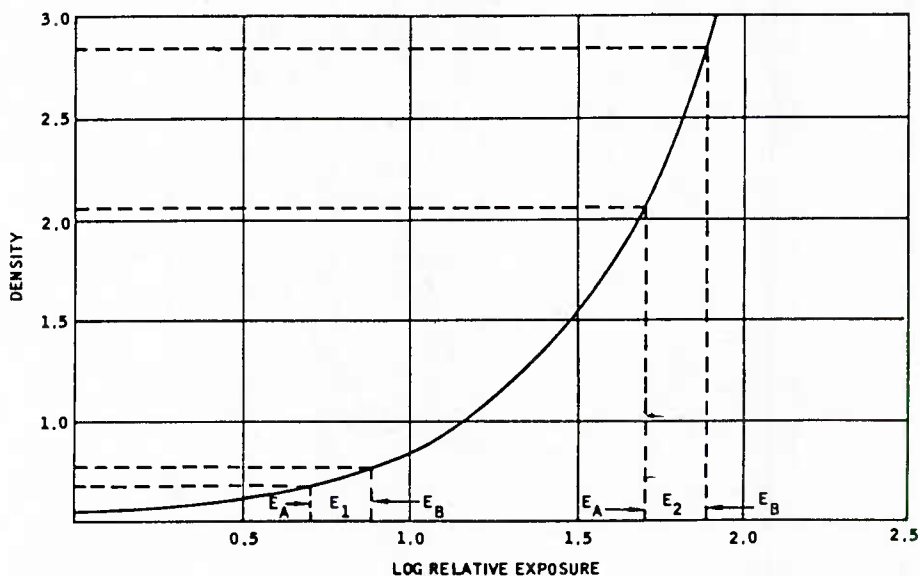


Figure 17. Film characteristic curve.<sup>6</sup>

5. *Standard Definitions of Terms Relating to Gamma X-Radiography*. Annual Book of ASTM Standards: Part 11, ASTM DES: E586-76, p. 630-631.

6. Army Materials and Mechanics Research Center, DARCOM Training Handbook 5330.19, Radiographic Inspection, p. 4-6, 6-30.

As we can see in Figure 16, the slope of a characteristic curve is continuously changing; the steeper the slope of the curve, the greater the film contrast and, therefore, the greater the flaw detection ability. For most films, the film contrast is greatest at higher densities. An exception to this is medical film, which exhibits maximum slope at mid-density range. This allows maximum contrast to be gained at lower exposures, an important consideration in medical applications. This benefit of reduced exposure, however, is accompanied by some loss of definition and requires specialized techniques to achieve a quality image. This type of film is only occasionally used in industrial radiography but has good potential for application to radiography of composites. Notice also in Figure 16 that the shapes of the curves (with the exception of the medical film) are quite similar, with only slight shape differences in the lower density portions. Increasing density is primarily dependent upon increasing amount of exposure, and there is no shape dependence on radiation quality (kilovoltage).

The location of the curve along the horizontal axis is a measure of another important film characteristic, film speed, that is, the relative amount of exposure needed to produce a desired film density. Film speed is inversely proportional to exposure for a fixed level of film density. High-speed films, such as type 1 and medical, require less exposure, while low-speed films, such as type 3 or 4, require more exposure to achieve the same density.

The mechanism that determines film speed depends primarily upon the size of the silver halide grains in the film emulsion and, to a lesser degree, upon the radiation quality (energy). High-speed, fast films contain relatively coarse grains (up to 0.001 mm or 0.0004 inch in diameter), while low-speed, slow films contain finer grains. When exposed to radiation, the larger grains are simply more likely to be sensitized, resulting in greater ability to produce film blackening. This increase in film speed with grain size, however, also results in a loss of radiographic definition and ability to detect details. The choice of film type is, therefore, a trade-off between radiographic quality and ease of exposure.

Another factor affecting the quality of a radiograph is the phenomenon of graininess. The ASTM defines graininess as "the visual impression of irregularity of silver deposit in a processed film."<sup>5</sup> Graininess often occurs when fast, coarse-grained film is exposed using high kilovoltage radiation. Under these conditions, exposed silver halide grains are most likely to form clumps of blackening, resulting in the visual impression of graininess, readily observable by the unaided human eye. This impression cannot arise from the reduction of individual silver halide grains, since their microscopic size (including that of even the coarsest grains) is far below the limits of unaided human vision. The fact that high kilovoltage radiation exposes several adjacent grains only partially accounts for its occurrence. The predominant factor contributing to graininess is that, upon exposure, silver halide grains are reduced to metallic silver in a random fashion over the area of the film, even when acted upon by a uniform radiation beam. Faster, coarse-grained films, requiring fewer absorption events, tend to exhibit a more uneven distribution of densities, whereas slower, finer-grained films tend to even out the random distribution effect, reducing observable graininess. Due to the random nature of this phenomenon, graininess will not necessarily always occur, but is statistically more apt to arise when coarse-grained film is exposed to high kilovoltage radiation.



Since graininess is a visual impression, a deviation from the normal development procedure by increasing either development time or temperature will result in greater observable film graininess. The use of fluorescent screens affects both film graininess and exposure, and will be discussed more fully in a later section.<sup>3</sup>

We have thus far examined the geometric, object, and film variables affecting the production of a quality radiograph. It is now apparent that while a change in each variable will produce a specific effect, beneficial or otherwise, a definite interrelationship exists among them which must be thoroughly understood by the radiographer. In particular, the selection of film based on a need for high contrast and good definition must be carefully considered along with film speed and graininess effects, faster films with larger grains offering more speed and economy along with poorer resolution and a greater chance of graininess occurring. A wide variety of films is available from film manufacturers to meet specific needs and requirements, and their recommendations for applications should be followed.

#### SECTION 4. EXPOSURE FORMULATION

In the previous sections, discussions centered on each of the primary variables involved in making a radiograph in order to highlight their cause and effect relationships. Since there are many variables involved which must all be optimized for each investigation, the radiographer must rely upon data provided by film manufacturers and isotope suppliers, as well as data recorded from his own past experiences. This information is generally presented in the form of charts, graphs, and tables, including film characteristic curves similar to those in Figure 16, radiographic equivalence factor tables as shown in Table 1, X-ray and gamma-ray exposure charts<sup>6</sup> similar to those in Figures 18, 19, and 20, and dated decay curves for gamma isotopes<sup>6</sup> similar to Figure 21.

When a radiographer sets out to produce a radiograph for a particular material specimen, he selects an appropriate radiation source, type of film, a reasonable source-to-film distance, and decides whether or not to use radiographic screens. (A discussion on the use of screens and other image enhancement techniques will be presented later.) Then, knowing the specimen thickness (or average thickness for a specimen of complex shape) and selecting a density level as required for high film contrast, he can use an X-ray exposure chart (or gamma ray exposure chart and isotope decay curve) prepared for the specific conditions selected to arrive at his preliminary settings. The radiographer uses the exposure chart prepared under conditions which most closely approximate those of his ongoing investigation, adjusting the preliminary settings obtained to account for the differences. In the case of X-radiography, the exposure chart allows him to choose kilovoltage, amperage and time settings (see Figure 18 or 19). For gamma radiography, with a value of source strength obtained from the isotope decay curve (see Figure 21), he must simply calculate an exposure time using the exposure factor obtained from the gamma ray exposure chart (see Figure 20). Therefore, once a series of exposure charts and isotope decay curves has been established for the specific X-ray machine and gamma isotopes to be used, it is a simple matter to select preliminary exposure settings. What must be understood, however, is how the exposure chart is produced, the limitations on its application, and how to adjust preliminary exposure settings to meet the conditions and image quality requirements of a particular investigation.

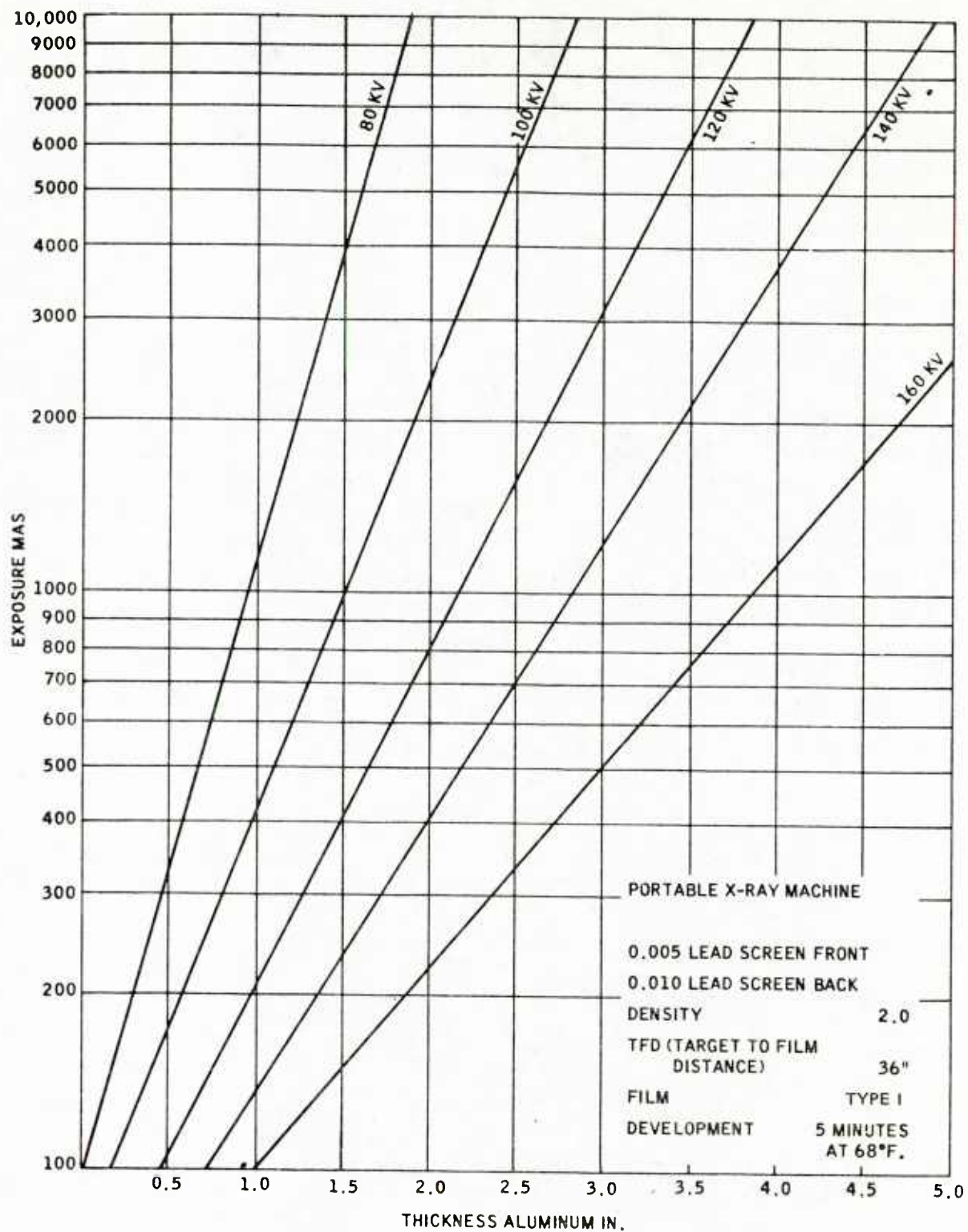


Figure 18. X-ray exposure chart.<sup>6</sup>

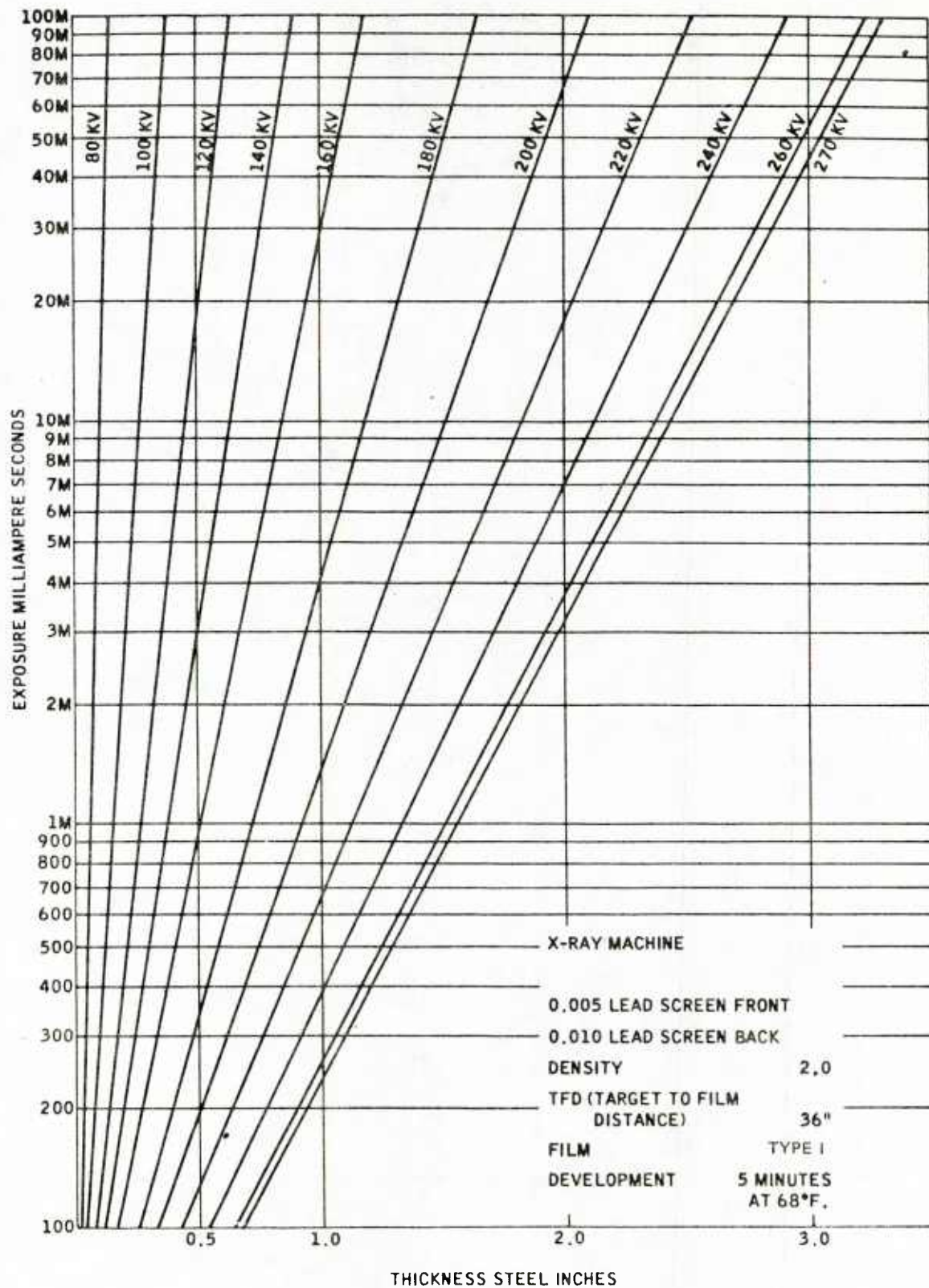


Figure 19. X-ray exposure chart.<sup>6</sup>

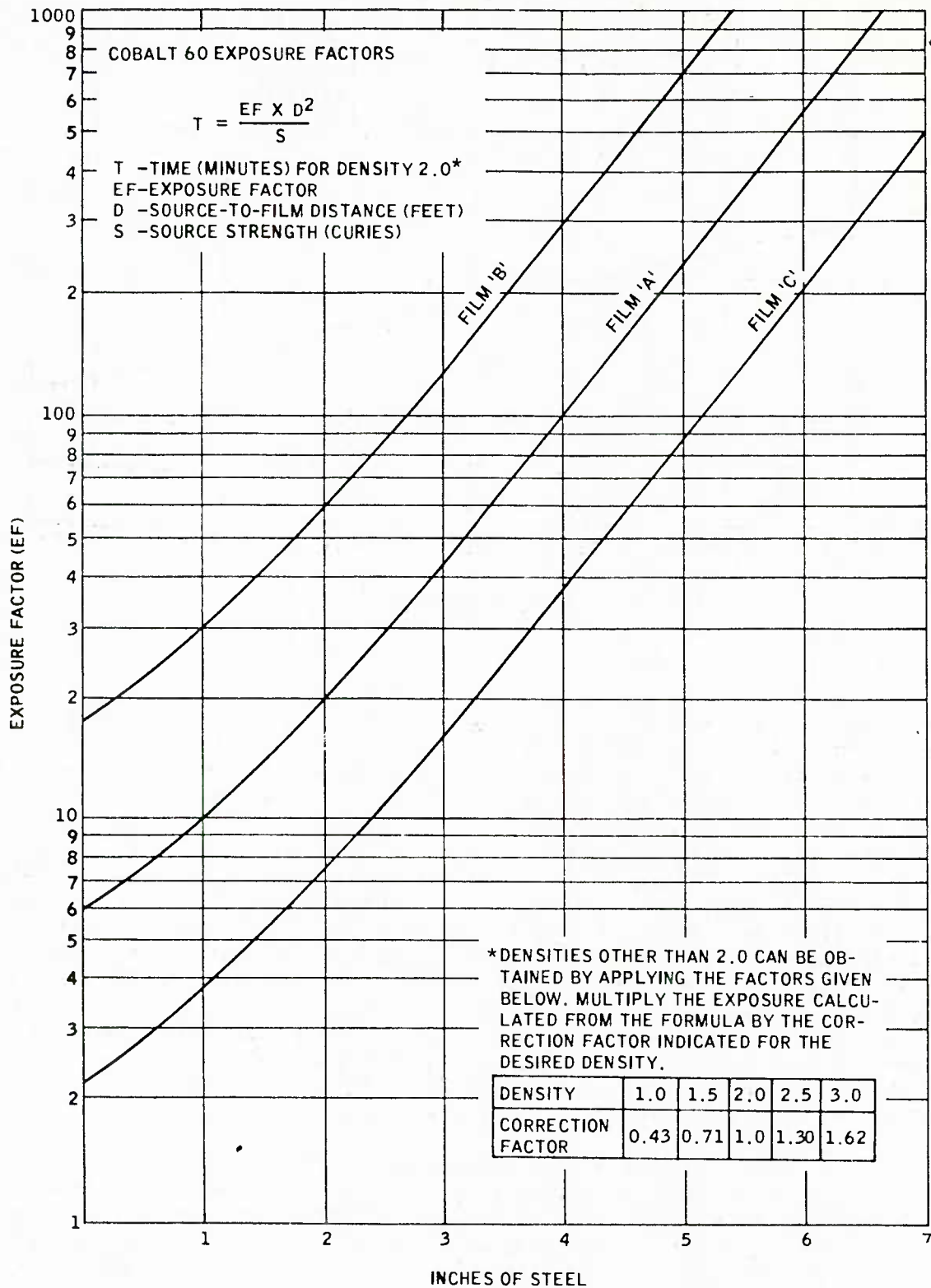


Figure 20. Gamma ray exposure chart.<sup>6</sup>



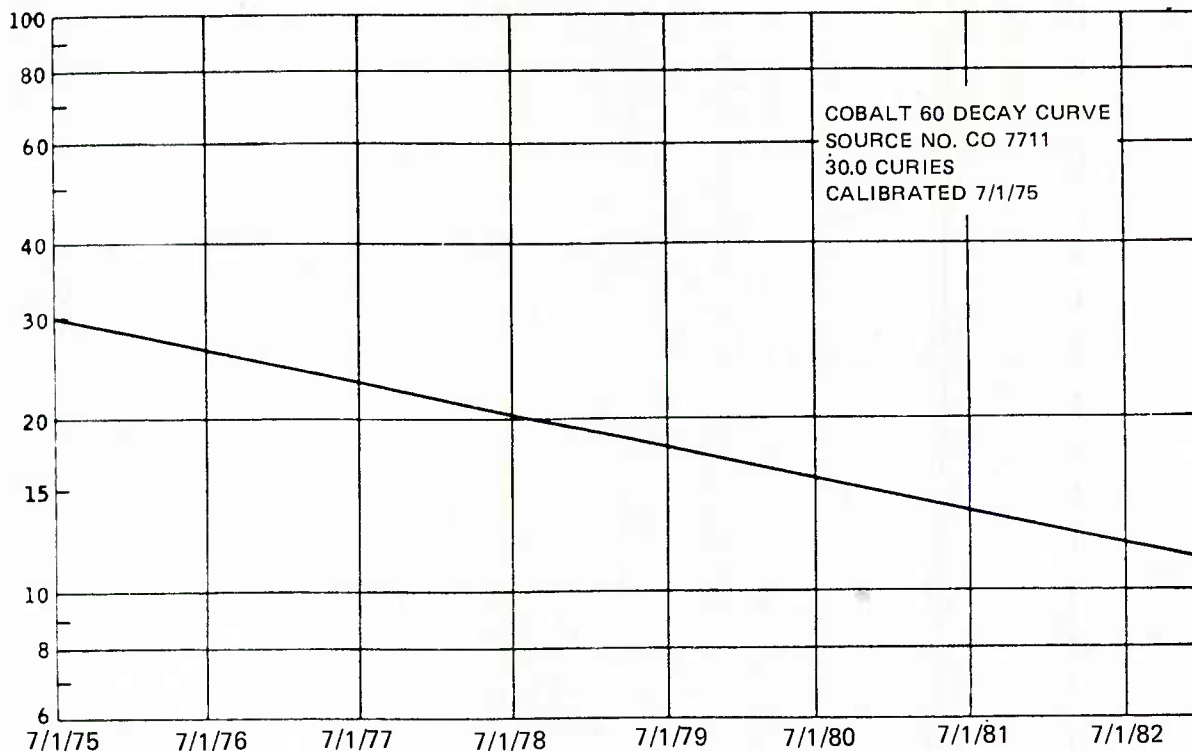


Figure 21. Dated decay curve.<sup>6</sup>

## X-Ray Exposure Charts

X-ray exposure charts, such as those shown in Figures 18 and 19, are prepared by the radiographer for a certain specific set of conditions -- type of material, specific X-ray machine, type of film, source (target)-to-film distance, type of screens (if any), development procedure, and a density chosen as the basis for the chart. These charts are prepared using a step wedge, or a wider step tablet, of a particular material, usually aluminum or steel, as these are the standards for the radiographic equivalence factor table. A series of radiographs is made at several selected exposure settings (milliamperes-minutes) and at a number of specific kilovoltages. The films are then uniformly processed under conditions selected as standard laboratory procedure. The resulting radiographs are images of the wedge with each step at a different film density. Using the density chosen as the basis for the exposure chart (measured by a densitometer), a corresponding value of material thickness, kilovoltage, and exposure can be recorded from each radiograph, interpolating between step thicknesses as necessary. These values are then plotted as a family of curves, as shown in Figures 18 and 19, with exposure laid off on a logarithmic scale and material thickness on a linear scale.

When radiographing a specimen of complex shape and thickness, exposure charts can be used only as a guide to selecting proper exposure settings, particularly since radiation will be scattered differently by a step wedge used in preparing the exposure chart than by a particular specimen. In fact, only if the conditions and materials of an investigation are identical to the specific set of conditions chosen in making the exposure chart, can proper settings be selected directly from the chart. When the conditions of an investigation differ from those of a prepared exposure chart, the following types of adjustments can be made:

1. For a difference in specimen material, a radiographic equivalence factor table (see Table 1) can provide a multiplier adjustment factor (assuming the specimen material is listed in the table) which is then applied to the exposure amount (milliamperere-seconds), holding the selected kilovoltage constant. For materials commonly used for composites, radiographic equivalence factor tables are not available. Therefore, the radiographer must either develop specific exposure charts for each of the commonly used composite matrix materials, or rely upon his own past experience and records of previous investigations.

2. An exposure adjustment for change in source-to-film distance can be easily calculated using the inverse square law for high kilovoltage settings but not for low kilovoltages (typically used for composites).

3. If a different type of film is selected (possibly to improve contrast and definition), a correction factor can be calculated using film characteristic curves similar to Figure 16.

4. If a different density is required (to improve film contrast), another similar type of exposure adjustment calculation can be made from the characteristic curve of the film used.

5. When radiographic screens are used and a change in either screen type or thickness is necessary, it is recommended that a specific exposure chart be prepared for each case. However, for the use of fluorescent screens, some data is available from film manufacturers for adjusting exposure settings (read from no-screen exposure charts) and for adjusting the source-to-film distance as a compensating measure.<sup>3</sup> Further discussions on the use of radiographic screens and other image enhancement techniques will follow later in this section.

6. Optimum development procedures for hand or automatic processing call for control of temperature and immersion time. Most manufacturers provide temperature-time charts which relate processing time to temperature changes within a range of ten degrees. An increase in developer temperature will decrease development time and cause a rapid increase in film density. Excessively high temperature should be avoided since this can result in film fogging. Excessively low temperature can result in poor or uneven development. An increase in development time will slightly increase the slope of the film characteristic curve (increasing film contrast) and shift the curve to the left (increasing film speed). Therefore, increasing the degree of development (time or temperature) can be beneficial for increasing film speed and contrast only up to certain limits. Once film fogging begins, however, the benefit may actually decrease since "net density" (total density less fog and film base density) may decrease. In addition to temperature and time considerations, the degree of development depends on the type of developer and its degree of activity.<sup>3</sup>

## Gamma Ray Exposure Charts

Figure 20 shows three gamma ray exposure charts prepared for a specific set of conditions: a specific radiation source (cobalt 60), a particular material (steel), specific film types (A, B, or C), standard manufacturer's recommended development procedures, and a film density basis of 2.0. These charts (rarely used for composites) provide for the simple calculation of exposure time for variations in source-to-film distance, D, and isotope source strength, S (see Figure 21). When radiographing a specimen of complex shape and thickness, gamma ray exposure charts can only be used

as a guide in calculating a preliminary exposure time. A final correct exposure setting can be arrived at by trial and error, with possible adaption of a two-film technique to obtain a quality image of different sections of a complex specimen.

For a detailed procedure of exposure calculations, see the examples given in the Appendix.

The preceding discussion has illustrated the procedures and data available to the radiographer for investigation of specimens of commonly encountered industrial metal materials. Radiographic investigation of composite materials, while similar in overall set-up and approach, has required the radiographer to refine and extend his capabilities, to meet the challenges posed by these new materials. Since composites are usually comprised of low-density materials, composite structures are generally radiographed at very low voltages, on the order of 20-100 kV (depending upon thickness, film, source-to-film distance, etc.). As discussed in a previous section, this type of soft radiation causes the film to be exposed predominantly to scattered radiation, and it is the control of this scatter which poses particular difficulties for the radiographer. The following discussion will present methods commonly used by the radiographer to direct, absorb, and restrict radiation in an effort to control scatter in industrial metal material investigations, and the limitations of these control methods when applied to the radiography of composites.

## Control of Scattered Radiation

For most industrial material investigations, a number of techniques and auxiliary items have been developed to aid the radiographer in controlling scatter and improving image quality. These methods and items include high density material filters, collimators, cones, diaphragms, and masking material, as well as the use of a variety of screen types including lead, fluorescent, and a combination of these called composite screens. Keeping in mind the fact that these items and techniques have been developed for investigation of higher density materials and higher energy radiation, it will become apparent that these methods can be used in some circumstances with composites, but usually offer very little control of scatter caused by the soft radiation used for composites.

The filters used are sheets of high atomic number material (lead, tin, copper or a combination of these) placed in the radiation beam at the tubehead or source (see Figure 22). Filter thickness is determined by the material type and thickness range of the specimen. In the case of high intensity radiation applications, the benefit of filters is their ability to selectively absorb the low energy parts of the radiation, allowing predominantly hard radiation to pass through the specimen and onto the film. In this manner, scatter can be reduced, and depending on the radiation quality, subject contrast can thereby be improved. However, as was pointed out earlier, since hard radiation tends to reduce subject contrast, the beneficial effects of filters will begin to predominate only when radiographing specimens with thicknesses equivalent to 40 mm or more of steel.<sup>7</sup> Because of their preferential absorption of low energy radiation, filters also allow a specimen with a wide range of thicknesses to be radiographed with a single exposure. This is termed "latitude" in radiography. Since composites are generally radiographed with relatively soft radiation, filters would have the effect of completely blocking out this soft radiation. Therefore, they are never considered when radiographing composites.

7. SCHNITGER, D., and MUNDAY, I. E. *Improvement of Contrast of X-Ray Images by the Use of Filters Between the Specimen and Film*. Brit. J. of NDT, November 1976, p. 162-164.



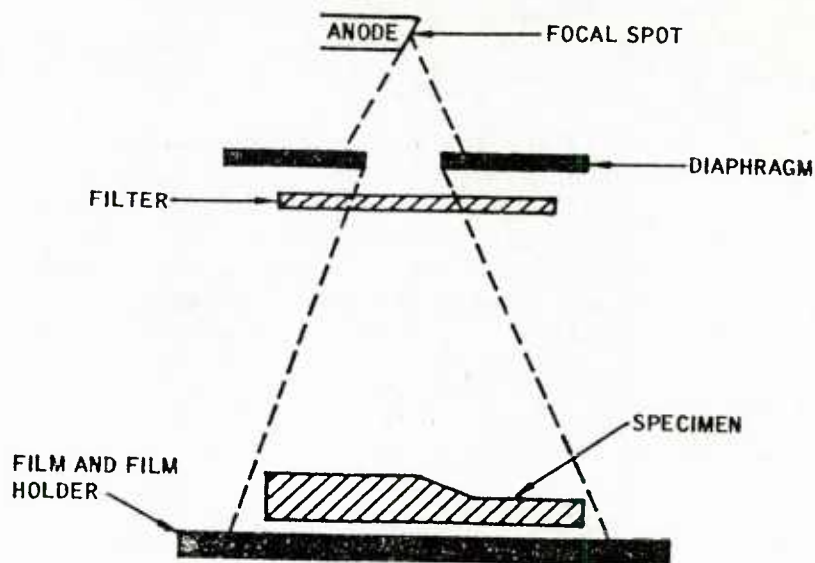


Figure 22. Filter.<sup>2</sup>

Diaphragms, collimators and cones are auxiliary items made of lead (see Figure 23) attached to an X-ray tubehead or surrounding a gamma-ray source. Due to their high density and specific configuration, they are used to limit the extent of the radiation beam. By limiting the beam to the area of the specimen only, side and back scatter and undercutting can be effectively reduced or eliminated. By limiting the beam to a specific portion of the specimen, internal scatter can be reduced. Many X-ray machines are equipped with adjustable diaphragms in order to facilitate limiting the beam extent for changes in source-to-film distance. While these auxiliary items have primary applications in the control of scatter from high quality radiation, they could also be used in soft radiation composite material investigations. However, since soft radiation tends to be absorbed rather than scattered by items adjacent to the radiographed specimen, and since internal scatter is a

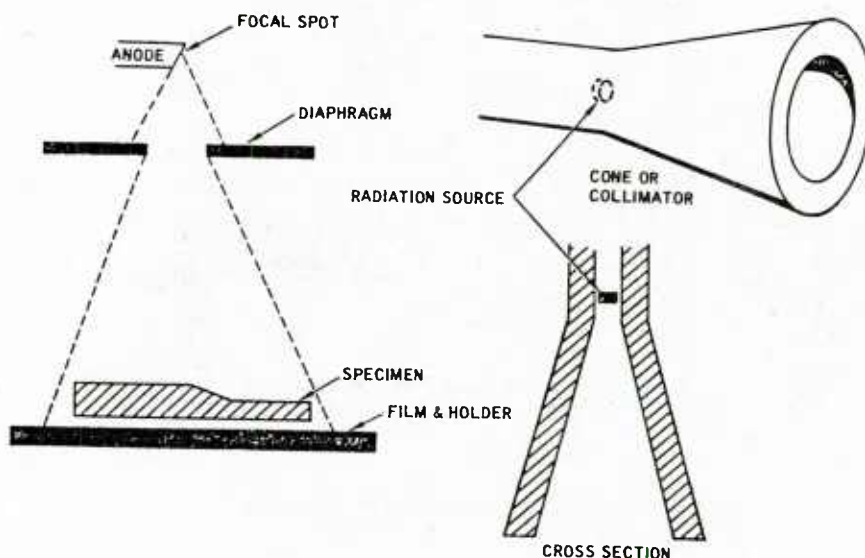


Figure 23. Diaphragm, collimator and cone.<sup>2</sup>

primary contributor to image formation with soft radiation, the use of these items does not afford much benefit. However, when thicker composite specimens are to be radiographed, the use of diaphragms, collimators, and cones could be beneficial.

In radiography, masking is the technique of surrounding all or part of a specimen with high density, absorbent material such as lead sheets, metallic shot, or barium clay (see Figures 24 and 25). Masks, like filters, control scatter by absorbing radiation which is not primarily involved with image formation and which may result in unwanted side, back, internal, or undercut scatter. Masks absorb both soft and higher energy rays, however, whereas filters are designed to absorb only soft rays. Again, this technique has its primary application in the control of scatter from high quality radiation, and its benefit in the control of soft radiation in composite materials investigation is questionable, depending on the thickness of the specimen.

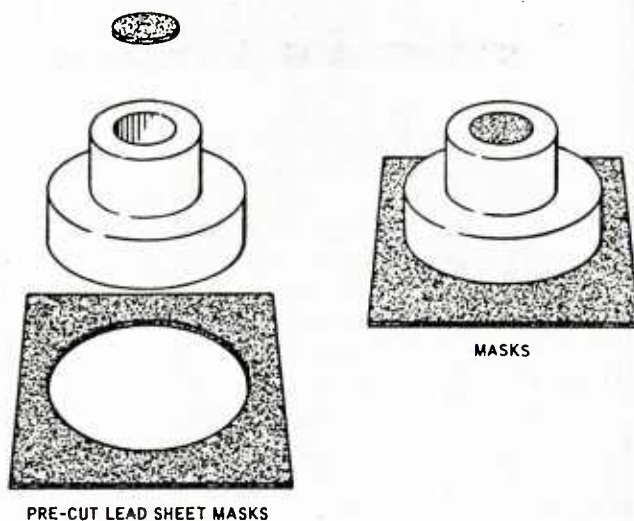


Figure 24. Lead masking technique.<sup>2</sup>

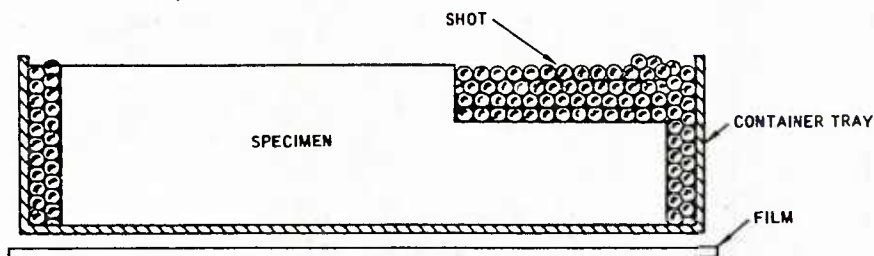


Figure 25. Masking with metallic shot.<sup>2</sup>

Radiographic intensifying screens are used in industrial radiography to shorten exposure time by enhancing the image producing radiation which strikes the film. Less than one percent of the radiation penetrating the film is actually absorbed by the grains in producing an image; the remainder passes completely through. Intensifying screens redirect or transform the radiation at the film surfaces in a manner to enhance image production. Presently, radiographic intensifying screens are of three basic types -- metallic, fluorescent, and composite.

Lead screens are by far the most commonly used in industrial radiography applications. They are available in the form of either lead foil mounted on thin cardboard or plastic, or as a lead oxide coating on a base sheet. These screens are used in pairs (front and back) with the film sandwiched in intimate contact between, and all three are encased in a film cassette. Typical front screen thicknesses range from about 0.005 to 0.010 inch, and back screens range from 0.010 to 0.030 inch. The back screen is usually thicker in order to absorb back scattered radiation. Lead screens, due to their inherent density, have the property of absorbing radiation while releasing photoelectrons which, in turn, react with the film emulsion to produce increased density. In addition, the front screens preferentially absorb soft scattered radiation while permitting primary image-forming radiation to pass through to further increase density. The amount of intensification produced in this way depends upon the amount and quality of the radiation reaching the screen through the specimen, as well as on the type of film. The effectiveness of the screen in improving film density is termed the intensification factor (I.F.), and is found by dividing the exposure amount used to produce a given radiographic density with no screens by the exposure amount needed to produce the same density with screens. Early industrial investigations<sup>8</sup> have shown that while lead screens can produce significant intensification in radiography conducted above 125 kV (or with gamma isotopes above this energy level), the use of front screens below this level will produce no practical intensifying action. The normal recommendation for low radiation investigations is therefore to use a back screen only, and the screen thickness appears to have no effect on image definition. Furthermore, since composite material specimens are generally radiographed well below the 125 kV radiation energy level, the use of lead front screens is of no practical value. As was true of filters, they would effectively eliminate the soft radiation. However, lead back screens have been found to be quite helpful when radiographing composites, both for image intensification and eliminating backscatter. For this reason, they are extensively used, and a minimum thickness of 0.010 inch is recommended.

Fluorescent screens are made by coating a plastic base sheet with either calcium tungstate or barium lead sulphate. For the radiography of composite materials, fluorescent screens are not recommended due to the poor image production effect associated with the spreading of their emitted light. These screens are used extensively in medical applications to improve image quality and where decreased exposure time is of paramount importance.<sup>3</sup> The use of medical films and filtering techniques, however, since they were developed for low-density human tissue, could be promising for low-density composite material applications. Unfortunately, due to the expense and complexity of the equipment and the uncertainty of obtaining quality results, very little work has been done in this area. On the other hand, more advanced techniques of microradiography and computer-based image enhancement of both direct fluorescent screen

8. HALMSHAW, R., and INST, F. *Radiographic Intensifying Screens*. Brit. J. of NDT, March 1972, p. 45-47.

images and finished radiographs are being actively developed for composite investigations and have produced amazingly good results. These techniques comprise the state-of-the-art in radiography and, in particular, composite radiography investigations, and will be discussed further in the following section, Composite Material Investigations.

The third type of radiographic intensifying screen, composite or fluorometallic, attempts to combine the best qualities of lead and fluorescent screens by utilizing the luminescence of a thin fluorescent layer and the electron image enhancement of a thin lead layer in combination.<sup>9</sup> For composite material investigations, composite intensifying screens would not be effective for the same reasons that lead or fluorescent screens are not recommended.

### Penetrators and Radiographic Sensitivity

Earlier in this discussion, the term sensitivity was used in relation to radiographic quality and image definition. The attainment of a minimum acceptable image quality level is a necessary part of any code or specification governing the acceptance or rejection of an item. For this reason, extensive work has been carried out in industrial radiography to establish methods for measuring radiographic image quality as a check on the adequacy of the radiographic technique. This has led to the adoption of standard items commonly referred to as penetrators and image quality indicators (IQI's). The ASTM defines a penetrator as a device employed to obtain evidence on a radiograph that the technique used is satisfactory.<sup>5</sup> It is not intended for judging the size of discontinuities, nor for establishing acceptance limits for materials or products.

In North America, the most commonly used penetrator is the ASTM plaque-type. An example of this type used for a one-inch thick material specimen, is shown in Figure 26. The penetrator material must be radiographically similar to the specimen being radiographed. That is, it must have similar radiation absorption properties. If a penetrator of material identical to the specimen material cannot be obtained, one of lower radiation absorption ability must be used, to insure that satisfactory evidence of image quality has been obtained.

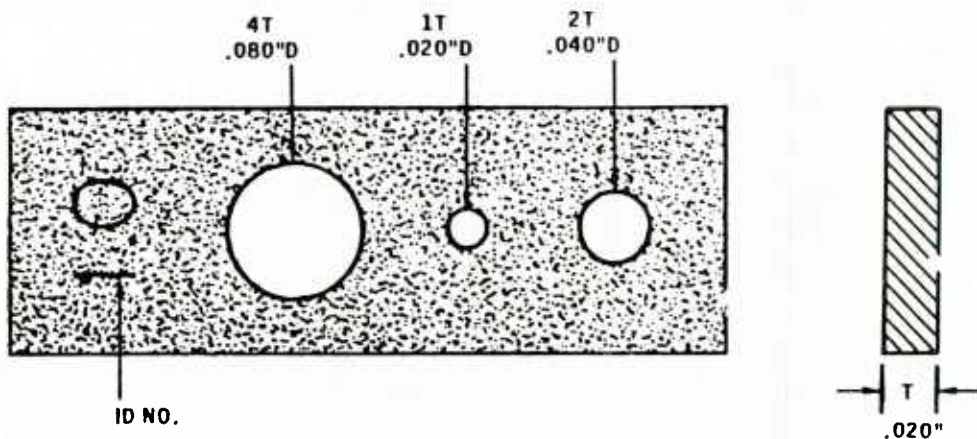


Figure 26. Standard penetrator for one-inch-thick material.<sup>2</sup>

9. DerBOGHOSIAN, S., and COATES, A. J. *Composite Screens Used as a Radiographic Aid*. Army Materials and Mechanics Research Center, AMMRC TR 81-11, March 1981.



The penetrameter method consists of placing the penetrameter, which contains carefully prepared defect indicators (the holes shown in Figure 26), onto the source side of the specimen under investigation, and proceeding with the exposure process. The penetrameter thickness and hole sizes are standardized to indicate a certain level of image quality. The penetrameter thus serves as a built-in defect of known thickness and known diameter. In this way, the ability to detect desired density, penetrameter outline, and defect size from the radiographed penetrameter image is an assurance that adequate imaging has occurred. This method is quite successful for industrial metal material investigations; but, as will become evident, it is not adequate for determining image quality in composite material investigations, due to the complexity of composite material composition and the type of defects associated with common composite materials.

Each ASTM penetrameter, as typified by the one shown in Figure 26, is identified by a lead number (ID No.) which indicates the maximum thickness of material for which the penetrameter can be normally used. A list of standard penetrameter sizes and the material thickness for which they are to be used is given in Table 2. The penetrameter serves to measure two indicators of image quality: contrast sensitivity and resolution. Most code requirements specify that adequate contrast sensitivity has been obtained if the outline of a penetrameter which is effectively two percent of the material specimen thickness is visible on the radiograph. For this reason, the penetrameter thicknesses (T), as shown in Table 2, are two percent of the material specimen thickness for which they are to be used. The density range for which a radiograph may be properly read is also specified in reference to penetrameters. One penetrameter can be used for each area of the radiograph where the specimen image density does not vary more than +30% or -15% of the penetrameter density. To cover an entire radiograph of widely divergent density, two penetrameters must be used, one

Table 2. STANDARD PENETRAMETER SIZES

| APPLIES TO DESIGN MATERIAL THICKNESS** (T <sub>m</sub> ) UP TO AND INCLUDING (INCHES)                     |       | ID NO. | "T"   | 1T HOLE DIA. | 2T HOLE DIA. | 4T HOLE DIA. |
|---|-------|--------|-------|--------------|--------------|--------------|
| 1/4"  | 0.25" | 25     | .005" | .010*        | .020*        | .040*        |
| 3/8   | 0.375 | 37     | .008  | .010*        | .020*        | .040*        |
| 1/2   | 0.5   | 50     | .010  | .010         | .020         | .040         |
| 5/8   | 0.625 | 62     | .013  | .013         | .025         | .050         |
| 3/4   | 0.75  | 75     | .015  | .015         | .030         | .060         |
| 7/8   | 0.875 | 87     | .018  | .018         | .035         | .070         |
| 1   | 1.0   | 1.0    | .020  | .020         | .040         | .080         |
| 1-1/8   | 1.125 | 1.1    | .023  | .023         | .045         | .090         |
| 1-1/4   | 1.25  | 1.2    | .025  | .025         | .050         | .100         |
| 1-1/2   | 1.5   | 1.5    | .030  | .030         | .060         | .120         |
| AND SO ON FOR EACH 1/4 INCH UP TO 2-1/2" AND THEN IN 1/2" INCREMENTS UP TO 8", AND THEN IN 1" INCREMENTS. |       |        |       |              |              |              |

\* MINIMUM HOLE SIZES REQUIRED BY THE STANDARD, DO NOT BEAR CORRECT RELATIONSHIP TO ID NO. OR THICKNESS OF THE PENETRAMETER.

\*\* DEFINED AS THE THICKNESS OF THE MATERIAL (T<sub>m</sub>) UPON WHICH THE THICKNESS OF THE PENETRAMETER IS BASED. FOR WELDS, THE MATERIAL THICKNESS SHALL BE THE THICKNESS OF THE STRENGTH MEMBER.



placed at the highest density region and the other at the lowest. This requirement was included in the specifications in order to control the density of radiographs, since density plays such an important part in sensitivity, contrast and defect detection ability.

The measurement of image resolution or detail definition is specified as the ability to see one of the three holes on the penetrameter image. The holes, labeled 1T, 2T and 4T in Figure 26, have diameters of 1, 2 and 4 times the penetrameter thickness, respectively. Therefore, a code specifying a 2-2T sensitivity (level 2) requires that the 2T hole on a penetrameter which is two percent of the specimen thickness be visible on the radiograph. A sensitivity level of 2-2T is the most common level specified for a wide range of aeronautical components and industrial investigations, including metal castings and weldments. The ability to attain this level of sensitivity, of course, depends upon the many factors discussed throughout this chapter, but, in particular, upon the type of film used. Specifying higher or lower sensitivity levels, such as 2-1T or 2-4T respectively, would depend upon the importance and intended use of the item under investigation.

Other penetrameters,<sup>3</sup> for example those specified by the ASME Boiler and Pressure Vessel Code and those required by the Armed Forces, are similar to the ASTM plaque-type, but have their own particular design. ASTM wire penetrameters have recently been introduced in North America. In Europe, a number of penetrameter designs are in use, including a wire-type DIN (German) IQI, a stepped BWRA (British Welding Research Association) IQI and a French standard (AFNOR) IQI. Where defects other than voids, inclusions, porosity, or other spherical-type defects have been expected, numerous types of special penetrameters, containing wires or beads, have been devised. What is important, however, is that a penetrameter must provide evidence of the sensitivity of the inspection process and must be representative of the defect conditions.

Concerning the use of penetrameters to measure the sensitivity of a composite material radiographic investigation, the question, of what type of penetrameter design or material should be used is difficult to answer; at this time, specifications are non-existent for adequate penetrameter measurement requirements for composite materials. There are a number of possible approaches to this problem. Penetrameters similar in design to those presently used could be made from a material representative of the particular composite specimen. However, at best this would yield only a rough measurement, because of the complex composition of most composite materials. In addition, the design of an adequate penetrameter is very difficult because of the many types of imperfections associated with composite specimens (fiber misalignment, fiber breaks, resin content irregularities, fiber matrix unbonds, damage considerations, moisture effects, etc.).

Another approach might be to incorporate simulated defects into the penetrameter. For example, in the inspection of a fiber-reinforced composite, a single ply of defective composite could be used as a comparative quality standard when radiographed together with the specimen. In any case, the selection of a penetrameter for adequate sensitivity measurements of the radiographic investigation of a particular composite material is a difficult problem. Most radiographers use no penetrameter, but rely totally on subjective observation and comparison to select a radiograph adequate for interpretative evaluation.

This raises some interesting questions about the capabilities and limitations of the human eye in detecting defects and imperfections on a radiographic image. In the following discussion, some of the factors which affect the viewing and interpretation

of radiographs will be presented in order to point out that image interpretation is a question of human skill, experience and training, and further, to demonstrate how these factors limit the usefulness of radiography as an inspection tool.

## Viewing and Interpreting Radiographs

Since radiographs are generally inspected visually, and since the sensitivity of a radiographic technique is generally measured by the size of the smallest penetrameter defect visible, the usefulness of any radiographic image depends upon its impact on the human eye. A simple approach toward improving inspection ability would be to produce as clear and sharp an image as possible. Yet, the following questions must also be considered:

1. What are the limitations in the ability of the eye to detect small, sharp detail?
2. What is the effect of blurred outlines on the visibility of an image of a given contrast?
3. What is the ability of the eye to recognize detail in the presence of film graininess?
4. What is the effect of image brightness on visual performance?
5. What is the effect of glare, i.e., extraneous light?

Halmshaw<sup>10</sup> has studied the preceding and other questions about viewing conditions and factors relating to ocular interpretation. The perception of an image is largely dependent upon the viewing conditions and the quality of the illuminator. Viewing conditions should combine a maximum of viewer comfort with a minimum of fatigue, in a viewing room with subdued lighting, rather than total darkness. Since the eye is not a perfect optical instrument, it is possible to have a defect image with too low a contrast to be seen or too small a size to be resolved. The most important single factor to be considered is that the performance of the eye is a function of the intensity of light which reaches it. This intensity depends both on the film density and the brightness capability of the illuminator. A radiograph of density 2.0 transmits only 1/100 of the illuminator screen light intensity, and a density of 3.0, only 1/1000 of the intensity. On a typical fine-grained film, the contrast at density 4.0 is three times greater than at density 1.0. This is a significant increase in film contrast which can be extremely beneficial for improving image interpretation, but only with the viewing facilities and illuminator capabilities to make full use of it. That is, the illuminator must provide light of sufficient intensity, free from glare, to illuminate the areas of interest, and it must diffuse the light evenly over that area. Commercially available high intensity illuminators, capable of viewing densities up to 4.0 and higher, are particularly recommended.

There is considerable experimental data on the ability of the eye to see small differences in brightness between two areas.<sup>10</sup> It has been concluded that, at a brightness of 10mL, the eye can detect a brightness difference of about 1.4%, which

10. HALMSHAW, R. *The Image on a Radiograph*. Proc. of a Symposium on Physics and Nondestructive Testing, Dayton, Ohio, September 1964, p. 171-193.

corresponds to a density difference on film of only 0.006 (0.02 in practice). This points out the incredible ability of the human eye to perceive extremely small brightness differences, and the need for an illuminator which is properly masked to avoid glare from bright light at the edges of the radiograph or glare transmitted by areas of low density.

When discussing the effect of blurred outlines on the visibility of an image, one is concerned with the influence of unsharpness on image visibility. While though there has been little work published on this subject,<sup>10</sup> it can be concluded that detail on the radiograph will be affected only when the blurred outline of a spherical defect reaches a width of 0.5 mm or more (when viewed at 10-in. distance). Furthermore, if sufficient blurring is present on the radiograph, the visibility of certain penetrameter holes does not insure that a defect of the same diameter and thickness will be visible. A penetrameter hole has a sharp boundary, whereas most defects are spherical with more or less rounded edges, causing a gradual density change. The penetrameter hole image will therefore have a sharper outline and will be seen more easily. The same is true of the effect of blurred outline and detectability of crack-type defects as compared to the visibility of a wire-type penetrameter (IQI). Moreover, the eye recognizes a long, thin defect more easily than a short one.

Some further thoughts about the factors which affect radiographic interpretation were also reported by Halmshaw.<sup>10</sup> He relates that the percentage of failures to perceive significant findings on a radiograph were surprisingly high among a group of experienced radiologists who independently examined 168 chest radiographs; 20-30% of the individuals had overlooked significant details. An analogous study on military photo-interpreters, Halmshaw reports, produced a 54% failure to report significant findings, and it was suggested that this was substantially due to failure of perception and not to mistakes in judgement. Halmshaw goes on to say that reading a radiograph is a process of visual searching, and that training should lead to a more orderly search pattern. However, he states, it has been shown that trained observers do not, or possibly cannot, adhere to any sort of orderly search pattern. There is therefore a tendency to concentrate on what one presupposes to be the significant areas of a radiograph, and to ignore (or not to see) important indications elsewhere on the film. Furthermore, the visual system's capacity for perception depends on identification with memory traces of prior experience; that is, there is no perception without recognition - the image which is perceived is in part constructed from remembered events. This explains, Halmshaw suggests, the expert's ability to immediately pinpoint a significant, but possibly small and low-contrast, detail on a radiograph.

In the following section, Composite Material Investigations, a discussion of computer-based radiographic image enhancement systems will be presented. With these systems, the interpretive role of a radiographer has been greatly reduced and, in many instances, virtually eliminated due to the capability of these computer systems for sorting and measuring enhanced defect images, and then automatically accepting or rejecting specimen items based upon pre-programmed specification requirements. This represents an exciting breakthrough in the limitations of radiography as an inspection tool, and with continued development, holds significant promise for future industrial and composite material radiographic investigations.



## SECTION 5. COMPOSITE MATERIAL INVESTIGATIONS

### Typical Applications

By far the most widely used radiographic technique for the inspection of composite materials is the straightforward radiographic method, as previously described in this report. It has been shown that the density on a radiograph depends upon the relative absorption of radiation by the material or defects in its path. In composite material investigations, the radiographer has had to deal with a vast spectrum of reinforcement and matrix material systems, together with a number of associated types of defects. In particular, some of the defect considerations investigated with radiography include: bond evaluations, curing effects, damage considerations, flaw content and growth, voids, failure mechanisms, fatigue behavior, fiber characteristics and fiber breaks, fracture characteristics, moisture effects, physical properties, resin content, and thermal effects. The need for detection of these types of defects and the general nature of composite systems has brought about a number of advancements in the traditional, straightforward radiographic technique, and has spurred the development of some new and promising techniques.

This section will focus on the methods and capabilities of some of these techniques, including microradiography, neutron radiography, the use of opaque additives, and the use of automatic computer-based radiographic image enhancement systems. However, we will begin by reviewing a number of composite material investigations which employed a more conventional radiographic technique.

In an early composite investigation, Owston and Connor<sup>11</sup> reported the initial results of an extended research program to determine the defects which initiate mechanical failure in carbon fiber-reinforced plastics, and to find nondestructive evaluation (NDE) methods of locating these defects. Approximately 40 specimens, some short rectangular bars, others cylindrical rings, were investigated. The rectangular bars were 1.5 in. x 0.75 in. x 0.08 in. thick, unidirectional with fibers running lengthwise, and were made by stacking carbon fiber-epoxy prepreg tapes. The cylindrical rings were 4.25-in. inside diameter by 0.1-in. wall thickness, and were an attempt to produce a tensile stress in unidirectional material without the complication of grips.

Good quality radiographs were obtained at 12 kV using a beryllium window X-ray tube, Kodak Microtex double-sided industrial film, and a source-to-film distance of 24 inches. Black industrial polyethylene was used as a film cassette in some cases, while other exposures were made without a cassette but with all the equipment enclosed in a dark room. Similar results were achieved in both cases. For the ring specimen, a strip of film backed with a thick strip of lead was fitted inside the ring, and the entire assembly was rotated in front of a collimated beam from the X-ray generator. The resulting radiographs revealed porosity in the specimens, but could not resolve the fibers, their orientation, or density.

The authors went on to present an interesting categorization of composite defects, together with the limitations of conventional radiography for their detection. Composite defects were classified into three groups:

11. OWSTON, C. N., and CONOR, P. C. *Failure Mechanisms in Carbon Fiber Reinforced Polymer and Their Relation to Non-Destructive Testing*. Composites, September 1970, p. 268-276.

Type 1 defects: Those of large proportions affecting wide areas or even the whole of a component, e.g., omission of a layer of prepreg in the layup of a component, faulty resin curing, incorrect compaction due to failure to close the mold correctly.

Type 2 defects: Smaller scale defects which are still the result of manufacturing technique, e.g., voidage, local misorientation of fibers, local variations in resin content, shrinkage cracks in the resin, and unavoidable features in the structure such as joints in prepreg sheets.

Type 3 defects: Very small defects, e.g., single misoriented fibers and their associated entrained air bubbles, piping along single fibers. These defects are the ultimate defects, the ones that cannot be avoided except under exceptionally rigorous manufacturing conditions.

The larger voids and cracks associated with Type 2 defects are readily detectable radiographically. Experience with the failure of test specimens has led Owston and Connors to believe that much attention should be paid to the significance of these defects. In some specimens containing large Type 2 defects, failure initiated at apparently insignificant Type 3 defects, implying that defect form and location can be very important.

The authors go on to say that variation in fiber fraction and orientation do not appear to be readily detectable using radiography or ultrasonics, although some indications can be obtained radiographically by using glass fiber tracers (a form of image enhancement).

In a more recent study, Roderick and Whitcomb<sup>12</sup> describe how a modified X-ray method can be used to show how fibers fail during fatigue of boron-epoxy laminates. The authors employed X-radiography in tracking fiber breakage in two notched boron-epoxy laminates, (+45/0/-45/0) and (90/±45/0) that were subjected to constant amplitude cyclic loads. Prior to the fatigue test, broken fibers were found only very close to the notch (as a result of machining). After  $10^6$  applied load cycles, a number of additional fibers were broken, as evidenced on the radiographs. At  $5 \times 10^6$  applied load cycles, more fiber breaks were recorded.

In this modified X-ray method, a high resolution glass photographic plate was used to record the image of the 1-mm thick specimens. The X-ray source was 12 inches from the laminate, which was laid on the photographic plate. The exposure was 5 minutes at 50 kV and 20 mA. After the plate was developed, it was rephotographed with a metallograph to produce a magnified image. The authors suggest that this technique can be used to locate fiber breaks on the glass plates themselves, and that the significance of this technique can be seen by noting the similarity between the images obtained in this study with thermographs of the same laminates at various stages of loading.

In a follow-up study, Roderick and Whitcomb<sup>13</sup> employed a similar technique to identify the primary fatigue mechanisms and to study the sequence of events during fatigue failure of notched boron-epoxy laminates. X-radiography and scanning electron

12. RODERICK, G. L., and WHITCOMB, J. D. *X-Ray Method Shows Fibers Fail During Fatigue of Boron-Epoxy Laminates*. J. Comp. Mat., v. 9, October 1975, p. 391-393.

13. RODERICK, G. L., and WHITCOMB, J. D. *Fatigue Damage of Notched Boron/Epoxy Laminates Under Constant Amplitude Loading*. N77-17165/OST, Report No. NASA-TM-X-73994, December 1976.



microscopy were used in combination to examine the fatigue processes in notched (0,  $\pm 45$ ) and (0,  $\pm 45$ , 90) laminates. Fiber breakage and matrix cracking were monitored. Fiber breakage was detected by taking radiographs at no load and periodically during fatigue testing. Soft, 50-kV radiation at 20 mA and a source-to-film distance of 30 cm were used to expose high resolution photographic glass plates which were processed and examined on a metallograph at 50X magnification. The breaks in the tungsten core of the boron fibers could easily be seen.

Examinations of each series of radiographs revealed that, initially, fatigue damage in both the (0,  $\pm 45$ ) and (0,  $\pm 45$ , 90) laminates occurred as interlaminar cracks around the edge of a notched hole. Then, whenever further damage developed, interlaminar cracks in the  $\pm 45$  degree plies began to propagate from the edge of the hole. Finally, in both type laminates, primarily  $\pm 45$  degree fibers broke (prior to two-piece failure) where interlaminar cracks in the  $\pm 45$  degree plies had occurred. The results of this study suggest that in boron-epoxy laminates, the 45 degree plies play a key role in the fatigue process, since fatigue starts as interlaminar matrix cracks in the  $\pm 45$  degree plies. Radiography has thus been shown to be a valuable investigative tool in the study of composite fatigue behavior.

In another investigation, Artis and Joiner<sup>14</sup> employed a stereo-microradiography technique together with a sulphur image enhancer to measure the relative performance of various classes of resin in carbon fiber composites. Unidirectional carbon-fiber-reinforced plates were fabricated with each of seven different resins, including: EPIKOTE 828 (epoxy), ARALDITE MY 753/HY 951 (epoxy), CRYSTIC 199 LV (polyester), CRYSTIC 272 and 625 LV (polyester), DV 19162 VARNISH (phenolic) and QX 13 Resin (polyimide). The plates fabricated were 7.62 cm x 7.62 cm x 0.2 cm thick, and were cut into 1.0 cm wide strips perpendicular to the fiber direction.

In order to enhance the radiographic image of very small voids (with diameters of five microns or less), a method of electron staining was developed. It was postulated that if the micropores of the carbon composite could be completely filled with a "staining" liquid having a sufficiently higher electron density than carbon, and furthermore, if the liquid could be kept from evaporating during radiography, then the pore network would predominate in the radiograph over the matrix. Molten sulphur was found to be an excellent medium, wetting all types of consolidated carbons, and was applied to the samples (after fine surface grinding), using a simple vacuum impregnation technique.

The samples were radiographed at 12 kV for 30 seconds with a source-to-film distance of 25.4 cm at an offset angle of  $11^\circ 18''$ , while they were placed in contact with the film and exposed in a light box. The radiographs were then enlarged using a microscopic technique, and stereo pairs were assembled by contact printing the films on Ilford 11/0 paper. This method of radiography proved particularly advantageous in that it allowed the examination of channel network pores within the specimen and not surface pores alone.

The stereo pairs produced showed voids in all the samples; however, the epoxy resins showed the least void occurrence. The voids in the polyester resin occurred along the fibers, the most probable source being air that was allowed to enter the composite due to the resin's low fiber wetting ability. Both phenolic and polyimide resins showed similar voids. The polyimide radiographs showed particularly bad striation, thought to be due to resin starvation.

14. ARTIS, L. J., and JOINER, J. C. *Methods of Measurement of the Relative Performance of Various Classes of Resins in Carbon Fibre Composites*. N73-31536/8, Report No. AQD/NM-000198, October 1972.

From their findings, the authors concluded that epoxy resins permit less void formation than the other resins, due to the epoxy resin's better wetting ability. They also concluded that the technique of stereo-microradiography could be extremely useful in the evaluation of carbon fiber composite materials, and that attempts should be made to devise a simple method of numerically quantifying the image produced.

## Microradiography

In order to improve image detail quality and radiographic sensitivity, a special radiographic method and related equipment were devised which best utilize the beneficial effects of very small focal spot size and improved, low kV subject contrast. This technique, microradiography, employs soft radiation in the 5 to 50 kV range, generated by special X-ray tubes with very small focal spots. The specimen must be kept in intimate contact with the film to minimize any optical enlargement effects. This is accomplished either by simple clamping devices or by using a vacuum pressure device. The film used is usually coated on one side only with a very fine grained emulsion (finer than that of typical X-ray films).

The microradiography technique is particularly suited to obtaining images of thin specimens of low density; for this reason, it is being used more and more extensively for composite material investigations. The detail and radiographic quality obtained with a successful application of this technique can be extremely good. However, there are some difficulties which must be considered when employing a low energy X-ray method such as this. One difficulty, depending upon the thickness of the specimen and the source-to-film distance used, is that exposure times can be very long, three hours or more. This exposure time could be reduced by decreasing the source-to-film distance to a minimum (which is an advantage of having a very small focal spot), but the specimen area intercepted by the radiation beam would also be reduced. Also, in the low kilovoltage range (20 kV or below), the inverse square law normally governing radiation intensity is violated due to the absorption of these low energy X-rays by the air. Moreover, the film cassette material also plays a part in radiation absorption and should be of minimum thickness and density. Many radiographers use plastic or paper film holders reinforced with tape and a thin lead back screen (0.005 or 0.01 inch thick). The paper holder should be of fine grained paper since radiation in the 20-50 kV range will transfer the holder paper grain image onto the film. The holders should also be free from dust, pencil, or paint smudges that would also be revealed on the radiograph and could be incorrectly interpreted as material defects. An extended daily warm-up period is required for microradiographic tubes which are highly susceptible to sudden voltage surges and usually require that a voltage regulator be installed in the line. In addition, care must be taken not to touch or jar the X-ray tube; because of its small focal spot size, even a slight movement can cause significant misorientation of the radiation beam. Beam misalignment can cause considerable blurring, particularly for investigations of specimens containing slots. Finally, since the objects radiographed are usually thin, the defect features to be detected are usually quite small and require some type of enlargement for adequate viewing and interpretation.

These difficulties and others were discussed by Huggins<sup>15</sup> who related the results of his recent investigations with low energy radiation. Huggins relates that at X-ray energies below about 60 kV, we begin to be concerned with the absorption of materials between the X-ray source and the film, other than the object being radiographed. As

15. HUGGINS, B. E. *Radiography with Low Energy Radiation*. Brit. J. of NDT, May 1981, p. 119-125.

X-ray energy is reduced, this absorption has two unwanted effects; it reduces the intensity of the beam thus increasing exposure time, and it preferentially absorbs the low energy components of the spectrum thus reducing radiographic contrast. For these reasons, use of plastic rather than aluminum-fronted cassettes is necessary with X-ray energies below about 40 kV. At around 16 kV, the granular structure of the plastic window begins to be apparent.

The material of the X-ray tube window has an increasingly marked effect on X-ray transmission below about 50 kV. Thus, if radiation of much less than this energy is required, the tube will need to have a low absorptive window. This will usually be of beryllium and have a thickness of less than 2 mm. A 1-mm window gives good transmission down to about 6 kV.

Radiation attenuation due to the air between the film cassette and the X-ray tube window begins to be significant below about 20 kV, depending on the focus-to-film distance used. The problem can be dealt with by using either a low density gas environment, such as hydrogen or helium, or by radiographing in a vacuum. Huggins used helium because it is safer than hydrogen, and its X-ray transmission is only marginally less. For example, with 4 kV X-rays, 200 mm of helium has a transmission of 99.6%. The corresponding transmission of air is 17%. Use of a vacuum, Huggins reports, could result in increased X-ray absorption, since the inlet and exit windows would need to be strong enough to support atmospheric pressure; helium on the other hand, can be contained in a vessel with extremely thin Mylar windows at either end. Huggins goes on to discuss various forms of enlargement techniques and the effects of film type and magnification, as well as the use of photographic plates on enlarged image detail and quality.

In an investigation similar to that of Roderick and Whitcomb,<sup>12,13</sup> Marcus and Stinchcomb<sup>16</sup> measured fatigue damage in boron-epoxy composite laminates using a micro-radiography technique. From previous investigations, it was evident to the authors that two different effects must be considered in order to understand the mechanical behavior (static and cyclic) of composite laminates with a stress raiser such as a circular hole. These effects are (1) The increased stress near the hole due to the local stress raiser effect, and (2) The interlaminar stresses occurring at and near the hole due to the presence of the free edge. See Figures 27-30 (given as Figures 3, 4, 5 and 6 in Ref. 16).

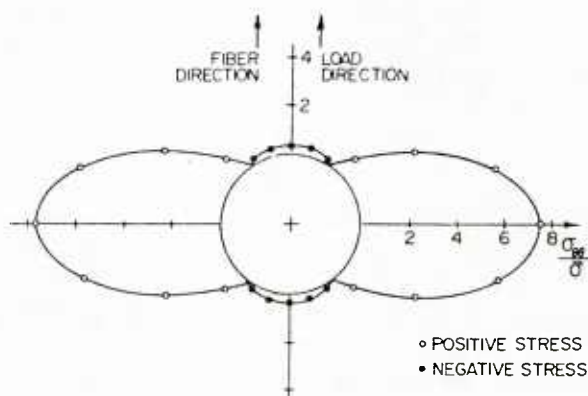


Figure 27. Circumferential normal stresses in 0-degree layers ( $z = h/2$  and  $7h/2$ ).<sup>16</sup>

16. MARCUS, L. A., and STINCHCOMB, W. W. *Measurement of Fatigue Damage in Composite Materials*. Exp. Mech., v. 15, no. 2, February 1975, p. 55-60.



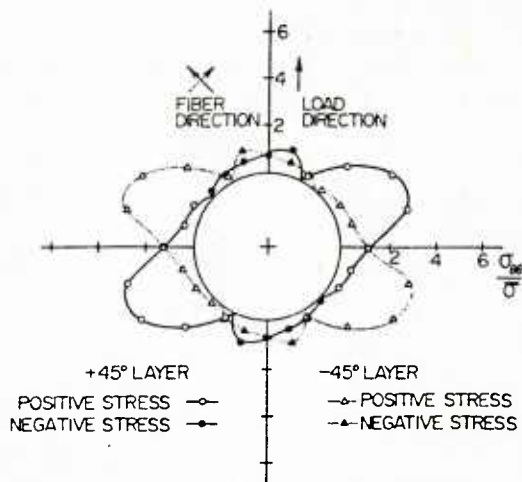


Figure 28. Circumferential normal stresses in 45-degree layers ( $z = 7h/4$  and  $9h/4$ ).<sup>16</sup>

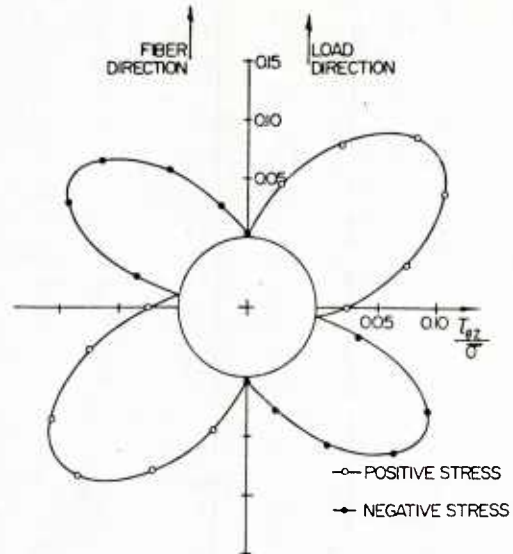


Figure 29. Interlaminar shear stresses in top 0-degree layer ( $z = 7h/2$ ).<sup>16</sup>

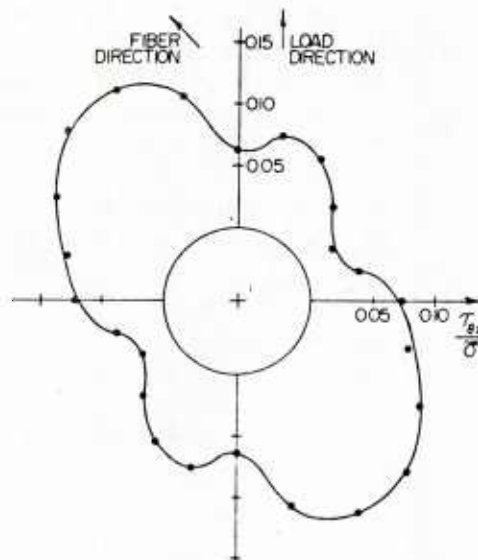


Figure 30. Interlaminar shear stresses in +45-degree layer ( $z = 9h/4$ ).<sup>16</sup>

In this investigation, a three-dimensional finite-element analysis was used to predict the static-stress distribution around a circular hole in a (0/±45/0) boron-epoxy plate. Data, obtained by thermographic and radiographic techniques during cyclic-strain tests on similar specimens, revealed the contribution of the two above-mentioned effects on the fatigue behavior of the composites. The tests performed were a series of strain-controlled tension-tension fatigue tests on a 0.05-inch (0/±45/0) specimen layed-up from AVCO 5505 prepreg tape.



For the radiographic investigation, a point X-ray source with a nickel filter, operating at 25 kV and 10 mA, produced radiation which was collimated by an 18-in. long by 7/8-in. diameter lead-shrouded tube. The thin specimen to be radiographed was placed between the end of the tube and a sheet of Polaroid Type 57 film. The exposure time was 25 seconds.

A sequence of radiographs of the specimen, corresponding to a similar series of thermographic images, was made by stopping the test at various points and performing the radiography. The comparisons showed that the more heavily damaged regions are also regions of more intense heat development.

The process by which the damage develops, as shown in the radiographs and by visual observation of the specimen during testing, is one in which the 0-degree layer longitudinal crack in the matrix develops first, followed by ejection of short pieces of the broken 45-degree fibers as the longitudinal crack propagates through the thickness and by delamination between the 45-deg layers. The authors noted that damage developed quickly in the material and then, for all purposes, stopped as could be seen by comparing the radiographs.

From the theoretical stress state around the hole and experimentally observed fatigue behavior noted, an analysis of the effects of the stress state on the fatigue behavior was made. The authors reported that the result of this investigation implied that a crack, although it initiates at points of greatest strain-energy density in the outer 0-degree layer, initiates preferentially in quadrants II and IV under the influence of the interlaminar shear stress in the underlying +45-degree layer. One must deduce this mechanism, suggest the authors, from a consideration of the stress state at the hole boundary.

In another investigation, Darlington and McGingley<sup>17</sup> discussed the benefits of contact microradiography over microphotography for determining fiber orientation and distribution in short fiber-reinforced plastics. The contact microradiography (CMR) technique consists of making a microradiograph of a 100-micron slice of the composite. This was compared to a microphotograph made on a polished microtomed section of a 100-micron slice of the same specimen. The microradiograph showed not only the parts of the fibers penetrating the polished surface, but also those underneath the surface to a depth of 100 microns. Therefore, a single circular spot indicated good fiber alignment along the axis, while blurred strip-like areas indicated that fibers were misaligned with the axis. Examples shown indicated gross misalignment at section corners and adjacent to complex shapes.

The use of a slice whose thickness was less than the mean fiber length suggested to the authors the possibility of estimating, from the radiograph, the orientation of the fibers to the plane of the cut. Therefore, the authors contended, one slice cut perpendicular to the moulded surface can give a good indication of the quality of the molding process by showing a 3-dimensional orientation distribution through the thickness. Also, the examination of a number of such cuts or a variety of cuts made at selected angles could be used for a more complete examination.

17. DARLINGTON, M. W., and MCGINGLEY, P. L. *Fibre Orientation Distribution in Short Fibre Reinforced Plastics*. J. of Mater. Sci., v. 10, 1975, p. 906-910.

## Automatic Computer-Based Radiographic Image Enhancement

While visual inspection and interpretation continues to be the most widely used technique for defect detection, the increasing need for more rapid and more accurate acceptance/rejection decisions has spurred the development of automatic, computer-based image enhancement and analysis systems. Over the past few years, a number of systems have been developed, some of which provide various forms of image enhancement, and others which provide both enhancement and image analysis.

In one of the earlier papers<sup>18</sup> on radiographic image enhancement, Vary states that, since the usual methods of direct or optically aided viewing require a high degree of eye accommodation, there is a growing effort to increase the amount of information retrievable from radiographs by means of image enhancement techniques. In this early report, radiographs of nuclear and aerospace components were studied with a closed-circuit television system to determine the advantages of electronic enhancement. The radiographic images were examined on a television monitor under various degrees of magnification and enhancement. The enhancement was accomplished by generating a video signal whose amplitude was proportional to the rate of change of image density. Points, lines, edges, and other density variations that were faintly registered in the original image were thus rendered in sharp relief.

With some exceptions, neither the normal nor enhanced video displays revealed details of the radiographs that could not be ultimately seen by direct-eye viewing or by means of simple optical aids. With proper back-lighting, magnification, and eye accommodation, vary states, there is actually little information in well-made radiographs that escapes detection. Conversely, the video system does retrieve all details revealed by close optical examination. However, all these details could not always be retrieved simultaneously with one setting of the enhancement controls (of this particular system), because the density response range of the system was not always adequate.

One problem that was aggravated by edge enhancement arose from film artifacts, such as the presence of defects in the film emulsion, graininess, scratches, water marks, dust, lint, etc. All these were, of course, enhanced along with other image details. In most instances, such artifacts that appeared in the enhancement could be readily identified and ignored, as in conventional radiographic examinations, after a little experience was gained in interpreting the enhanced images.

Overall, the video system proved to be a valuable tool for the examination of radiographs. Over 100 samples of radiographs were examined and interpreted with the aid of the enhancer. Each was found to contain some detail that was either missed or difficult to see without enhancement.

In a more recent report, Jacoby<sup>19</sup> described his ongoing investigations in the use of automatic computer-based signal processing techniques for image enhancement of radiographs of aerospace composite structures. He begins by pointing out that improvement of the visual image does not mean finding increasingly small flaws more reliably, but that an NDT technique should detect all the flaws that would adversely influence the performance of the composite structure. "The problem," Jacoby explained,

18. VARY, A. *Investigation of an Electronic Image Enhancer for Radiographs*. Mater. Eval., December 1972, p. 259-267.

19. JACOBY, M. H. *Nondestructive Testing of Composites*. Proc. of the Inst. of Environmental Sciences, Tech. Paper, Lockheed Missiles and Space Co., Sunnyvale, California, 1980.

"is due less to the NDT techniques themselves than to the current dependency on subjective evaluations of data by inspectors. The lack of consistency in the interpretation of X-ray images has been called 'the weakest link' in the whole inspection process."

Automatic computer-based signal processing techniques improved the interpretation and evaluation of NDT data in two important ways. First, the data was enhanced to accentuate details which would otherwise not be apparent to the observer and second, the enhanced data was automatically evaluated by the computer, and the item was accepted or rejected on the basis of a predetermined defect size criterion without relying exclusively on the subjective interpretation of an inspector.

The paper described how several new and innovative signal processing techniques for image data enhancement and restoration have been combined to provide an automatic computer-based method for measuring voids on radiographs of graphite/epoxy composite structures. The techniques employed included high-pass filtering, low-pass filtering (smoothing), thresholding, requantization, and contrast stretching to produce a binary image from a radiograph. Then the computer--in this case a Data General Eclipse 130--evaluated the binary image, counted voids, measured them, and either accepted or rejected the item.

Once an optimum quality radiograph had been obtained, the image enhancement system began its automatic analysis. The first step was to scan the radiograph with a Sierra Scientific LSV TV camera, 1.5. The resulting video output was digitized by a Biomation A/D converter, and the digitized image was stored in the computer memory as a 512 x 512 pixel (picture element) array - each pixel quantized to one of 512 gray shades (from black to 0, to white at 511). The radiograph was thus converted into a form that the computer could manipulate and analyze. See Figure 31 (given as Figure 1 by Jacoby<sup>19</sup>). The contrast of the digitized image was then stretched to accommodate the full gray scale range. (This was a simple proportioning operation.) See Figure 32 (given as Figure 2 by Jacoby<sup>19</sup>).

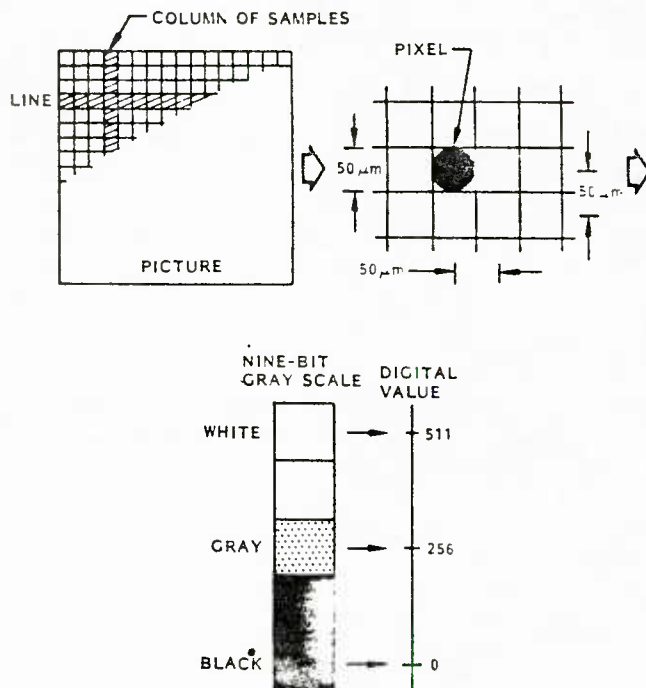


Figure 31. Sampling and digitizing an image.<sup>19</sup>



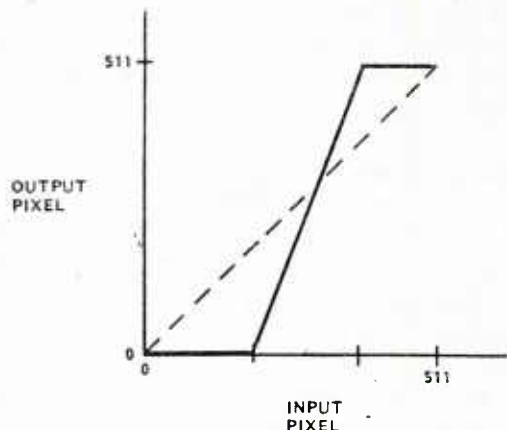
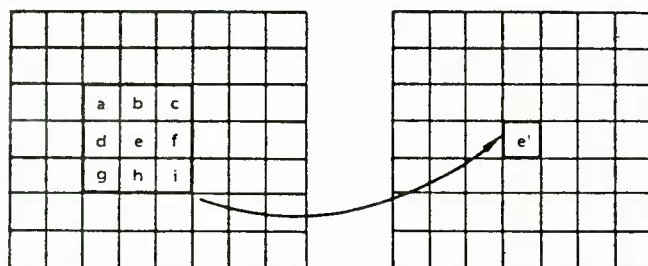


Figure 32. Contrast stretching.<sup>19</sup>

Since unwanted noise signals were introduced by the TV camera preamp and increased exponentially with optical density on the radiograph, they had to be minimized by "smoothing" the digitized image using low-pass filtering. That is, the effect of random noise was statistically nullified by producing a second 512 x 512 pixel array where each new pixel,  $e'$ , was assigned a new gray scale value taken as the average of its former location value,  $e$ , averaged with those of its eight adjacent pixel neighbors. See Figure 33 (given as Figure 3 by Jacoby<sup>19</sup>). It was also pointed out how another troublesome feature, image density gradient, which occurs in radiographs of complex shaped specimens, could be removed by curve fitting and rescaling. The technique, called "field-flattening," fits a polynomial to the observed image density gradient, subtracts the original and fitted curves, and displays the remainder which results in a mapping of defect locations. See Figure 34 (given as Figure 4 by Jacoby<sup>19</sup>). The process is performed on a line-by-line basis over the whole X-ray image and demonstrates the extraordinary value and capability of the computer.

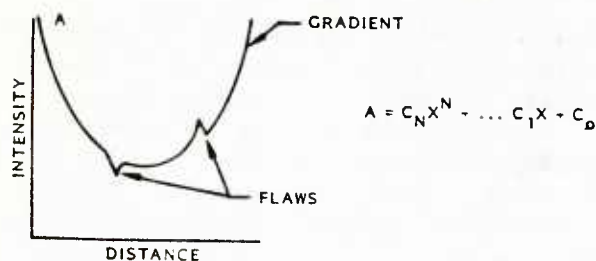
After the field flattening process, the image was then "thresholded" to locate flaws such as voids, cracks, and porosity; i.e., after some preliminary statistics had been calculated, a square window size (typically 35 x 35 pixels) was arrived at through which pixels were observed as a group or array. The window size was set so that approximately 10% (statistically) of the pixels were below a certain threshold density. Each array of pixels which was below the threshold density was labeled a *candidate flaw pixel*. In this particular candidate pixel array, all pixels below the threshold were turned into a white binary image (marked 511), and all pixels above the threshold were turned into a black binary image (marked 0). See Figure 35 (given as Figure 5 by Jacoby, Ref. 19). This technique highlighted the candidate



$$e' = \frac{1}{9} (a + b + c + d + e + f + g + h + i)$$

Figure 33. Low-pass filtering. The value of pixel  $e$  is replaced by  $e'$  calculated as shown.<sup>19</sup>





- FOR A WINDOW (TYPICALLY 35 x 35 PIXELS), PRODUCE A HISTOGRAM OF INTENSITIES IN THE WINDOW
- SET A THRESHOLD SO THAT N% (TYPICALLY 10%) OF THE PIXELS PASS THE THRESHOLD TEST
- THE N% OF PIXELS ARE CONSIDERED CANDIDATE FLAW PIXELS

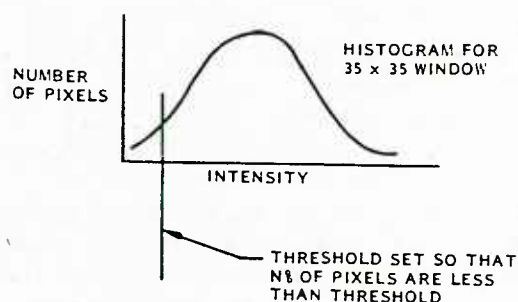
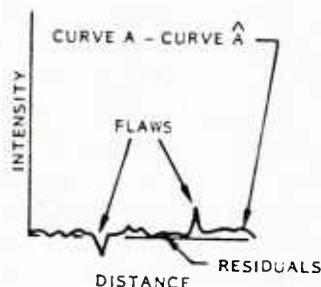
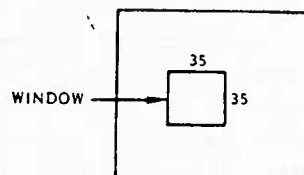
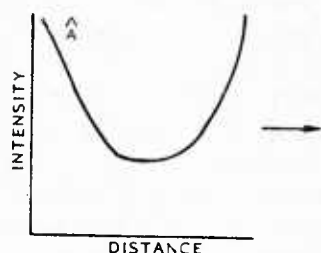


Figure 34. Field flattening.<sup>19</sup>

Figure 35. Thresholding.<sup>19</sup>

array in full contrast. (If white pixels overlapped row-to-row vertically or horizontally, the entire 35 x 35 pixels were grouped together as one defect group and imaged white; if not, the entire array was imaged as some weighted gray tone.) See Figure 36 (given as Figure 6 by Jacoby, Ref. 19). The defect candidates had thus been judged and imaged as enhanced flaw locations. This was done over the entire radiograph on a window-by-window basis to produce a binary image.

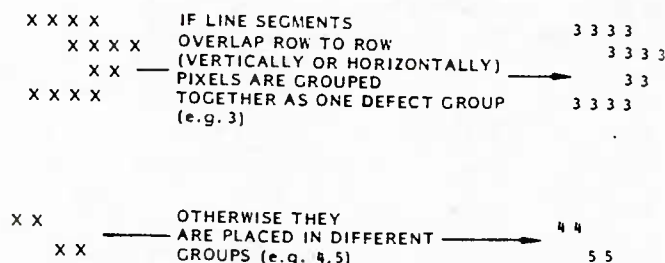


Figure 36. Grouping flaw pixels by line overlap.<sup>19</sup>

In the final step, the flaw sizes (adjacent areas of white defect group locations) were measured by the computer and a report was printed out. The report listed the number of flaws falling within specified flaw size ranges. The results were compared against predetermined specifications, and the specimen was either accepted or rejected by the computer. The radiographer simply positioned the film on the light table under the TV camera and instructed the computer where to search. Control then reverted to the computer, and the analysis of the film was done automatically.

In another similar paper,<sup>20</sup> Jacoby describes an investigation of a glass-wrapped, rubber insulated, cylindrical pressure vessel. In this investigation, field flattening was performed to eliminate the density gradients caused by the cylindrical shape of the specimen. This was followed by a specially developed spacial filtering technique using Fourier analysis to decompose the two-dimensional matrix of brightness values that represents the image into a linear combination of elementary functions. The filtered spectrum is then transformed back into the image domain to clearly reveal cuts in the rubber insulation. The image was then smoothed to reduce noise indications and to permit efficient evaluation by the computer. In this way, a small vertical cut on the left-hand side of the filtered image and a high-density inclusion (neither of which were perceived on the original radiograph) became apparent.

In another report, Roberts and Vary<sup>21</sup> described the computer facility at the NASA-Lewis Research Center and how it was used to provide enhanced radiographic images in near real time of a carbon-fiber-reinforced epoxy composite fan frame ring for an aircraft gas turbine. The results of inspections by ultrasonic C-scan and paper radiography were also shown. The two methods of digital image enhancement used were brightness (or contrast) expansion and high-pass filtering. These were not applied to a radiograph, but to a thin-film radiographic sensing search which sensed an X-ray field at one face and displayed a visible image on its opposite face. A television camera accepts the visible radiation, converts it to a standard television signal, and passes it on to the computer for image enhancement.

The ultrasonic C-scan showed only the extent of delamination damage, while the radiograph clearly delineated the damaged areas. The electronic images showed the same damaged areas as the radiograph, as well as subtle variations in the damaged zones that were not evident in the radiograph.

This preliminary study showed that digital image analysis offers the advantage of immediate results, while revealing radiographic information that would not otherwise be evident in a conventional radiograph. Two types of irregularity were evident in the multi-ply composite element. One was major mechanical damage producing broken fibers and separated plies. The other was the junction of differently-oriented plies. For these types of irregularities in this type of material, computer-assisted radiographic inspection was clearly superior to either ultrasonic C-scan or film-based radiography.

In another report, Yakushev and Dolmatovski<sup>22</sup> used an X-ray fluoroscopic (visual) and photographic method to monitor erosion-resistant asbestos plastic articles for

20. JACOBY, M. H. *Image Processing for Nondestructive Evaluation*. Tech. Paper, Lockheed Missiles and Space Co., Sunnyvale, California, 1980.

21. ROBERTS, E., and VARY, A. *Inspection of Composites Using a Computer Based Real Time Radiographic Facility*. NASA-TM-X-73504, 1976.

22. YAKUSHEV, V. F., and DOLMATOVSKI, M. G. *Monitoring the Quality of Asbestos Plastics by an X-Ray Method*. Sov. J. NDT, v. 10, no. 6, November - December 1974, p. 727-729.

nonuniform reinforcement distribution, voids, differences in resin content, and degree of cure. Low kilovoltage, soft X-radiation was used to produce images on both high-contrast (slow) film, and on a visual fluorescent screen with a magnification of 1.5. In this investigation, the film images were found to be superior to the visual fluoroscopic examination, revealing structural inhomogeneities and regions of differing binder concentration, whereas the visual fluoroscopic screens revealed only the structural inhomogeneities.

In another report, Holloway, Shelton and Mitchell<sup>23</sup> have overviewed the field of radiographic image processing. They concluded that many trade-offs exist between resolution, sensitivity and speed. Whatever trade-off is made, the improvements frequently come at the expense of greater initial capital investment.

The results of their paper suggest several potential advantages of image processing:

- greater operator convenience and less fatigue,

- less time between the discovery of an anomaly and initiation of corrective action,

- decreased direct inspection cost,

- fewer rejects at later stages of production run.

The greatest disadvantage is the increased cost of the equipment.

Another report by Johnson<sup>24</sup> on the use of computer-based radiographic inspection emphasizes that this type of process reduces corrective response time sufficiently to close the loop in a manufacturing-inspection process at minimal loss of sensitivity. Furthermore, Johnson demonstrated that it is neither necessary nor desirable to reject all but flaw-free products. Economics dictates that discontinuities smaller than some limit-value should not be rejected. Thus, the major reason for introducing a computer into the inspection process is to reduce variability, not necessarily to increase sensitivity.

## Stereoradiography

In order to determine the depth of a flaw within a specimen, a number of stereo methods have been devised. These methods involve the making of a pair of radiographs of the same specimen, but with the tube head either shifted laterally or rotated with respect to the perpendicular to the film plane. These radiographs are then examined simultaneously and, with suitable markers placed on the specimen surfaces, the depth location of the defect within the specimen can be determined.

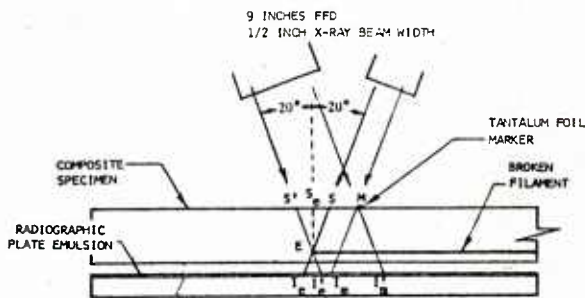
In one of these methods, commonly termed stereoradiography, two radiographs are made from two positions of the X-ray tube separated by a nominal inter-eye distance. The radiographs are then viewed with a stereoscope, a device which permits the left eye to see only the left eye position radiograph and the right eye to see only the radiograph made in the right eye position. With this viewing technique,

23. HOLLOWAY, J. A., SHELTON, W. L., and MITCHELL, J. *Image Processing of Industrial Radiographs*. AFML-TR-75-46, March 1975.

24. JOHNSON, D. P. *Inspection Uncertainty: The Key Element in Nondestructive Inspection*. Mater. Eval., v. 34, no. 6, June 1976.

the brain causes the image to be seen in its correct 3-dimensional spacial relationship, as with normal vision, and defects are seen to stand out. This method, however, does not readily afford an actual depth measurement of a defect, but serves to provide spacial visualization.

With another technique, termed double-exposure or parallax method, an actual depth measurement can be made. In a recent report by Martin, Moore and Tsang,<sup>25</sup> a double-exposure method was used to measure the depth location of boron filament defects in a metal matrix composite. In order to obtain clear filament definition, a narrow-beam microradiography technique was used to make a stereographic pair of radiographs taken at known offset angles to the titanium-boron specimens. Using the measured shift of a known marker location, the depth of the defect was calculated by triangulation. Figure 37 (given as Figure 3 in Ref. 25) clearly illustrates the derivation and set-up used in making the two triangulation radiographs from which the measurements for the defect depth determinations ( $S_e E$ ) were made. The  $20^\circ$  triangulation angle was a nominal value selected to minimize the effect of errors in setting up the equipment. A small source-to-film distance was selected to reduce exposure time. A marker was made from 0.002-in. thick tantalum foil. Distance measurements were made at 100X magnification with a microscopy equipped with a filar eyepiece. From these measurements, the distances  $I'_e I'_m$  and  $I_e I_m$  could be computed.



To find the depth of the broken filament ( $S_e E$ ) by radiographic triangulation, set a marker (M) on the specimen and take two exposures at  $\pm 20$  degrees from the normal to the composite surface. The image distances  $I_e I_m$  and  $I'_e I'_m$  can be measured on the radiograph. The defect depth  $S_e E$  can be determined by solving the right triangles  $S'S_e E$  or  $SS_e E$ . This is done as follows:

1. Note that  $S'M - SM = S'S$ ,  
and  $S'M = I'_e I'_m$  and  $SM = I_e I_m$ .
2. Therefore  $S'S = I'_e I'_m - I_e I_m$ .
3. Since  $S_e S = S'S/2$ ,  
then  $S_e S = (I'_e I'_m - I_e I_m)/2$ .
4. Solving right triangle  $S_e SE$  gives  $S_e E = S_e S \cot 20^\circ$ ,  
or  $S_e E = (I'_e I'_m - I_e I_m)/2 \times \cot 20^\circ$ .

Figure 37. Derivation of relationship for determining defect depth.<sup>25</sup>

From the results obtained, the authors calculated the defect depth to be 0.009 inch. The composite had been fabricated using four layers of 4-mil boron filaments alternately sandwiched between five 0.0008-in. thick titanium alloy sheets. After diffusion bonding, the composite thickness was 0.045 in., which gives a nominal thickness of 0.009 in. for each layer; thus the defect was located in the first filament layer under the X-ray entry surface.



## Opaque Additives and Image Enhancement

In an early work by Shelton,<sup>26</sup> significant improvements were made in image quality and sensitivity by impregnating subject materials with contrasting liquids, such as tetrabromethane (TBE), to increase image definition of voids and small cracks in graphite, and to provide clearer weave patterns in composite materials.

The radiography of graphite presents certain difficulties; at X-ray energies where differential absorption is greatest, graphite, because of its low atomic number (Z), is more effective as a scatterer than as an absorber of radiation. Therefore, the processes of scatter and absorption occur at the same time and are in conflict. This difficulty becomes even more pronounced as the graphite shapes become more complex. Radiographic images of graphite rocket nozzle inserts, nose tips, nose cones, etc., are often unclear and lack sharpness around the edges. To overcome this problem, one approach taken by Shelton was to impregnate the materials with a solution of a higher atomic number compound so that differential absorption of the X-rays would improve the contrast on the resultant radiograph, and greater resolution of the structure of the material would be obtained. Tetrabromethane (TBE) was selected for this work.

Multidirectional carbon/carbon composites and graphite of various thicknesses were used as the materials to be impregnated. The impregnation procedure involved four basic steps:

- 1) Preparation of the specimen by removal of moisture and surface contamination.
- 2) Contacting, as by soaking or sponging the specimen with tetrabromethane solution for a period of time sufficient to allow the TBE to penetrate into the cracks or voids present in the specimen.
- 3) X-raying the impregnated specimen.
- 4) Removal of the impregnant from the specimen.

The time required for impregnating the piece to be inspected depends upon the thickness and the porosity of the material. The TBE can be completely removed from the impregnated article by evaporation with heat and pressure. A well ventilated area is necessary because TBE is toxic. Demonstration of the practical application of this technique was accomplished on eleven three-D multidirectional carbon/carbon rocket nozzle inserts. The radiographs of the impregnated inserts were much clearer and contained more detail, revealing the presence of cracks and pores that were not discernible when TBE was not used. Even the multidirectional nature of the laminated composite could be detected. Assurance that the TBE had been completely removed was obtained by radiographing an item before the TBE had been applied and after it was removed, and comparing the two radiographs. In general, therefore, the impregnation technique using TBE as an opaque additive gave much more detail to the shape of the pores and their interconnection. Other conditions, such as microcracks, were also made evident.

26. SHELTON, W. L. *Improved Radiographic Techniques for Graphite and Carbon/Carbon Composite Materials*, Proc. 8th Symp. on Nondestructive Evaluation in Aerospace Systems and Nuclear Applications, San Antonio, Texas, April 1971, p. 134-154.

In a graphite-epoxy composite investigation, Chang and Couchman et al<sup>27</sup> used the TBE opaque additive technique to monitor damage zone growth, matrix cracks parallel to fibers and delaminations between plies. A conventional X-ray technique is not suitable for the detection of delaminations in graphite-epoxy or carbon-epoxy composites, partly because carbon has a low attenuation coefficient for X-rays. Small differences in attenuation caused by planar delaminations and voids are indistinguishable on a radiograph. In this investigation, center-slit specimens were fabricated from Modmor II/Narmco 5208 graphite-epoxy laminates with orientations of (0/±45), (0/±45/90), and (±45). Tensile ramp and sawtooth cyclic loadings at different levels were applied to these specimens in an effort to correlate a failure mechanism with the level and mode of loading by monitoring the real-time damage zone growth. The X-ray technique consisted of introducing the opaque additive, TBE, into a prepared center-slit opening in the specimen using a hyperdermic syringe. As the stress level in the neighborhood of the slit area was increased by increasing load, the TBE in the slit opening tended to enter the voids and delaminations by capillary action. The additive was found to have no deleterious effect on the matrix and fibers. When the testing time exceeded 2 hours, it was necessary to reapply the TBE to compensate for evaporation loss.

The experimental results were presented in the form of a time-sequence of radiographs of damage zones and plots of the damage length as a function of stress level, see Figures 38 and 39 (given as Figures 5 and 6 by Chang, Couchman et al<sup>27</sup>). It was

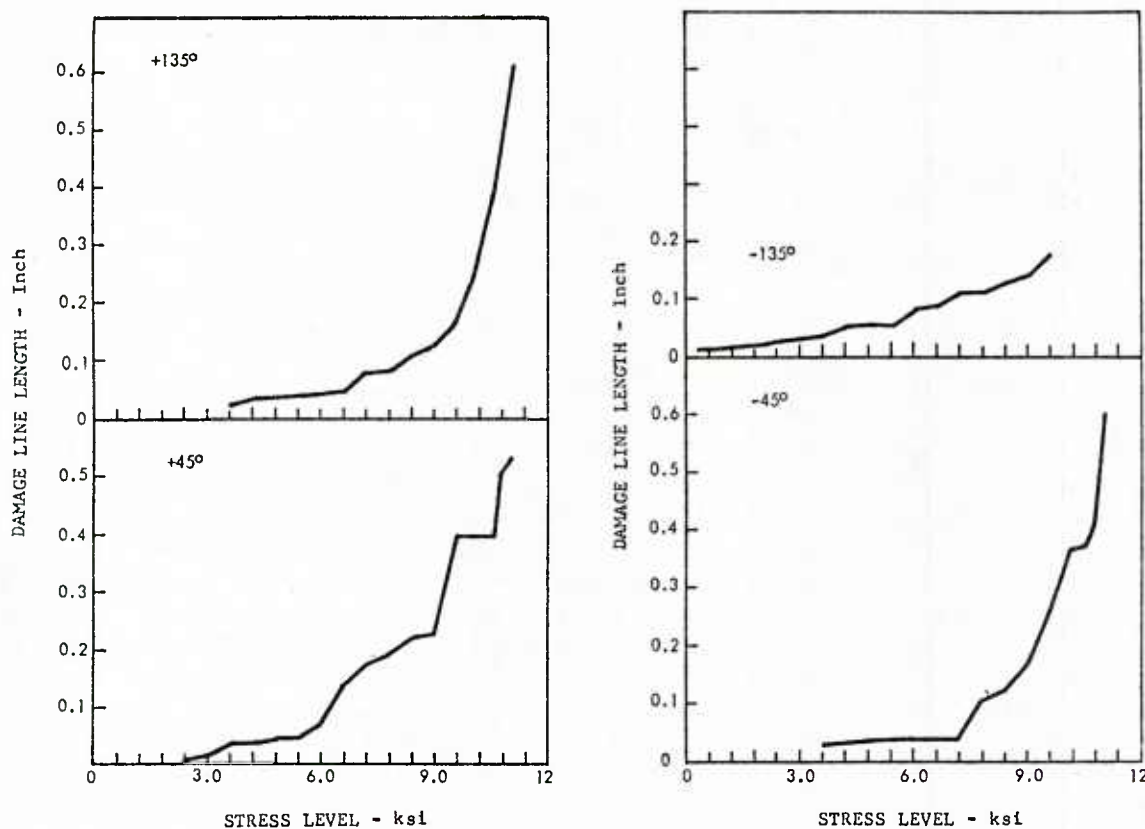


Figure 38. Damage line growth for a  $[\pm 45]_{3s}$  specimen under ramp loading.<sup>27</sup>

27. CHANG, F. H., COUCHMAN, J. C., EISENMANN, J. R., and YEE, B. G. W. *Application of a Special X-Ray Nondestructive Testing Technique for Monitoring Damage Zone Growth in Composite Laminates*. ASTM-STP 580, 1975, p. 176-190.

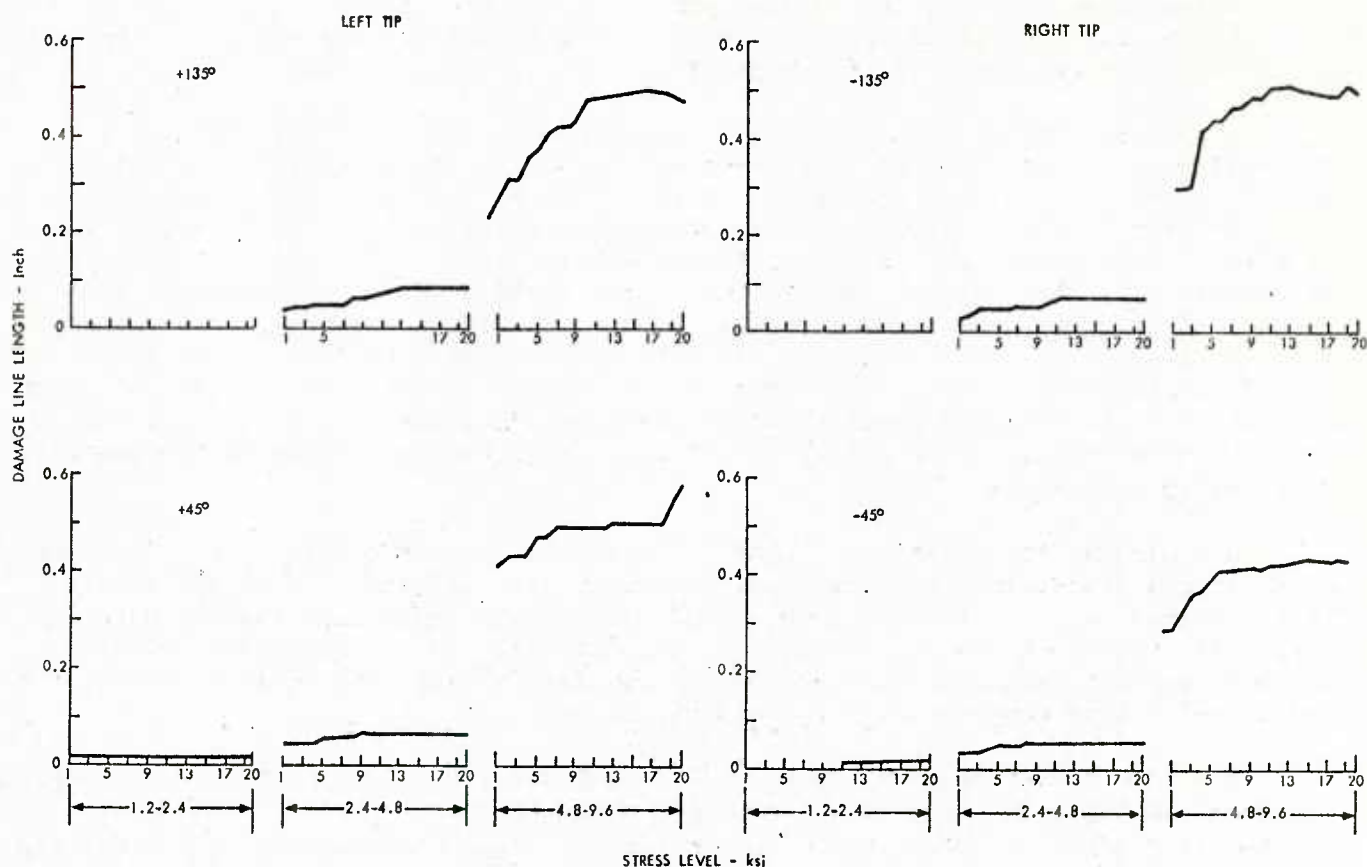


Figure 39. Damage line growth for a  $[\pm 45]_{3s}$  specimen under cyclic loading.<sup>27</sup>

established that this modified X-ray technique using TBE as an opaque additive can be very helpful in enhancing the radiographic image and in assessing the damage growth zone surrounding discontinuities in fibrous composite laminates. The method is efficient and can be economically applied in real time for stress concentration studies in composites. In addition, it was found that this technique can be used simultaneously with an acoustic emission monitoring technique for residual serviceability evaluation of composite components.

In a follow-up study of the same three types of graphite-epoxy composites, Chang and Gordon et al<sup>28</sup> employed the same technique of adding TBE to slits in the specimens to more fully characterize damage growth. Again, using specific tensile ramp loading and constant amplitude cyclic loading, it was evident that the main reason the specimen under cyclic loading could withstand higher stress was because sufficient time had elapsed for the load to be redistributed as the damage propagated.

In addition, the failure mechanism for this type of composite was made observable by the introduction of TBE. Specifically, the question of whether matrix crazing or delamination between plies occurred first appeared to be resolved. It appeared that delaminations always originated from damage lines caused by matrix crazings.

28. CHANG, F. H., GORDON, D. E., RODINI, B. T., and McDANIEL, R. H. *Real-Time Characterization of Damage Growth in Graphite/Epoxy Laminates*. J. Compos. Mater., v. 10, July 1976, p. 182-192.



Once delamination started, the failure process would be accelerated until total failure occurred. The modified TBE X-ray technique also allowed the actual stress redistribution, characteristic of this type of laminate, to be observed.

In a related study, Sendeckyj<sup>29</sup> investigated the effect of TBE-enhanced X-ray inspection on fatigue life of graphite-epoxy composite specimens in order to either support or dispel fears of the unknown effects of the penetrant on the post-inspection behavior of these composites. He noted that some investigators had suggested TBE as being a good penetrant and, thus, a good wetting agent. Therefore, there exists the possibility that TBE may be absorbed by the resin leading to changes in the mechanical properties of the composite. Also noted was the existing possibility of dissociation of the TBE, leading to evolution of nascent bromine which is known to plasticize graphite fibers. Based upon a statistical analysis of the data obtained from the fatigue tests of graphite-epoxy specimens, Sendeckyj reported there is no statistical evidence for an effect of TBE-enhanced X-ray inspection on fatigue life of ( $\pm 45$ ) graphite-epoxy.

In a similar study, Ratwani<sup>30</sup> investigated the unknown effect of diiodobutane (DIB) on the post-inspection compression fatigue life of graphite-epoxy laminates. Test specimens were fabricated from a (0/ $\pm 45$ /90/0/ $\pm 45$ ) laminate using the Hercules AS/3501-6 graphite-epoxy system with and without DIB. He concluded that DIB does not have any detrimental effect on the compression fatigue life of this type of composite under room temperature dry environments.

In a more recent study by Sendeckyj, Maddux and Tracy,<sup>31</sup> side-by-side comparisons of damage indications obtained by using TBE-enhanced X-ray, through-transmission ultrasonic C-scan, and holographic nondestructive inspection methods on various composite specimens were presented and discussed. Specific results were presented for (a) graphite-epoxy specimens containing fatigue induced damage regions from surface notches and through-the-thickness circular holes and (b) hybrid composite specimens containing static loading induced damage regions near central through-the-thickness slits. The results showed that the TBE enhanced radiographic method gives the most detailed information on the nature and planar distribution of damage. It is capable of finding fiber fractures, matrix cracks and delaminations. The ultrasonic C-scans gave the least information. The holographic method, using thermal loading, provided information on delaminations near the specimen surfaces and cracks in the surface plies. This information, in conjunction with that provide by the TBE-enhanced radiographs, gave an accurate description of the damage region.

The authors also made the following recommendations: (1) an X-ray opaque fluid that is not as toxic as TBE should be found and used in future applications, and (2) a procedure for using enhanced radiographs for getting information on the through-the-thickness distribution of damage in composites should be developed. X-raying the specimen edgewise, making stereo-pair radiographs and constructing a three-dimensional X-ray image of the damage by using tomography were suggested as possibilities.

29. SENDECKYJ, G. P. *The Effect of Tetrabromomethane-Enhanced X-Ray Inspection on Fatigue Life of Resin-Matrix Composites*. Compos. Tech. Review, v. 2, no. 1, Winter 1980, p. 9-10.

30. RATWANI, M. M. *Influence of Penetrants Used in X-Ray Radiography on Compression Fatigue Life of Graphite/Epoxy Laminates*. Compos. Tech. Review, v. 2, no. 1, Winter 1980, p. 10-12.

31. SENDECKYJ, G. P., MADDUX, G. E., and TRACY, N. A. *Comparison of Holographic, Radiographic, and Ultrasonic Techniques for Damage Detection in Composite Materials*. Proc. of 1978 Int. Conf. on Composite Materials, Toronto, Canada, April 1978, p. 1037-1056.



In another study using opaque additives for radiographic stereo-mode image enhancement, Joiner<sup>32</sup> investigated carbon-epoxy specimens impregnated with molten sulphur to better reveal the extent and distribution of voids. Shear and transverse strength measurements were also made on the composites, and the effect of voids on these properties was investigated.

For the radiographic examination, the specimens were impregnated under vacuum with molten sulphur at 140°C for 4 hours. The specimens were then cooled and excess sulphur was removed using very fine emery paper to give a visually clean surface. The specimens were then radiographed in a light tight box by exposure to 12 kV X-rays for 30 seconds at a source-to-film distance of 25.4 cm and an offset angle of 11.5 degrees. The samples were then rotated by 180 degrees and a second radiograph taken. This formed a stereoradiographic image pair allowing easy examination of the void distribution throughout the sample.

This work indicates that the modified radiographic technique used is capable of determining the extent and distribution of voids in carbon-fiber composites. Voids of micron size were detected and their effects on composite shear and transverse strengths were demonstrated and explained. Joiner says that, if it can be established that sulphur impregnation does not have a significant effect on the composite properties, the present examination technique will be capable of extension to form the basis of a nondestructive testing technique for the quality control assessment of fabricated items.

In another recent and somewhat imaginative image enhancement investigation by Crane, Chang and Allinikov,<sup>33</sup> it was shown that the addition of boron fibers to the edges of graphite-epoxy prepreg tapes facilitated the radiographic inspection of both the distribution and integrity of fibers on a tape-by-tape level within the component. The technique consisted of adding a boron fiber to the edges of each composite tape. This extra fiber was first coated with a dilute solution of the epoxy matrix and methyl ethyl ketone and then dusted with a powdered fluorescent dye to enhance its visibility. The coated fiber appeared as a distinct bright yellow line against the black background of the graphite tape (during fabrication) and would permit automated inspection of the tape position with simple optical readers.

Since the ability to radiographically see the individual tungsten cores of the boron fibers in thick laminates was open to question, a 50-ply thick composite plate with boron fiber additions was fabricated and examined. The plate was radiographed using 25 kV and 3 mA for 120 seconds on Type M Kodak film. Remarkably, almost all the boron fibers were clearly visible on the radiograph, except in a few cases of overlap. The tungsten core of the boron filament, since it is more radiographically opaque, permitted a tape-by-tape level examination for ply orientation and sequencing, fiber washing and waviness and ply overlap or underlap. A three-point bending test performed on the composite suggested that the small addition of the boron fibers did not affect the mechanical properties.

The authors felt that two points concerning the use of boron fibers in graphite-epoxy composites should be mentioned. First, the use of boron marker fibers would be limited in their application to composite structures where the radius of curvature is greater than approximately 0.635 cm, depending on the strength of the boron fiber

32. JOINER, J. C. *The Determination of Voids in Carbon Fibre Composites*. Report AQD/NM-000296, 1974.

33. CRANE, R. L., CHANG, F., and ALLINIKOV, S. *The Use of Radiographically Opaque Fibers to Aid the Inspection of Composites*. Mater. Eval., v. 36, no. 10, September 1978, p. 69-71.

used. Second, it was pointed out that since the boron in the fiber is more dense to neutrons than the surrounding composite, it would also serve as a marker fiber for a neutron radiograph of the structure. Information concerning the internal structure of the composite could be easily obtained using this technique since the boron sheath of the fiber is larger by a factor of 40 than the tungsten boride core.

In a recent overview study by Prakash<sup>34</sup> on nondestructive testing of composites, a number of NDT techniques, including microradiography, were evaluated for their applicability to assess internal features such as voids, fiber volume fraction, fiber wash or misoriented fibers, interlaminar and translaminar cracks, lay-up orders, latent defects, etc. Prakash also commented on the use of opaque additives. The two types of composite samples used for this study were carbon fiber-reinforced plastics (cfrp) and glass fiber-reinforced plastics (grp). Cfrp samples were made with commercially available carbon fiber prepeg sheet containing HM-S (Type 1) carbon fibers in 828/DDM/BF<sub>3</sub>400 epoxy resin and using a compression molding technique. Grp samples were made with E-glass fibers and epoxy resin by the hand lay-up method. The samples were made to deliberately contain a wide spectrum of internal defect features.

For the radiographic studies, a commercially available low voltage beryllium window X-ray generator was employed. For 2.5-mm thick cfrp laminates, good radiographs were obtained using a 7 minute exposure time with 12 kV and 0.5 mA.

It was found that radiographs provide a good overall view of frp laminates under inspection (e.g., general fiber orientation, fiber wash or misorientation, fiber kinks, or wrinkles, etc.) and foreign objects or inclusions are easily detected. Cracks aligned parallel to the direction of X-ray beam travel (i.e., translaminar cracks) are also readily revealed. Thermal or shrinkage cracks are generally present in the form of translaminar cracks, especially in cross-ply cfrp laminates, because of the thermal anisotropy of various prepreg layers. These cracks can best be detected using an X-radiography technique.

It was also determined in this study that X-radiography does not appear suitable for the measurement of fiber volume fraction. Interlaminar defects, such as voids, do not have an appreciable dimension in the direction of X-ray beam travel and are therefore not detectable by this technique.

Prakash concluded his discussion on radiography of composites by commenting on the feasibility of some of the recently developed techniques. Regarding the use of a sulphur penetration technique to enhance void images, he notes that the rate of sulphur penetration into microvoids in large structures may be too slow to be of any use on economical grounds, and that the effects of sulphur impregnation on the mechanical properties has not been established and may prove to be impractical. In reference to the impregnation of delaminated specimens with a dense filler (lead oxide in a gelatin) to obtain radiographs which provide an indication of the degree of delamination cracking, Prakash notes that total penetration of the crack cannot be guaranteed.

He also notes that, if tracer filaments of high density (such as lead silicate) are introduced while making the laminate, it may be possible to follow the lay-up, but that the results obtained cannot be totally relied upon because tracer fibers may not move in the same manner as the surrounding fibers.

34. PRAKASH, R. *Nondestructive Testing of Composites*. Composites, October 1980, p. 217-224.

In a final comment, Prakash notes that the technique of micro-radiography or X-ray microscopy, which consists of cutting a very thin slice of an frp sample, obtaining a radiography, and subsequently optically enlarging the radiograph, has also been used to establish fiber orientation, etc., in grp and cfrp samples, but that it is difficult to visualize how this technique could be applied on a production scale.

## Neutron Radiography

Neutron radiography, like X- or gamma radiography, depends upon the differential absorption of neutrons by the specimen material. However, while X-rays interact with the atomic orbiting electrons, neutrons interact with the atom's nucleus. There is no well-ordered relationship between neutron absorption and scattering coefficients and material atomic number as there is for X-rays (where absorption and scatter generally increase with atomic number). Neutrons, particularly those with low velocities (thermal neutrons), exhibit a random variation of absorption from element to element. The range of absorption coefficients for neutrons is 0.03 to 90, considerably exceeding that for X-rays (0.13 to 4.0), which allows for greater flexibility and excellent contrast in neutron radiographs. Furthermore, elements with adjacent atomic numbers may have widely different neutron absorption coefficients, and some low atomic number elements (such as hydrogen) can attenuate neutrons much more strongly than some high atomic number elements (such as lead). Thus, thicker sections of high atomic number materials can be radiographed with neutrons in a much shorter time than with X- or gamma rays. Also, neutron radiographs can exhibit a sharp contrast between elements which have similar absorption coefficients for X- or gamma rays but quite different ones for neutrons, such as boron and carbon, cadmium and barium.

Unfortunately, however, since neutrons are unchanged particles, they exhibit negligible direct photographic effects on film, and neutron energy must be somehow converted to produce a radiographic image. Two techniques using converter foils are presently employed to accomplish this. The first technique is direct exposure wherein the film is sandwiched between two layers of foil (gadolinium, rhodium, indium, or cadmium) and exposed. The foils become radioactive when exposed to the neutrons and emit beta or gamma radiation which, in turn, expose the film to produce an image. The second technique is a transfer exposure method wherein the converter foil alone is exposed to the neutron radiation passing through the specimen. The radioactive foil is then placed in intimate contact with the film for sufficient time to expose the film and produce an image. Converter foils of gold, indium and dysprosium have been used in this technique.

The most common source of neutrons for neutron radiography is a nuclear reactor which provides a horizontal beam of thermal neutrons of high intensities but limited to only a few inches in diameter. This permits short exposure times but may require numerous radiographs for imaging large objects. Neutron beams which do not spread significantly and which contain few gamma rays are desirable for promoting high resolution in the radiographic image. Electronic and isotopic sources (such as californium-252) of neutrons are also available.

While neutron radiography is most frequently used when X- or gamma ray techniques are unable to perform a desired inspection task, it is also considered a useful complement to those techniques. For example, the detection of hydrogen pockets within a metal container are readily detected by neutron radiography. Other applications include the inspection of brazed joints, tires, printed circuits and the location of core materials in investment castings.



Neutron radiography is being explored as an inspection tool for numerous composite materials (such as boron fiber-aluminum, boron-epoxy or bonded honeycomb structures). Neutron radiography is also being used together with X-radiography to inspect fiber-reinforced plastic composites, with resin voids being detected by the neutrons and fiber orientation by the X-rays. Bondline defects in certain adhesively bonded composite/metal structures have also been accurately and reliably inspected by neutron radiography.

In a 1977 report, Dance and Petersen<sup>35</sup> used neutron radiography to inspect the structural integrity of adhesive bondlines between a laminated aluminum alloy skin and the rib/spar in an airframe wing box, see Figure 40 (given as Figure 2 by Dance and Petersen<sup>35</sup>). The laminated skin consisted of three 0.063-inch aluminum layers bonded to each other and to the rib/spar with 0.005-inch epoxy adhesive. The hydrogen content of organic materials, such as epoxy adhesives, typically ranges from 8 to 12 percent. It is readily evident, therefore, that even very thin bondlines can be easily imaged using neutron radiography. Furthermore, the neutron radiography technique is not troubled by discontinuities, such as those occurring at bondline overlap edges, as are acoustic and ultrasonic techniques. This is particularly important because of the nature of the stresses in the bonded joint. The edges should be the area of most effective inspection.

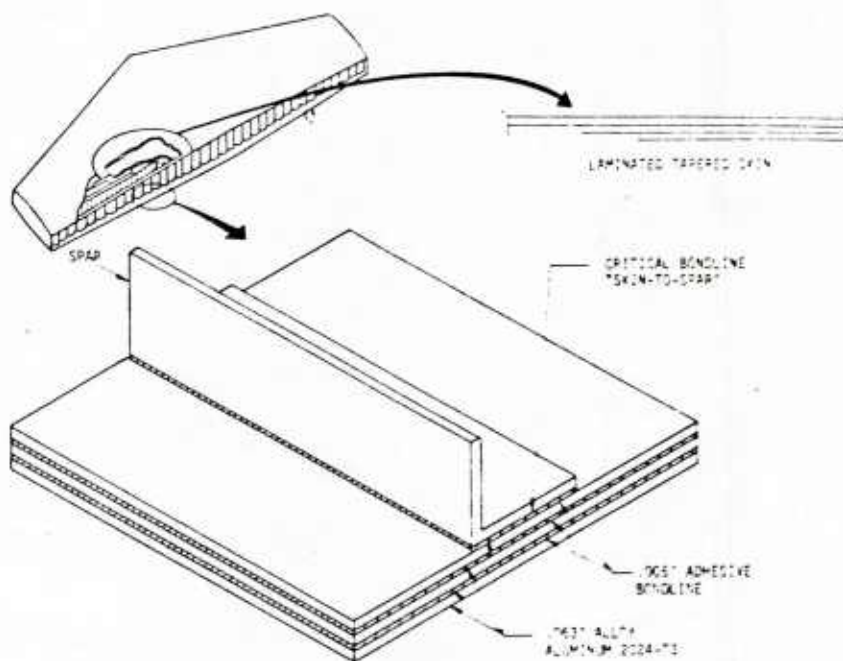


Figure 40. Adhesively-bonded primary structure test specimen.<sup>35</sup>

The authors discussed their inspection for bondline voids and gross porosity using epoxy adhesives with and without neutron radiography image enhancement additives. The two adhesives investigated were Narmco 6800 and Hysol 9512. Both were used as received

35. DANCE, W. E., and PETERSEN, D. H. *Verification of the Structural Integrity of Laminated Skin-To-Spar Adhesive Bondlines by Neutron Radiography*. J. Appl. Polymer Sci., Applied Polymer Symposium 32, 1977, p. 399-410.



from the vendor and as modified by the addition of a gadolinium oxide neutron radiography image enhancer. A number of specimen assemblies were prepared to include a variety of void fractions by the addition of different amounts of acetone to the epoxy resins prior to adhesive application.

Neutron radiographic inspection was performed using a 2.8 mg californium-252 source. The thermal neutron flux was approximately  $10^4$  n/cm<sup>2</sup>-sec. Industrial X-ray film, types SR-54 and AA were used. A 0.001-inch-thick vapor-deposited gadolinium metal film was used as a converter, see Figure 41 (given as Figure 3 by Dance and Petersen<sup>35</sup>). In addition to neutron radiographic inspection, each critical bondline, between the laminated skin and rib/spar, was tested for strength in order to correlate observed void fractions and strength predictions. Radiographs were made of all the specimen assemblies and bondline voids were clearly visible in all cases. However, it was obvious that the gadolinium oxide image enhancer significantly improved the contrast whenever used.

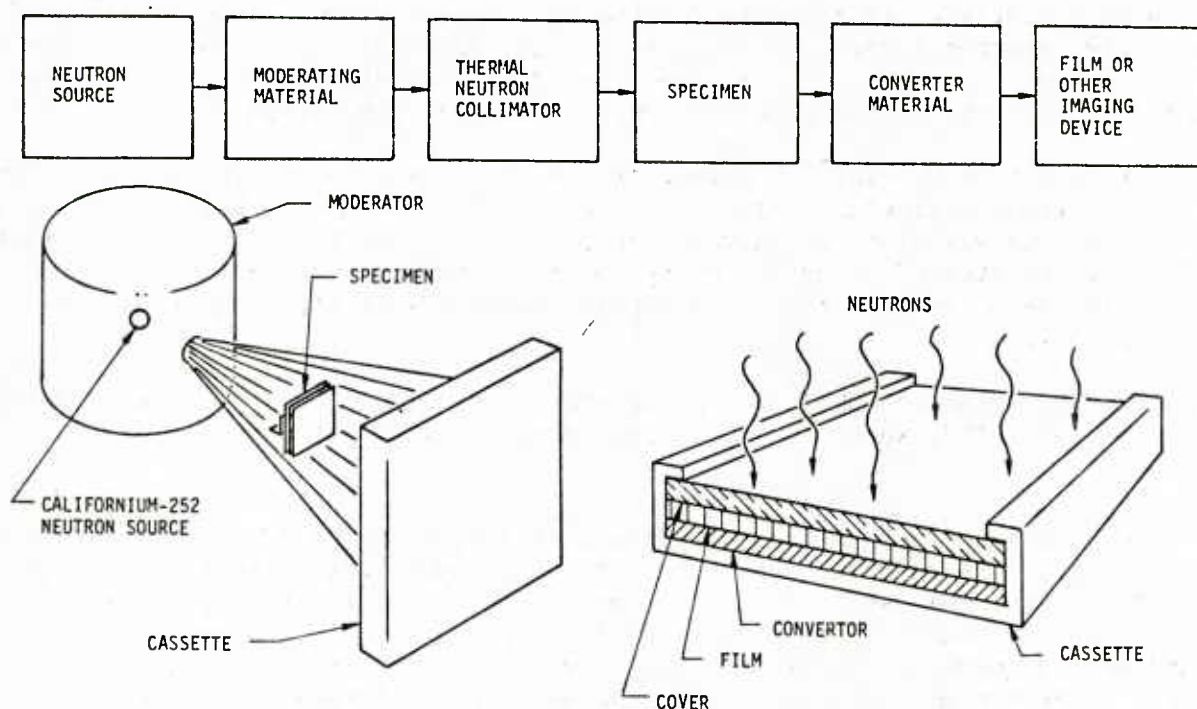


Figure 41. Neutron radiographic imaging.<sup>35</sup>

From the data obtained, the authors concluded that the value of neutron radiography for assessing the serviceability of this type of laminated structure had been clearly demonstrated. They also concluded that the use of gadolinium oxide as an image enhancer greatly improves radiographic contrast and is effective for rapid inspection and strength prediction of adhesively bonded joints.

In an early preliminary study of penetrating radiation techniques for the inspection of multidirectional reinforced resin matrix composites, Cook and Gully<sup>36</sup> investigated a number of techniques including neutron radiography, conventional film X-radiography and the X-ray Vidicom television imaging technique.

36. COOK, J. L., and GULLEY, L. R. *Penetrating Radiation Inspection of Multidirectional Reinforced Resin Matrix Composites*. Materials 1971 Proc., 16th Nat. Symp. Soc. Aerospace Materials and Process Eng., Anaheim, California, April 1971, p. 345-354.

The composites investigated included a woven quartz fiber-phenolic resin flat panel which was approximately 30 inches long, 6 inches wide and 3/8 inch thick. All of the panels were evaluated by both conventional film X-radiography and neutron radiography. Since the composite matrix material was a phenolic resin which contained hydrogen atoms of high neutron capture cross-section, it was anticipated that neutron radiography would be a successful method for defect detection. Several composite samples were fabricated. Some were doped with paraffin and some with a gadolinium salt to enhance the absorption of neutrons. In addition, several small diameter flat-bottom holes were placed in some samples to simulate defects.

The neutron radiographs of the undoped composites were no better, and usually of poorer quality than the X-ray film of the same samples. Only the addition of a doping agent, particularly gadolinium nitrate, provided the contrast and density necessary for quality radiographs. Weave irregularities in the reinforcement were better evaluated by conventional film radiography.

The authors concluded that, while further enhancement by doping may lead to improved analysis, neutron radiography must be considered of limited value for inspecting resin matrix composites. The disadvantage of utilizing a reactor source of neutrons also places restrictions on the potential application of this method.

A recent report by Martin<sup>37</sup> concerned the feasibility of measuring composite resin content by radiographic (including gauging) techniques. The use of both low kV X-rays and thermal neutrons was also considered. In particular, Martin attempted to detect resin-rich or resin-starved areas caused by porosity and curing variables. It was assumed that the X- or neutron radiation interacted only with the resin and fibers, and not the porosity.

Graphite fiber (Thornel 300) reinforced epoxy resin (Narmco 5208) composite test panels (0.25" x 4" x 10") were fabricated from prepreg tape approximately 2" wide and 0.005" thick.

Based upon calculations of the composite mass absorption coefficient versus resin content for both X-rays and neutrons, and upon roughly equivalent experimental data, Martin concluded that the use of X-rays for measuring composite resin content is not feasible because of insufficient sensitivity for detecting small changes in composite density and mass absorption coefficient due to variations in resin content. Although changes in the neutron mass absorption coefficient due to changes in the resin content are significantly larger than the corresponding situation for X-rays, Martin also concluded that the neutron film technique is not sensitive enough for practical measurement of resin content. Martin also concluded that the use of neutron gauging is feasible for detecting changes in resin content of  $\pm 1$  percent, but that further experimental work would be necessary to determine the practicality of using neutron gauging for measuring composite resin content.

In a 1972 report by Youshaw<sup>38</sup>, the feasibility of applying neutron radiography to the inspection of massive fiberglass composites was studied. There are several manufacturing anomalies, such as resin-rich regions, which are thought to be beyond

37. MARTIN, B. G. *An Analysis of Radiographic Techniques for Measuring Resin Content in Graphite Fiber Reinforced Epoxy Resin Composites*. Mater. Eval., v. 35, no. 9, September 1977, p. 65-68.

38. YOUSHAU, R. A. *Neutron Radiography of Massive Fiberglass Composite Structures Feasibility Study*. AD-752 457, 1972.

the limits of ordinary X-radiography and the other tools of nondestructive testing. In view of the low atomic numbers of the resin constituents in composites and the large cross section for reaction with neutrons for these elements, Youshaw determined that abnormalities such as resin-rich regions could be expected to react with a neutron beam.

Fiberglass sonar domes were fabricated manually by applying successive layers of resin-impregnated strips of glass fibers to a female mold, and squeezing the strips to remove entrapped air. For the neutron radiography work, gadolinium screens were selected for the prompt emission technique and indium screens for the transfer or induced method of obtaining an image.

Youshaw summarized that this study showed that the boron constituent of the fiberglass severely attenuated neutrons at thermal energies, necessitating long exposure times to obtain film darkening. Simultaneously, the hydrogen of the binding resin very efficiently scattered neutrons, which acted to fog the film. Considering the thickness of the sonar domes, Youshaw concluded that neutron radiography is not a suitable inspection tool for this item. Furthermore, it was demonstrated that conventional X-radiography can be usefully applied.

## APPENDIX

### Exposure Calculations

Example 1. A uniform two-inch-thick specimen of magnesium is to be radiographed with X-rays (Figure 18). Assuming the screening and source-to-film distance of 36" specified, determine proper exposure settings to obtain a density of 3.0 with Type 1 film (see Figure 16).

Step 1. From Table 1, with assumed low kilovoltage X-rays, the radiographic equivalence factor for magnesium is 0.6. For an equivalent aluminum thickness of 1.2 inches (2.0" x 0.6"), a 2.0 density with Type 1 film can be obtained (see Figure 18) with either of the following settings:

80 kV - 1800 mas (milliampere-seconds)

100 kV - 560 mas

120 kV - 270 mas

Since maximum subject contrast, better definition and greater sensitivity is achieved with the lowest possible kilovoltage, preliminary settings of 80 kV for 1800 mas (30 mam) are chosen.

Step 2. To adjust these 2.0 density settings for a desired density of 3.0, refer to Figure 16, Type 1 film. The log relative exposure for a 2.0 density is approximately 1.55 and for a 3.0 density is approximately 1.78. The difference between these log relative exposure values is 0.23. The antilogarithm of 0.23 is 1.70. Therefore, the exposure setting to obtain the desired 3.0 density (keeping the 80 kV setting constant) is adjusted as follows:

$$30 \text{ mam} \times 1.7 = 51 \text{ mam}$$

Step 3. A 3.0 density on Type 1 film can be obtained with setting of 80 kV and 51 mam (3 milliamperes for seventeen minutes or any other equivalent combination).

Example 2. For the two-inch-thick magnesium specimen of Example 1, determine proper exposure settings to obtain the same 3.0 density with Kodak Type 3 film. This is a slower film with smaller grains, capable of yielding higher film contrast, better definition and greater sensitivity.

Step 1. From Figure 16, the log relative exposure for a 3.0 density with Type 1 film is 1.78, and with Type 3 film is 2.12. The difference between the log relative exposures is 0.34. The antilog of 0.34 is 2.188. Therefore, the exposure setting to obtain the desired 3.0 density with Type 3 film is adjusted as follows:

$$51 \text{ mam} \times 2.188 = 111.6 \text{ mam}$$

Step 2. A 3.0 density on Type 3 film can be obtained with settings of 80 kV and 111.6 mam (5 milliamperes for 18.6 minutes or 4 milliamperes for approximately 28 minutes or equivalent). Shorter exposure time with this type film could be obtained by increasing the kilovoltage setting, but this would lessen the beneficial contrast, definition and sensitivity effects gained from using a slower film.



Example 3. A standard in radiography is that the source-to-film distance should be at least 8 to 10 times the specimen thickness. To reduce exposure time at the possible expense of image quality, it is decided that a 20" source-to-film distance be used. The exposure settings should be determined to obtain a 3.0 density for the specimen and conditions of Examples 1 and 2.

Step 1. From the inverse square law, it is known that radiation intensity varies inversely with the square of the distance. Therefore, keeping the selected kilovoltage constant, the exposure setting for a 20" source-to-film distance is adjusted by a multiplier factor of  $20^2/36^2 = 400/1296 = 0.3086$ .

Step 2. For Example 1, the exposure setting becomes  $51 \text{ mam} \times 400/1296 = 15.75 \text{ mam}$ . Therefore, a 3.0 density on Type 1 film with a source-to-film distance of 20" will be obtained with settings of 80 kV and approximately 16 mam.

Step 3. For Example 2, the exposure setting becomes  $111.6 \times 400/1296 = 34.4 \text{ mam}$ . Therefore, a 3.0 density on Type 3 film with a source-to-film distance of 20" can be obtained with settings of 80 kV and 34.4 mam.

Although this report is primarily concerned with the radiography of composite materials, exposure charts are rarely prepared for composites. Magnesium was therefore given as the specimen material in the above examples, due to the fact that it is the lightest metal listed in the radiographic equivalence factor table, and thus, serves best to approximate the range of exposure settings arrived at for radiographing composite material structures. Unless the radiographer has already prepared a specific exposure chart for the particular type of composite material under investigation, he must rely upon his past experience to arrive at a good approximation for preliminary exposure settings. Once the preliminary radiograph is developed and observed, the radiographer can then proceed to adjust the exposure settings following the same procedures used in the above examples. This process is time consuming and exacting. Moreover, since no radiographic equivalence factor table is available for commonly used composite matrix materials, a simple adjustment cannot be made when changing from one material to another, and the entire procedure must be repeated for each separate composite matrix material to be investigated.

## LITERATURE CITED

1. Army Materiel Command Pamphlet, *Quality Assurance Guidance to Nondestructive Testing Techniques*, AMCP-702-10, April 1970, p. 30-31.
2. Army Materials and Mechanics Research Center, DARCOT Training Handbook 5330.19, Radiographic Inspection, p. 2-17.
3. *Radiography in Modern Industry*. Eastman Kodak Co., 1979, p. 44-130.
4. MIL-HDBK-333 (USAF), April 1974, p. 4-34.
5. *Standard Definitions of Terms Relating to Gamma X-Radiography*. Annual Book of ASTM Standards: Part 11, ASTM DES: E586-76, p. 630-631.
6. Army Materials and Mechanics Research Center, DARCOT Training Handbook 5330.19, Radiographic Inspection, p. 4-6, 6-30.
7. SCHNITGER, D., and MUNDAY, I. E. *Improvement of Contrast of X-Ray Images by the Use of Filters Between the Specimen and Film*. Brit. J. of NDT, November 1976, p. 162-164.
8. HALMSHAW, R., and INST, F. *Radiographic Intensifying Screens*. Brit. J. of NDT, March 1972, p. 45-47.
9. DerBOGHOSIAN, S., and COATES, A. J. *Composite Screens Used as a Radiographic Aid*. Army Materials and Mechanics Research Center, AMMRC TR 81-11, March 1981.
10. HALMSHAW, R. *The Image on a Radiograph*. Proc. of a Symposium on Physics and Nondestructive Testing, Dayton, Ohio September 1964, p. 171-193.
11. OWSTON, C. N., and CONOR, P. C. *Failure Mechanisms in Carbon Fiber Reinforced Polymer and Their Relation to Non-Destructive Testing*. Composites, September 1970, p. 268-276.
12. RODERICK, G. L., and WHITCOMB, J. D. *X-Ray Method Shows Fibers Fail During Fatigue of Boron-Epoxy Laminates*. J. Comp. Mat., v. 9, October 1975, p. 391-393.
13. RODERICK, G. L., and WHITCOMB, J. D. *Fatigue Damage of Notched Boron/Epoxy Laminates Under Constant Amplitude Loading*. N77-17165/OST, Report No. NASA-TM-X-73994, December 1976.
14. ARTIS, L. J., and JOINER, J. C. *Methods of Measurement of the Relative Performance of Various Classes of Resins in Carbon Fiber Composites*. N73-31536/8, Report No. AQD/NM-000198, October 1972.
15. HUGGINS, B. E. *Radiography with Low Energy Radiation*. Brit. J. of NDT, May 1981, p. 119-125.
16. MARCUS, L. A., and STINCHCOMB, W. W. *Measurement of Fatigue Damage in Composite Materials*. Exp. Mech., v. 15, no. 2, February 1975, p. 55-60.
17. DARLINGTON, M. W., and MCGINGLEY, P. L. *Fibre Orientation Distribution in Short Fibre Reinforced Plastics*. J. of Mater. Sci., v. 10, 1975, p. 906-910.
18. VARY, A. *Investigation of an Electronic Image Enhancer for Radiographs*. Mater. Eval., December 1972, p. 259-267.
19. JACOBY, M. H. *Nondestructive Testing of Composites*. Proc. of the Inst. of Environmental Sciences, Tech. Paper, Lockheed Missiles and Space Co., Sunnyvale, California, 1980.
20. JACOBY, M. H. *Image Processing for Nondestructive Evaluation*. Tech. Paper, Lockheed Missiles and Space Co., Sunnyvale, California, 1980.
21. ROBERTS, E., and VARY, A. *Inspection of Composites Using a Computer Based Real Time Radiographic Facility*. NASA-TM-X-73504, 1976.
22. YAKUSHEV, V. F., and DOLMATOVSKI, M. G. *Monitoring the Quality of Asbestos Plastics by an X-Ray Method*. Sov. J. NDT, v. 10, no. 6, November - December 1974, p. 727-729.
23. HOLLOWAY, J. A., SHELTON, W. L., and MITCHELL, J. *Image Processing of Industrial Radiographs*. AFML-TR-75-46, March 1975.
24. JOHNSON, D. P. *Inspection Uncertainty: The Key Element in Nondestructive Inspection*. Mater. Eval., v. 34, no. 6, June 1976.
25. MARTIN, G., MOORE, J. F., and TSANG, S. *The Radiography of Metal Matrix Composites*. Mater. Eval., April 1972, p. 78-86.
26. SHELTON, W. L. *Improved Radiographic Techniques for Graphite and Carbon/Carbon Composite Materials*. Proc. 8th Symp. on Nondestructive Evaluation in Aerospace Systems and Nuclear Applications, San Antonio, Texas, April 1971, p. 134-154.
27. CHANG, F. H., COUCHMAN, J. C., EISENMANN, J. R., and YEE, B. G. W. *Application of a Special X-Ray Nondestructive Testing Technique for Monitoring Damage Zone Growth in Composite Laminates*. ASTM-STP 580, 1975, p. 176-190.
28. CHANG, F. H., GORDON, D. E., RODINI, B. T., and McDANIEL, R. H. *Real-Time Characterization of Damage Growth in Graphite/Epoxy Laminates*. J. Compos. Mater., v. 10, July 1976, p. 182-192.
29. SENDECKYJ, G. P. *The Effect of Tetrabromomethane-Enhanced X-Ray Inspection on Fatigue Life of Resin-Matrix Composites*. Compos. Tech. Review, v. 2, no. 1, Winter 1980, p. 9-10.
30. RATWANI, M. M. *Influence of Penetrants Used in X-Ray Radiography on Compression Fatigue Life of Graphite/Epoxy Laminates*. Compos. Tech. Review, v. 2, no. 1, Winter 1980, p. 10-12.
31. SENDECKYJ, G. P., MADDUX, G. E., and TRACY, N. A. *Comparison of Holographic, Radiographic, and Ultrasonic Techniques for Damage Detection in Composite Materials*. Proc. of 1978 Int. Conf. on Composite Materials, Toronto, Canada, April 1978, p. 1037-1056.
32. JOINER, J. C. *The Determination of Voids in Carbon Fiber Composites*. Report AQD/NM-000296, 1974.
33. CRANE, R. L., CHANG, F., and ALLINIKOV, S. *The Use of Radiographically Opaque Fibers to Aid the Inspection of Composites*. Mater. Eval., v. 36, no. 10, September 1978, p. 69-71.
34. PRAKASH, R. *Nondestructive Testing of Composites*. Composites, October 1980, p. 217-224.
35. DANCE, W. E., and PETERSEN, D. H. *Verification of the Structural Integrity of Laminated Skin-To-Spar Adhesive Bondlines by Neutron Radiography*. J. Appl. Polymer Sci., Applied Polymer Symposium 32, 1977, p. 399-410.
36. COOK, J. L., and GULLEY, L. R. *Penetrating Radiation Inspection of Multidirectional Reinforced Resin Matrix Composites*. Materials 1971 Proc., 16th Nat. Symp. Soc. Aerospace Materials and Process Eng., Anaheim, California, April 1971, p. 345-354.
37. MARTIN, B. G. *An Analysis of Radiographic Techniques for Measuring Resin Content in Graphite Fiber Reinforced Epoxy Resin Composites*. Mater. Eval., v. 35, no. 9, September 1977, p. 65-68.
38. YOUSHAU, R. A. *Neutron Radiography of Massive Fiberglass Composite Structures Feasibility Study*. AD-752 457, 1972.

## BIBLIOGRAPHY

### Typical Applications

- ALLEY, B. J. *X-Ray Fluorescence Analysis of Composite Propellants for Army Missile Systems*. AD-A044 686/4st, June 1977.
- ASHLEY, D. G. *Measurement of Glass Content in Fibre/Cement Composites by X-Ray Fluorescence Analysis*. NDT International, April 1979, p. 56-60.
- AWERBUCH, J., and HAHN, H. T. *Hand Object Impact Damage of Metal Matrix Composites*. J. Compos. Mater., v. 10, July 1976, p. 231-257.
- BABYLAS, E. *Radiographic Testing of Glass Fiber Reinforced Plastic Material*. AD-312 991, 1976.
- BAILEY, C. D., FREEMAN, S. M., and HAMILTON, J. M. *Detection and Evaluation of Impact Damage in Graphite/Epoxy Composites*. Mater. and Processes in Service Performance Soc. for Adv. of Mater. and Processing Eng., 9th Tech. Conf., Atlanta, Georgia, October 1977, p. 491-503.
- BASLER, G., HAMBURG, A., and SCHMEISSER, H. *Radiometric Inspection of Glass Fibre Reinforced Pipes by Means of an Image Analyzing System*. Materialpruefung, v. 19, no. 9, 1977, p. 361-365.
- BREWER, W. D., and KASSEL, P. C. *Flash X-Ray Technique for Investigating Ablative Material Response to Simulated Re-Entry Environments*. Int. J. of NDT, v. 3, 1972, p. 375-390.
- BULLOCK, R. E. *Mechanical of a Boron-Reinforced Composite Material Radiation-Induced of Its Epoxy Matrix*. J. Compos. Mater., v. 8, January 1974, p. 97-101.
- COMPTON, W. A., STEWARD, K. P., and MNEW, H. *Composite Materials for Turbine Compressors*. AD-835 373, June 1968.
- COOK, J. L. *Multidirectional Fiber-Reinforced Resin Matrix Composites*. AD-883 978/9st, February 1971.
- COOK, J. L., REINHART, W. W., and ZIMMER, J. E. *Development of Nondestructive Testing Techniques for Multidirectional Fiber-Reinforced Plastics*. AD-746 592, 1971.
- CRANE, R. L. *Measurement of Composite Ply Orientation Using a Radiographic Fringe Technique*. Mater. Eval., v. 34, no. 4, April 1976, p. 79-80.
- CRANE, R. L. *Nondestructive Inspection of Composites and Adhesively Bonded Structures*. AD-770 823, 1980.
- CRISCUOLO, E. L., and POLANSKY, D. *Application of Radiographic Specifications*. Nondestructive Testing, v. 20, no. 2, March-April 1962, p. 114-118.
- CROSSMAN, F. W. et al. *Initiation and Growth of Transverse Cracks and Edge Delamination in Composite Laminates, Part 2 - Experimental Correlation*. J. of Compos. Mater. Supplement, v. 14, 1980.
- DASTIN, S. J., and LUBIN, G. *Adhesive Bonding High Modulus Composite Aircraft Structures*. Adhesive Age, June 1971, p. 28-32.
- EPSTEIN, G. *Nondestructive Test Methods for Reinforced Plastic/Composite Materials*. AD-686 466, February 1969.
- EVANGELIDES, J. S., and MEYER, P. A. *Investigation of the Properties of Carbon-Carbon Composites and Their Relationship to Nondestructive Test Measurements*. AD-753 874/8st, August 1974.
- FRENCH, C. R. *Radiographic Examination of Large Filament-Wound, Solid-Propellant Motor Cases*. Mater. Eval., v. 24, no. 8, August 1966, p. 412-416.
- GOSSE, H. J., KAITATZIDI, M., and ROTH, S. *Testing Procedures for Carbon Fiber Reinforced Plastic Components*. N77-30182/8st, July 1975.
- HAGEMAIER, D. J. *Bonded Joints and Nondestructive Testing*. Nondestructive Testing, February 1972, p. 38-48.
- HAGEMAIER, D. J. *NDT of Aluminum-Brazed Titanium Honeycomb Structures*. Nondestructive Testing (London), v. 9, no. 3, June 1976, p. 107-116.
- HAGEMAIER, D. J., McFAUL, H. J., and MOUA, D. *Nondestructive Testing of Graphite Fiber Composite Structures*. Mater. Eval., v. 29, no. 6, June 1971, p. 133-140.
- HAGEMAIER, D. J., McFAUL, H. J., and PARKS, J. T. *Nondestructive Testing Techniques for Fiberglass, Graphite Fiber and Boron Fiber Composite Aircraft Structures*. Mater. Eval., v. 28, no. 9, September 1970, p. 194-204.
- HASTINGS, C. H., and GRUND, M. V. *Radiographic Inspection of Reinforced Plastics and Resin-Ceramic Composites*. Nondestructive Testing, v. 19, no. 5, September-October 1961, p. 347-351.
- HENDRON, J. A., GROBLE, K. K., and WANGARD, W. *The Determination of the Resin-to-Glass Ratio of Glass-Epoxy Structures by Beta Ray Back Scattering*. Mater. Eval., v. 22, no. 5, May 1964, p. 213-216.
- JONES, R. C., and CHRISTIAN, J. L. *Analysis of an Improved Boron/Aluminum Composite*. ASTM STP 497, 1972, p. 439-468.
- KOENIG, J. R., and FORNARO, G. F. *Evaluation of the Compressive Properties of a Special 3DQP*. AD-A044 031/3st, September 1976.
- LAYNE, W. S., and PATRICK, R. L. *Interfacial Interaction in Composite Structures*. AD-665 697, November 1967.
- LISIN, V. A. *A Method of Detecting a Defective Layer in Double-Layer Articles Using the Radiometric Method of Electron Flaw Detection*. Sov. J. of NDT, May 1979, p. 801-803.
- LITTLETON, H. E. *Collimated Scanning Radiography*. SAMPE Journal, May-June 1978, p. 21-23.
- LOHSE, K. H. *Application of Photographic Extraction Techniques to Nondestructive Testing of Graphites and Other Materials*. AFML-TR-70-162, November 1970.
- MAIGRET, J. P., and JUBE, G. *Advanced NDT Methods for Filament Wound Pressure Vessels and Composites in General*. Materials 1971, SAMPE 16th Nat. Symp. and Exhib., v. 16, April 1971, p. 123-137.
- MANTEI, J. E. *An Examination of Factors That Effect the Mechanical Properties of Boron-Aluminum Composites*. AD-837 408/4st, June 1968.
- MARCUS, L. A., STINCHCOMB, W. W., and TURGAY, H. M. *Fatigue Crack Initiation in a Boron-Epoxy Plate With a Circular Hole*. AD-780 106/1st, February 1974.
- MATHERS, G. B. *Nondestructive Inspection Techniques for Multilayer Circuit Boards*. Mater. Eval., v. 25, no. 6, June 1967, p. 148-152.
- MOOL, D. L., and VANNIER, R. K. *X-Ray Inspection of the AWACS Radome Attachment Locations*. Mater. Eval., October 1972, p. 211-213.



- MOORE, J. F., and MARTIN, G. *Research and Development of Nondestructive Testing Techniques for Composites*. AD-825 636/4st, AFML-TR-67-166, November 1967.
- NEVADUNSKY, J. J., LUCAS, J. J., and SALKIND, M. J. *Early Fatigue Damage Detection in Composite Materials*. J. Compos. Mater., v. 9, October 1975, p. 394-408.
- NEVADUNSKY, J. J., SALKIND, M. J., and LUCAS, J. J. *Fatigue Damage Behavior in Composite Materials*. AD/A-001 944/8st, September 1974.
- Nondestructive Testing: Radiography*. Defense Documentation Center, Alexandria, Virginia, AD-769 100/9, November 1973.
- OWSTEN, C. N., and JAFFE, E. H. *Nondestructive Testing and Inspection Applied to Composite Materials and Structures*. AD-739 780, February 1972.
- PROUDFOOT, E. A. *Nondestructive Testing Techniques for Advanced Composites*. AD-714 296, September 1970.
- REYNOLDS, W. N. *Problems of Nondestructive Testing in Carbon Fibers and Their Composites*. Int. Conf. Carbon Fibres and Their Comp., Appl. Pap., 1971, p. 52/1-52/5.
- REYNOLDS, W. N. *Testing of Fibre-Bonded Composites*. SPI Reinf. Plas./Compos. Div., Proc. 24th Ann. Tech. Conf., Washington, Sect. 14B, February 1969.
- SALKIND, M. J. *Early Detection of Fatigue Damage in Composite Materials*. J. Aircr., v. 13, no. 10, October 1976, p. 764-769.
- SCHULTZ, A. W. *Development of Nondestructive Methods for the Quantitative Evaluation of Advanced Reinforced Plastic Composites*. AD-875 229, 1970.
- STONE, D. E. W. *Nondestructive Inspection of Composite Materials for Aircraft Structural Applications*. Brit. J. of NDT, March 1978, p. 65-75.
- STONE, D. E. W. *Some Problems in the Nondestructive Testing of Carbon Fiber-Reinforced Plastics*. Carbon Fibres, 2nd Int. Conf. Proc., 18-20 February 1974, Paper 28, Plast. Inst., London, 1974.
- STONE, D. E. W. *The Use of Radiography in the Nondestructive Testing of Composite Materials*. AD-894 884, December 1971.
- WANG, A. S. D., and CROSSMAN, F. W. *Initiation and Growth of Transverse Cracks and Edge Delamination in Composite Laminates, Part 1. - An Energy Method*. J. of Compos. Mater. Supplement, v. 14, 1980.
- X-Ray Eye for Quality Control*. British Plastics, v. 42, no. 9, September 1969.
- ZURBRICK, J. R. *Development of Nondestructive Methods for the Quantitative Evaluation of Glass-Reinforced Plastics*. AFML-TR-66-269, March 1967.

### **Microradiography**

- BOOGEND, W. J., VAN ZUYLEN, P., and FONTIJN, L. A. *An Unconventional 150 kv Microfocus X-Ray Equipment for NDT Purposes*. November 1976, p. 175-178.
- FONTIJN, L. A., and PEUGEOT, R. S. *An Operational 150 kv Microfocus Rod Anode X-Ray System for Nondestructive Testing*. NDT International, October 1978, p. 229-235.
- GUGAN, K. *A Fine Focus High Intensity, Medium Energy X-Ray Source*. J. Sci. Instr., v. 42, 1965.
- HOTHAM, C. A., JONES, R. W., and TAYLOR, J. L. *Microfocal Radiography Using the Electron Microscope*. Brit. J. of NDT, November 1981, p. 306.
- SMITH, R. L. *The Effect of Scattering on Contrast in Microfocus Projection X-Radiography*. Brit. J. of NDT, September 1980, p. 236-239.
- WILLIAMS, R. D. *General Applications of Microfocus X-Ray Techniques to the Field of NDT*. 3rd Annual Symp. on NDT of Aircraft and Missile Components, 1962.

### **Automatic Computer Based Radiographic Image Enhancement**

- CLOSIER, M. J. *Automatic Product Analysis Using X-Rays*. NDT International, April 1981, p. 59-65.
- GOSSELIN, R. M. *Automatic Nondestructive Testing with X-Rays*. Brit. J. of NDT, January 1973, p. 17-22.
- HALL, E. L., et al. *A Survey of Preprocessing and Feature Extraction Techniques for Radiographic Images*. IEEE Trans. Computers C-20, no. 9, September 1971, p. 1032-1044.
- HALMSHAW, R., and JAKINS, B. G. *Optical and Digital Image Processing Applied to Radiographs*. Brit. J. of NDT, July 1977, p. 197-199.
- HARRINGTON, T. P., and DOCTOR, P. G. *Data Analysis Methods for Nondestructive Evaluation*. Battelle Pacific Northwest Labs, Report BN-SA-1056, October 1979.
- HESSE, P. W., CRISCUOLO, E. L., and POLANSKY, D. *Radiographic Image Enhancement by Spatial Frequency Filtering*. Brit. J. of NDT, July 1973, p. 101-107.
- HUNT, A. C. *The Effect of Masking in T. V. Image Intensifier Fluoroscopy*. Brit. J. of NDT, January 1981, p. 12-13.
- HUNT, B. R. *Digital Image Processing*. Proc. IEEE 63, no. 4, April 1978, p. 693-708.
- PEARSON, J. J., FISCHLER, M. A., FIRSCHEIN, O., and JACOBY, M. *Application of Image Processing Techniques to Automatic Radiographic Inspection*. Proc. EIA 7th Annual AIPR Symposium, 1977.
- SCHAGEN, P. *X-Ray Imaging Tubes*. NDT International, February 1981, p. 9-14.

### **Stereo Radiography**

- ADHIKARI, B. C., CHANDA, D. K., and JANA, S. *On the Determination of the Depth of a Planar Defect by Radiography*. Brit. J. of NDT, Tech. Note, September 1979, p. 249-251.
- HALMSHAW, R., and HALSTEAD, F. *Defect Size Measurement by Radiography*. Brit. J. of NDT, September 1979, p. 245-248.



## Opaque Additives

- CHANG, F. H., GORDON, D. E., and GARDNER, A. H. *A Study of Fatigue Damage in Composites by Nondestructive Testing Techniques*. ASTM-STP 636, 1977, p. 57-72.
- JENSEN, D. L., and SPENCE, L. M. *Radiographic Enhancement Results and Structural Performance Effects of Diiodobutane on Graphite/Epoxy Structures*. Lockheed Missiles and Space Company, Inc., Sunnyvale, California 94086.
- KORNISHIN, K. I. *Application of Contrasting Liquids in Roentgenography*. *Industr. Laboratory*, v. 30, no. 4, April 1964, p. 560-561.

## Neutron Radiography

- CARTER, A. C., MARTYN, N. P. W., and WILSON, C. G. *Enhancement of Neutron Radiographic Contrast*. *Brit. J. of NDT*, January 1980, p. 21-24.
- HERMAN, H. *Nondestructive Evaluation of Materials with Cold Neutron Beams*. AD-A053 073, December 1973.
- HOLLAND, B. G. *Contrast Enhancement in Neutron Radiography Using a Gaseous Penetrant*. *Brit. J. of NDT*, July 1980, p. 172-174.
- HOLLOWAY, J. A., and STUHRKE, W. F. *Low Voltage and Neutron Radiographic Techniques for Evaluating Boron Filament Metal Matrix Composites*. AD-829 621/2st, February 1968.
- JACKSON, C. N., BARTON, J. P., and PROUDFOOT, E. A. *Neutron Radiography Facility at the Hanford Engineering Development Laboratory*. *Mater. Eval.*, June 1979, p. 55-61.
- WILSON, C. R. *Neutron Radiography Complements X-Rays*. *Metal Progress*, v. 98, no. 2, August 1970, p. 75-76.

## X-Ray Diffraction

- BARRETT, C. S., and PREDECKI, P. *Stress Measurement in Polymetric Materials by X-Ray Diffraction*. *Polym. Eng. and Sci.*, v. 16, no. 9, September 1976, p. 602-608.
- BRYDGES, W. T., BADAMI, D. V., JOINER, J. C., and JONES, G. A. *The Structure and Elastic Properties of Carbon Fibers*. *Appl. Polym. Symp.*, no. 9, 1969, p. 255-261.
- PREDECKI, P., and BARRETT, C. S. *Stress Measurement in Graphite/Epoxy Composites by X-Ray Diffraction from Fillers*. *J. Compos. Mater.*, v. 13, January 1979, p. 61-71.
- SCHIERDING, R. G. *Measurement of Whisker Orientation in Composites by X-Ray Diffraction*. *J. Compos. Mater.*, v. 2, no. 4, October 1968, p. 448-457.
- SPERI, W. M., and JENKINS, C. F. *Effect of Fiber-Matrix Adhesion on the Properties of Short Fiber Reinforced ABS*. *Polym. Eng. and Sci.*, v. 13, no. 6, November 1973, p. 409-414.

# DISTRIBUTION LIST

| No. of<br>Copies | To   |
|------------------|--|
|                  | Commander, U.S. Army Aviation Research and Development Command,<br>4300 Goodfellow Boulevard, St. Louis, MO 63120            |
| 10               | ATTN: DRDAV-EGX  |
| 1                | DRDAV-D  |
| 1                | DRDAV-N  |
|                  | Project Manager, Advanced Attack Helicopter, 4300 Goodfellow Boulevard,<br>St. Louis, MO 63120                               |
| 2                | ATTN: DRCPM-AAH-TM   |
| 1                | DRCPM-AAH-TP   |
|                  | Project Manager, Black Hawk, 4300 Goodfellow Boulevard, St. Louis, MO 63120  |
| 2                | ATTN: DRCPM-BH-T   |
|                  | Project Manager, CH-47 Modernization, 4300 Goodfellow Boulevard, St. Louis,<br>MO 63166                                      |
| 2                | ATTN: DRCPM-CH-47-MT   |
|                  | Project Manager, Aircraft Survivability Equipment, 4300 Goodfellow Boulevard,<br>St. Louis, MO 63120                         |
| 2                | ATTN: DRCPM-ASE-TM   |
|                  | Project Manager, Cobra, 4300 Goodfellow Boulevard, St. Louis, MO 63120   |
| 2                | ATTN: DRCPM-CO-T   |
|                  | Project Manager, Advanced Scout Helicopter, 4300 Goodfellow Boulevard,<br>St. Louis, MO 63120                                |
| 2                | ATTN: DRCPM-ASH  |
|                  | Project Manager, Tactical Airborne Remotely Piloted Vehicle/Drone Systems,<br>4300 Goodfellow Boulevard, St. Louis, MO 63120 |
| 2                | ATTN: DRCPM-RPV  |
|                  | Project Manager, Navigation/Control Systems, Fort Monmouth, NJ 07703   |
| 2                | ATTN: DRCPM-NC-TM  |
|                  | Commander, U.S. Army Materiel Development and Readiness Command,<br>5001 Eisenhower Avenue, Alexandria, VA 22333             |
| 4                | ATTN: DRCMT  |
| 2                | DRCPM  |
|                  | Director, Applied Technology Laboratory, Research and Technology Laboratories<br>(AVRADCOM), Fort Eustis, VA 23604           |
| 2                | ATTN: DAVDL-ATL-ATS  |
|                  | Director, Research and Technology Laboratories (AVRADCOM), Moffett Field,<br>CA 94035  |
| 2                | ATTN: DAVDL-AL-D   |

No. of  
Copies

To

Director, Langley Directorate, U.S. Army Air Mobility Research and Development  
Laboratories (AVRADCOM), Hampton, VA 23365

2 ATTN: DAVDL-LA, Mail Stop 266

Commander, U.S. Army Avionics Research and Development Activity,  
Fort Monmouth, NJ 07703

2 ATTN: DAVAA-O

Director, Lewis Directorate, U.S. Army Air Mobility Research and Development  
Laboratories, 21000 Brookpark Road, Cleveland, OH 44135

2 ATTN: DAVDL-LE

Director, U.S. Army Industrial Base Engineering Activity, Rock Island Arsenal,  
Rock Island, IL 61299

4 ATTN: DRXIB-MT

Commander, U.S. Army Troop Support and Aviation Materiel Readiness Command,  
4300 Goodfellow Boulevard, St. Louis, MO 63120

1 ATTN: DRSTS-PLC

1 DRSTS-ME

2 DRSTS-DIL

Office of the Under Secretary of Defense for Research and Engineering,  
The Pentagon, Washington, D.C. 20301

1 ATTN: Dr. L. L. Lehn, Room 3D 1079

12 Commander, Defense Technical Information Center, Cameron Station,  
Alexandria, VA 22314

Headquarters, Department of the Army, Washington, D.C. 20301

2 ATTN: DAMA-CSS, Dr. J. Bryant

1 DAMA-PPP, Mr. R. Vawter

1 DUSRDE(AM), Mr. R. Donnelly

Director, Defense Advanced Research Projects Agency, 1400 Wilson Boulevard,  
Arlington, VA 22209

1 ATTN: Dr. A. Bement

Commander, U.S. Army Missile Command, Redstone Arsenal, AL 35809

1 ATTN: DRSMI-ET

1 DRSMI-RBLD, Redstone Scientific Information Center

1 DRSMI-NSS

Commander, U.S. Army Tank-Automotive Command, Warren, MI 48090

1 ATTN: DRSTA-R

1 DRSTA-RCKM

1 Technical Library

1 DRSTA-EB

| No. of<br>Copies | To   |
|------------------|--|
| 1                | Commander, U.S. Army Armament Research and Development Command, Dover, NJ 07801                                |
| 1                | ATTN: DRDAR-PML  |
| 1                | Technical Library  |
| 1                | Mr. Harry E. Pebly, Jr., PLASTEC, Director   |
| 1                | Commander, U.S. Army Armament Research and Development Command,<br>Watervliet, NY 12189                        |
| 1                | ATTN: DRDAR-LCB-S  |
| 1                | SARWV-PPI  |
| 1                | Commander, U.S. Army Armament Materiel Readiness Command, Rock Island, IL 61299                                |
| 1                | ATTN: DRSAR-IRB  |
| 1                | DRSAR-IMC  |
| 1                | Technical Library  |
| 1                | Commander, U.S. Army Foreign Science and Technology Center, 220 7th Street, N.E.,<br>Charlottesville, VA 22901 |
| 1                | ATTN: DRXST-SD3  |
| 1                | Commander, U.S. Army Electronics Research and Development Command,<br>Fort Monmouth, NJ 07703                  |
| 1                | ATTN: DELET-DS   |
| 1                | Commander, U.S. Army Electronics Research and Development Command,<br>2800 Powder Mill Road, Adelphi, MD 20783 |
| 1                | ATTN: DRDEL-BC   |
| 1                | Commander, U.S. Army Depot Systems Command, Chambersburg, PA 17201   |
| 1                | ATTN: DRSDS-PMI  |
| 1                | Commander, U.S. Army Test and Evaluation Command, Aberdeen Proving<br>Ground, MD 21005                         |
| 1                | ATTN: DRSTE-ME   |
| 1                | Commander, U.S. Army Communications-Electronics Command,<br>Fort Monmouth, NJ 07703                            |
| 1                | ATTN: DRSEL-LE-R   |
| 1                | DRSEL-POD-P  |
| 1                | Director, U.S. Army Ballistic Research Laboratory, Aberdeen Proving Ground,<br>MD 21005                        |
| 1                | ATTN: DRDAR-TSB-S (STINFO)   |
| 1                | Chief of Naval Research, Arlington, VA 22217   |
| 1                | ATTN: Code 472   |
| 1                | Headquarters, Naval Material Command, Washington, D.C. 20360   |
| 1                | ATTN: Code MAT-042M  |
| 1                | Headquarters, Naval Air Systems Command, Washington, D.C. 20361  |
| 1                | ATTN: Code 5203  |



No. of  
Copies

To

Headquarters, Naval Sea Systems Command, 1941 Jefferson Davis Highway,  
Arlington, VA 22376

1 ATTN: Code 035

Headquarters, Naval Electronics Systems Command, Washington, D.C. 20360

1 ATTN: Code 504

Director, Naval Material Command, Industrial Resources Detachment, Building 75-2,  
Naval Base, Philadelphia, PA 19112

1 ATTN: Technical Director

Commander, U.S. Air Force Wright Aeronautical Laboratories, Wright-Patterson  
Air Force Base, OH 45433

1 ATTN: AFWAL/MLTN

1 AFWAL/MLTM

1 AFWAL/MLTE

1 AFWAL/MLTC

National Aeronautics and Space Administration, Washington, D.C. 20546

1 ATTN: AFSS-AD, Office of Scientific and Technical Document Information

National Aeronautics and Space Administration, Marshall Space Flight Center,  
Huntsville, AL 35812

1 ATTN: R. J. Schwinghammer, EH01, Dir., M&P Lab

1 Mr. W. A. Wilson, EH41, Bldg 4612

2 Metals and Ceramics Information Center, Battelle Columbus Laboratories,  
505 King Avenue, Columbus, OH 43201

Hughes Helicopters-Summa, M/S T-419, Centinella Avenue and Teale Street,  
Culver City, CA 90230

2 ATTN: Mr. R. E. Moore, Bldg. 314

Sikorsky Aircraft Division, United Aircraft Corporation, Stratford, CT 06497

2 ATTN: Mr. Melvin M. Schwartz, Chief, Manufacturing Technology

Bell Helicopter Textron, Division of Textron, Inc., P.O. Box 482,  
Fort Worth, TX 76101

2 ATTN: Mr. P. Baumgartner, Chief, Manufacturing Technology

Kaman Aerospace Corporation, Bloomfield, CT 06002

2 ATTN: Mr. A. S. Falcone, Chief, Materials Engineering

Boeing Vertol Company, Box 16858, Philadelphia, PA 19142

2 ATTN: R. Pinckney, Manufacturing Technology

2 R. Drago, Advanced Drive Systems Technology

Detroit Diesel Allison Division, General Motors Corporation, P.O. Box 894,  
Indianapolis, IN 46206

2 ATTN: James E. Knott, General Manager

| No. of<br>Copies | To   |
|------------------|--|
| 2                | General Electric Company, 10449 St. Charles Rock Road, St. Ann, MO 63074<br>ATTN: Mr. H. Franzen   |
| 2                | AVCO-Lycoming Corporation, 550 South Main Street, Stratford, CT 08497<br>ATTN: Mr. V. Strautman, Manager, Process Technology Laboratory  |
| 2                | United Technologies Corporation, Pratt & Whitney Aircraft Division, Manufacturing Research and Development, East Hartford, CT 06108<br>ATTN: Mr. Ray Traynor                   |
| 2                | Grumman Aerospace Corporation, Plant 2, Bethpage, NY 11714<br>ATTN: Richard Cyphers, Manager, Manufacturing Technology<br>Albert Greci, Manufacturing Engineer, Department 231 |
| 2                | Lockheed Missiles and Space Company, Inc., Manufacturing Research, 1111 Lockheed Way, Sunnyvale, CA 94088<br>ATTN: H. Dorfman, Research Specialist                             |
| 2                | Lockheed Missiles and Space Company, Inc., P.O. Box 504, Sunnyvale, CA 94086<br>ATTN: D. M. Schwartz, Dept. 55-10, Bldg. 572   |
| 1                | Mr. R. J. Zentner, EAI Corporation, 198 Thomas Johnson Drive, Suite 16, Frederick, MD 21701  |
| 2                | Director, Army Materials and Mechanics Research Center, Watertown, MA 02172<br>ATTN: DRXMR-PL  |
| 1                | DRXMR-PR   |
| 1                | DRXMR-K  |
| 1                | DRXMR-FD   |
| 10               | DRXMR-OC, Dr. Richard Shuford  |

U.S. Army Aviation Research and Development Command,  
St. Louis, Missouri 63120  
QUALITY CONTROL AND NONDESTRUCTIVE EVALUATION  
TECHNIQUES FOR COMPOSITES - PART IV:  
RADIOGRAPHY - A STATE-OF-THE-ART REVIEW -  
Frank P. Alberti, University of Lowell,  
Lowell, Massachusetts 01854

Technical Report AVRADCOM TR 82-F-4 (AMMRC TR 82-40),  
June 1982, 75 pp - illus-tables, Contract No.  
IPAO5-3363, O/A Project 1807119,  
Final Report, December 1980 to May 1981

AO  
UNCLASSIFIED  
UNLIMITED DISTRIBUTION

Key Words  
Composite materials  
Quality assurance  
Nondestructive  
evaluation

Author's Abstract on reverse side of  
OO Form 1473 of this report

U.S. Army Aviation Research and Development Command,  
St. Louis, Missouri 63120  
QUALITY CONTROL AND NONDESTRUCTIVE EVALUATION  
TECHNIQUES FOR COMPOSITES - PART IV:  
RADIOGRAPHY - A STATE-OF-THE-ART REVIEW -  
Frank P. Alberti, University of Lowell,  
Lowell, Massachusetts 01854

Technical Report AVRADCOM TR 82-F-4 (AMMRC TR 82-40),  
June 1982, 75 pp - illus-tables, Contract No.  
IPAO5-3363, O/A Project 1807119,  
Final Report, December 1980 to May 1981

AD  
UNCLASSIFIED  
UNLIMITED DISTRIBUTION

Key Words  
Composite materials  
Quality assurance  
Nondestructive  
evaluation

Author's Abstract on reverse side of  
OO Form 1473 of this report

U.S. Army Aviation Research and Development Command,  
St. Louis, Missouri 63120  
QUALITY CONTROL AND NONDESTRUCTIVE EVALUATION  
TECHNIQUES FOR COMPOSITES - PART IV:  
RADIOGRAPHY - A STATE-OF-THE-ART REVIEW -  
Frank P. Alberti, University of Lowell,  
Lowell, Massachusetts 01854

Technical Report AVRADCOM TR 82-F-4 (AMMRC TR 82-40),  
June 1982, 75 pp - illus-tables, Contract No.  
IPAO5-3363, O/A Project 1807119,  
Final Report, December 1980 to May 1981

AO  
UNCLASSIFIED  
UNLIMITED DISTRIBUTION

Key Words  
Composite materials  
Quality assurance  
Nondestructive  
evaluation

Author's Abstract on reverse side of  
OO Form 1473 of this report

U.S. Army Aviation Research and Development Command,  
St. Louis, Missouri 63120  
QUALITY CONTROL AND NONDESTRUCTIVE EVALUATION  
TECHNIQUES FOR COMPOSITES - PART IV:  
RADIOGRAPHY - A STATE-OF-THE-ART REVIEW -  
Frank P. Alberti, University of Lowell,  
Lowell, Massachusetts 01854

Technical Report AVRADCOM TR 82-F-4 (AMMRC TR 82-40),  
June 1982, 75 pp - illus-tables, Contract No.  
IPAO5-3363, O/A Project 1807119,  
Final Report, December 1980 to May 1981

AO  
UNCLASSIFIED  
UNLIMITED DISTRIBUTION

Key Words  
Composite materials  
Quality assurance  
Nondestructive  
evaluation

Author's Abstract on reverse side of  
OO Form 1473 of this report

U.S. Army Aviation Research and Development Command,  
St. Louis, Missouri 63120  
QUALITY CONTROL AND NONDESTRUCTIVE EVALUATION  
TECHNIQUES FOR COMPOSITES - PART IV:  
RAUIOGRAPHY - A STATE-OF-THE-ART REVIEW -  
Frank P. Alberti, University of Lowell,  
Lowell, Massachusetts 01854

Technical Report AVRADCOM TR 82-F-4 (AMMRC TR 82-40),  
June 1982, 75 pp - illus-tables, Contract No.  
IPA05-3363, O/A Project 1807119,  
Final Report, December 1980 to May 1981

AO  
UNCLASSIFIED  
UNLIMITED DISTRIBUTION

Key Words  
Composite materials  
Quality assurance  
Nondestructive  
evaluation

Author's Abstract on reverse side of  
DO Form 1473 of this report

U.S. Army Aviation Research and Development Command,  
St. Louis, Missouri 63120  
QUALITY CONTROL AND NONDESTRUCTIVE EVALUATION  
TECHNIQUES FOR COMPOSITES - PART IV:  
RAUIOGRAPHY - A STATE-OF-THE-ART REVIEW -  
Frank P. Alberti, University of Lowell,  
Lowell, Massachusetts 01854

Technical Report AVRADCOM TR 82-F-4 (AMMRC TR 82-40),  
June 1982, 75 pp - illus-tables, Contract No.  
IPA05-3363, O/A Project 1807119,  
Final Report, December 1980 to May 1981

AO  
UNCLASSIFIED  
UNLIMITED DISTRIBUTION

Key Words  
Composite materials  
Quality assurance  
Nondestructive  
evaluation

Author's Abstract on reverse side of  
DO Form 1473 of this report

U.S. Army Aviation Research and Development Command,  
St. Louis, Missouri 63120  
QUALITY CONTROL AND NONDESTRUCTIVE EVALUATION  
TECHNIQUES FOR COMPOSITES - PART IV:  
RADIOGRAPHY - A STATE-OF-THE-ART REVIEW -  
Frank P. Alberti, University of Lowell,  
Lowell, Massachusetts 01854

Technical Report AVRADCOM TR 82-F-4 (AMMRC TR 82-40),  
June 1982, 75 pp - illus-tables, Contract No.  
IPA05-3363, O/A Project 1807119,  
Final Report, December 1980 to May 1981

AO  
UNCLASSIFIED  
UNLIMITED DISTRIBUTION

Key Words  
Composite materials  
Quality assurance  
Nondestructive  
evaluation

Author's Abstract on reverse side of  
DO Form 1473 of this report

U.S. Army Aviation Research and Development Command,  
St. Louis, Missouri 63120  
QUALITY CONTROL AND NONDESTRUCTIVE EVALUATION  
TECHNIQUES FOR COMPOSITES - PART IV:  
RAUIOGRAPHY - A STATE-OF-THE-ART REVIEW -  
Frank P. Alberti, University of Lowell,  
Lowell, Massachusetts 01854

Technical Report AVRADCOM TR 82-F-4 (AMMRC TR 82-40),  
June 1982, 75 pp - illus-tables, Contract No.  
IPA05-3363, O/A Project 1807119,  
Final Report, December 1980 to May 1981

AO  
UNCLASSIFIED  
UNLIMITED DISTRIBUTION

Key Words  
Composite materials  
Quality assurance  
Nondestructive  
evaluation

Author's Abstract on reverse side of  
DO Form 1473 of this report



R



60526